ESTIMATING LIVE FUEL MOISTURE CONTENT IN OKLAHOMA PLANTS

By

ANTIGONE JANE BURKE

Bachelor of Science in Botany

Kent State University

Kent, Ohio

2019

Submitted to the Faculty of the
Graduate College of the
Oklahoma State University
in partial fulfillment of
the requirements for
the Degree of
MASTER OF SCIENCE
May, 2023

ESTIMATING LIVE FUEL MOISTURE CONTENT IN OKLAHOMA PLANTS

Thesis Approved:

Dr. Bryan Murray

Thesis Adviser

Dr. Courtney Duchardt

Dr. Hamed Gholizadeh

Dr. Rodney Will

ACKNOWLEDGEMENTS

I would first like to thank my advisor Dr. Bryan Murray and my committee members Dr. Courtney Duchardt, Dr. Hamed Gholizadeh, and Dr. Rodney Will, as well as Dr. Henry Adams for their contributions to this project and their guidance and support throughout my time here at Oklahoma State. I also thank my fantastic technicians Amna Dar, Ronie Loffelmacher, and Maddie Watts who were instrumental to the success of this project. Thank you to Anna Moeller for helping me learn (to love) R, statistical assistance, and always being a kind and approachable mentor. Thanks also to Dr. Tyson Ochsner and his lab, for aiding me in my soil analyses and for sharing soil moisture data. Thank you to my parents Jill and Ian Burke for encouraging me (from afar) when I needed it most. Lastly, thank you, most especially, to Zachary Harmon for being my greatest support throughout this degree— I don't think I could have done it without you.

Name: ANTIGONE BURKE

Date of Degree: MAY, 2023

Title of Study: ESTIMATING LIVE FUEL MOISTURE CONTENT IN OKLAHOMA PLANTS

Major Field: NATURAL RESOURCE ECOLOGY AND MANAGEMENT

Abstract: Live fuel moisture content (LFM) is an important variable in fire danger rating systems. LFM collection is time and resource intensive and plant water relations vary within and between species. Consequently, the best approach for estimating LFM is unknown. Few studies have investigated LFM in the state of Oklahoma, and current estimates of LFM have not been validated. The objectives of this study were to evaluate the use of environmental and remote sensing proxies for estimating LFM in Oklahoma plants. I found that LFM can be accurately estimated using either hyperspectral leaf-level reflectance or environmental proxies. My analysis of several remote sensing vegetation indices identified the Water Index and VIgreen as the best suited indices for approximating LFM. Using functional group, photoperiod, vapor pressure deficit, and rainfall I was able to estimate LFM in Oklahoma plant communities. In addition to these findings, I identified a need to reevaluate current methods for estimating LFM. By advancing our understanding of LFM and how best to predict it, my results can be used in fire danger rating systems to protect lives and preserve natural resources.

TABLE OF CONTENTS

LIST OF TABLES

Table Page

LIST OF FIGURES

Figure Page

CHAPTER I

LITERATURE REVIEW

This year, the UN Environment Programme published their 2022 Emissions Gap Report, which revealed that under current emissions global warming is projected to reach 2.8° C by the end of the century (United Nations Environment Programme 2022). The 2014 Intergovernmental Panel on Climate Change warned that this business-as-usual level of warming will have drastic environmental impacts (Intergovernmental Panel on Climate Change 2014). The U.S. Global Change Research Program's Fourth National Climate Assessment (2017) reported warming temperatures, decreasing annual precipitation, and intensifying droughts in much of the western and southern USA. In the U.S. Climate Change Science Program's 2008 report, they described that these climate change impacts, and others, will exacerbate wildfire conditions (U.S. Climate Change Science Program 2008). In addition to climate change, expanding wildland-urban-interfaces (WUIs) are increasing wildfire risk throughout the USA (Radeloff et al. 2018). Burke et al. (2021) estimate that the number of houses in the USA's wildland-urban-interface is increasing at a rate of one million per year. Figures from the United States Environmental Protection Agency (2022a) using data from Monitoring Trends in Burn Severity (2022) show increasing landscape damages and lengthening fire seasons.

They also revealed increasing annual acreage burned throughout the USA but especially in the west and southwest.

Wildfires can cause loss of life, and significant direct and indirect financial burden in the USA. Data compiled by St. Denis et al. (2020) include reports of 222 fatalities during wildfire incidents from 1999-2014 and Butler et al. (2017) found that wildfires cause the death of approximately 20 USA wildland firefighters per year. In addition to direct casualties, wildfires cause indirect deaths, health complications, and negative health impacts (Youssouf et al. 2014, Reid et al. 2016, Chen et al. 2021, Nanjappan et al. 2021). Costs other than healthcare include mitigation, suppression, evacuations, industry/infrastructure/private losses, and ecosystem damages (Dale 2010, Ingalsbee 2010, Thomas et al. 2017, Prestemon et al. 2022). Thomas et al. (2017) estimate that the annual economic burden related to wildfires could be as much as $347 billion. Ingalsbee (2010) attributed accelerating costs to expanding WUIs and increasing megafires (a nontechnical term sometimes defined as fires burning over 100,000 acres (Tedim et al. 2018)). These rising costs are expected to continue (Prestemon et al. 2022).

Directly or indirectly, wildfires can damage and alter ecosystems and ecosystem services (Shakesby and Doerr 2006, Laughlin and Fulé 2008, Smith et al. 2011, Dickens and Allen 2013, Alba et al. 2015, Horn and St. Clair 2016, Thomas et al. 2017, Day et al. 2019, Vukomanovic and Steelman 2019, Köster et al. 2021). Shakesby and Doerr (2006) found that wildfires cause increased erosion, and decreased soil stability and organic matter. They found that wildfires reduce water interception, retention, and infiltration while increasing overland flow and runoff. Wildfires can facilitate plant invasion which can hinder native plant succession (Dickens and Allen 2013, Coates et al. 2016, Horn and

St. Clair 2016). In their review of threatened species, Kelly et al. (2020) found that over 4,400 faced threats from altered fire regimes. These indirect damages coupled with direct damages create compounding expenses. For example, wildfires cause direct losses to agriculture (lost crops, timber, and livestock), but can indirectly taint crops and damage vital ecosystem services like soil health and hydrologic processes (Shakesby and Doerr 2006, Krstic et al. 2015, Hays 2017, Köster et al. 2021, Dillis et al. 2022).

The San Diego Declaration on Climate Change and Fire Management suggests that to prepare for a future with increased wildfire hazard monitoring and prediction will be essential (Oswald and The Association for Fire Ecology Board of Directors 2007). Fire danger rating systems predict wildfire potential and behavior and inform resource investment (Hardy and Hardy 2007). The US National Fire Danger Rating System (NFDRS) was first released in 1972 and is the most widely used fire danger rating system in the USA (Schlobohm and Brain 2002). Since its release, the NFDRS has undergone three revisions. Diagrams for Versions 1 and 2 are available in Bradshaw et al. (1984), Version 3 in Burgan (1988), and Version 4 in Jolly (2018). The NFDRS has adjusted as fire ecology advanced (ex. the addition of season/daylength, vapor pressure deficit, and improved methods for estimating fuel moisture content) and technology advanced (ex. hourly measurements and the use of satellite imagery). Key variables maintained in each iteration are slope, windspeed, temperature, relative humidity, precipitation, habitat/land use, estimates of time-lagged dead fuel moisture, and estimates of live fuel moisture content (LFM).

Of scientific and management interest is the significance and variability of LFM and the accuracy of current estimates. Early in the development of fire danger rating

systems the importance of LFM, the water content of nondormant living vegetation, to fire danger was realized (Deeming et al. 1972). LFM is calculated as the proportion of water in live vegetation:

$$\text{LFM (\%)} = \frac{fresh\ mass - dry\ mass}{dry\ mass} \times 100$$

Where $fresh\ mass$ is the mass of a freshly clipped vegetation sample from living vegetation and $dry\ mass$ is the mass of that same sample after being oven dried, typically for at least 24 hours.

High LFM decreases wildfire risk by increasing time to ignition and slowing the rate of consumption (Nelson Jr 2001). Moisture content dictates fuel flammability and living vegetation can either contribute to available fuels or serve as a heat sink (Loomis et al. 1979, Dimitrakopoulos and Papaioannou 2001). In some instances and locations, live fuels are the most abundant fuels (Castro et al. 2003, Weise et al. 2005). For example, low LFM may have been the dominant cause of the 2007 Zaca Fire in California which burned 240,000 acres (Dennison and Moritz 2009). LFM has been shown to be related to number of total and/or large fires, area burned, and fire behavior (ex. rate of spread, heat content) (Jolly 2007, Dennison et al. 2008, Chuvieco et al. 2009, Dennison and Moritz 2009, Arganaraz et al. 2016, Qi et al. 2016, Rossa et al. 2016).

Despite its long use in fire models and acknowledged importance, the best approach for estimating LFM is not agreed upon. This is likely due to LFM in-situ data being limited, mostly to historically fire-prone locations like California, and the complexity of plant-water relations (Deeming et al. 1972, Countryman 1974, Bradshaw et al. 1984, Snyder et al. 2006, Capps et al. 2021). As a result, there are ongoing efforts to

increase the availability of LFM data (National Fuel Moisture Database 2009, Yebra et al. 2019) and to explore the role of plant ecophysiology in LFM (Fares et al. 2017, Jolly and Johnson 2018, Pivovaroff et al. 2019, Nolan et al. 2020, Resco de Dios 2020, Scarff et al. 2021). Recently, the term pyro-ecophysiology (or pyrophysiology) has been used to describe the study of the ecophysiological interactions between plants and fire (Jolly and Johnson 2018, Resco de Dios 2020). Through the study of pyro-ecophysiology we can improve our understanding of LFM (Fares et al. 2017, Jolly and Johnson 2018, Pivovaroff et al. 2019, Resco de Dios 2020, Scarff et al. 2021).

Variation in plant species' morphology and physiology influence plant water content and flammability (Dimitrakopoulos 2000, Dimitrakopoulos and Papaioannou 2001). Additionally, plants manage and avoid water stress through a number of different morphological and physiological approaches (Al-Tawaha et al. 2017, Seleiman et al. 2021). These adaptations can influence LFM, for example, drought tolerant species, with the ability to reduce transpiration during water stress, would theoretically exhibit slower rates of LFM decline. These variations are likely why, in several studies, water status has been shown to vary among co-occurring species (Sobrado 1986, Pellizzaro et al. 2007a, Pellizzaro et al. 2007b, Pivovaroff et al. 2019, Costa-Saura et al. 2021, Brown et al. 2022). In addition to inter-species variations, plant water content varies temporally— diurnally, seasonally, annually— and spatially— within and between habitats (Klepper 1968, Sobrado 1986, Smith et al. 1995, Touchette 2006, Pellizzaro et al. 2007b, Kauf et al. 2015, Wright et al. 2015, Nolan et al. 2016, Costa-Saura et al. 2021, Brown et al. 2022). These factors and others, like stress history, interact and make plant water status difficult to predict.

There is sufficient evidence that LFM's impact on wildfire behavior is threshold dependent (Viegas et al. 2001, Schoenberg et al. 2003, Pellizzaro et al. 2007b, Dennison et al. 2008, Dennison and Moritz 2009, Jurdao et al. 2012, Weir and Scasta 2014, Arganaraz et al. 2016, Nolan et al. 2016). These thresholds occur at critical LFM values whereafter there is significant increase in fire activity (ex. acres burned). However, estimated critical LFM thresholds vary between species, systems, and studies. Dennison et al. (2008) and Dennison and Moritz (2009) found critical LFM thresholds of 71% and 79% in southern California chaparral, but Schoenberg et al. (2003) found a critical LFM threshold of 90% for the same region. In Argentina, Arganaraz et al. (2016) found thresholds of 67% in grasslands, 105% in forests, and 121% in shrublands. Pellizzaro et al. (2007b) estimated the critical threshold of the Western Mediterranean Basin to be about 100% and in Spain, Jurdao et al. (2012) found thresholds of ~127% in grasslands and ~106% in shrublands. Nolan et al. (2016) found critical moisture thresholds of Australian woodlands to be as high as ~167%. These thresholds likely vary due to pyro-ecophysiology.

Globally, many researchers have had success estimating plant water status from environmental proxies. In Spain, Castro et al. (2003) were able to estimate LFM using models containing temperature, soil water, relative humidity, date, and the Canadian Buildup Index. Buildup Index is calculated from the Canadian Forest Fire Danger Rating System's Duff Moisture Code and Drought Code (Van Nest and Alexander 1999). In the same region Viegas et al. (2001) also found LFM was correlated to the Buildup Index and Drought Code. The meteorological-based Keetch-Byram Drought Index (KBDI, Keetch and Byram (1968)) was used in Greece to estimate forest LFM (Dimitrakopoulos and

Bemmerzouk 2003). For four Mediterranean species Pellizzaro et al. (2007a) found the best estimate of LFM was either soil moisture content or the Drought Code. California *Adenostoma fasciculatum* LFM was predicted by Capps et al. (2021) using date, day length, temperature, relative humidity, precipitation, windspeed, and solar radiation. In the latest version of the NFDRS, LFM is estimated using the Growing Season Index which is derived from photoperiod, vapor pressure deficit, and minimum temperature (Jolly et al. 2005, Jolly 2018). In Utah, Qi et al. (2012) found soil moisture was a better proxy for LFM than remote sensing vegetation indices.

Vegetation indices estimate plant traits from remotely sensed canopy or leaf reflectance. Vegetation indices are calculated using the known reflective properties of plants, and how traits (like stress or water content) influence reflectance in particular wavelengths/regions of the electromagnetic spectrum. This approach is popular because it typically is less time-consuming and expensive than field collection, nondestructive, and applicable at large spatial scales. Due to these benefits and the lack of available LFM data, there is interest in using remote sensing to estimate plant water content and many studies have done so successfully. For example, the Water Index (WI, (Peñuelas et al. 1992)) and the Normalized Difference Water Index (NDWI, (Gao 1996)) were used to monitor changes in the relative water content of California chaparral species by Serrano et al. (2000). Chuvieco et al. (2004) estimated LFM in Mediterranean species using the Normalized Difference Vegetation Index (NDVI, (Rouse et al. 1974)) and remotely sensed surface temperature. In the woodlands of Australia Nolan et al. (2016) predicted LFM using the Visible Atmospherically Resistant Index (VARI, (Gitelson et al. 2002)). A summary of vegetation indices for approximating plant water status can be found in

Roberto et al. (2012). Several projects have had greater success estimating LFM by combining remote sensing and environmental predictors (García et al. 2008, Myoung et al. 2018, Costa-Saura et al. 2021).

Located in the south-central USA, Oklahoma is part of the Southern Great Plains ecoregion (United States Environmental Protection Agency 2022b). The Southern Great Plains are dominated by grasslands, characterized by strong east-west precipitation and north-south temperature gradients, host to diverse flora and fauna, and were historically moderated by grazing, fire, and drought (U.S.D.I. National Park Service 2008). Agencies predict that climate change will cause more extreme weather in the Southern Great Plains, like heatwaves, intense rainfall events, and drought (Meehl and Tebaldi 2004, United States Environmental Protection Agency 2016, U.S. Global Change Research Program 2018). Although the Southern Great Plains has historically experienced droughts, even under moderate emission scenarios Cook et al. (2015) project unprecedent megadroughts in the future. This prediction is corroborated by the findings of Lin et al. (2013) who reported continuous soil moisture declines in Oklahoma from 1980 to 2009 and by the climate change simulations of Gensini et al. (2023). Moreover, the historically dipole nature of precipitation in the Southern Great Plains — modulating from pluvial (significantly wet) to drought years— may be becoming more extreme, possibly due to climate change (Christian et al. 2015, Chen and Wang 2022). And these dipole events are linked to megafires in the Southern Great Plains because wet years result in increased biomass which can become available fuel during consequent dry years (Van Speybroeck et al. 2011, Krueger et al. 2016, Scasta et al. 2016, Lindley et al. 2019).

Of the megafires investigated by Lindley et al. (2019), the majority were associated with Southern Great Plains wildfire outbreaks. Southern Great Plains' wildfire outbreaks and megafires have been linked to low-level thermal ridges (which create high surface temperatures), high winds, and dry conditions, especially drought (Lindley et al. 2007, Van Speybroeck et al. 2007, Reid et al. 2010, Lindley et al. 2011a, Lindley et al. 2011b, Lindley et al. 2013, Weir et al. 2017, Lindley et al. 2019). Other factors linked to large fires in the Southern Great Plains are growing populations/wildland-urban-interfaces (Van Speybroeck et al. 2007, An et al. 2015, Nagy et al. 2018, Radeloff et al. 2018) and historic fire suppression (Bidwell et al. 2016, Donovan et al. 2017b, Pyne 2017, Lindley et al. 2019).

When compared to the previous decade, Donovan et al. (2017a, 2017b) reported an average increase of ~85 large wildfires per year, an average percent increase in area burned of ~1200%, and ~36% average increase in likelihood of annual large wildfire occurrence in the Southern Great Plains. These increases were generally much greater than in the Northern Great Plains (Donovan et al. 2017b). Their findings are substantiated by the wildfire risk model of An et al. (2015) which estimated the greatest increase in the contiguous USA would be in the Southern Great Plains (and Louisiana). Scasta et al. (2016) also predict that the potential for large fires in the Southern Great Plains will increase. In Oklahoma, according to Monitoring Trends in Burn Severity data, nine out of the ten largest wildfires since 1984 have occurred in the last twelve years, the largest in the last seven (Monitoring Trends in Burn Severity 2022).

These large wildfires are costly and dangerous. Of especial financial concern in the Southern Great Plains are losses to agriculture— the primary land use (U.S.D.I.

National Park Service 2008). For example, the meat industry of Oklahoma supplies over 25,000 jobs and a total economic output near $15 billion and the forestry industry has an economic impact of over $5 billion (The North American Meat Institute 2016, Starr et al. 2018). In 2017, Oklahoma State University Cooperative Extensionist Derrell Peel, estimated losses to the cattle industry incurred by the Northwest Complex fires to be $14.6 million (Hays 2017). During the 2010-2011 SGPWOs, The Texas Forest Service estimated that 175 million cubic feet of timber and $1.6 billion in profits were lost (Texas Forest Service Communications 2011).

Presently there is a knowledge gap regarding LFM in Oklahoma, and the National Fuel Moisture Database contains no data from the state (National Fuel Moisture Database 2022). When compiling this literature review, I found four studies investigating LFM in Oklahoma that were limited to *Juniperus virginiana* or tallgrass prairie. Weir and Scasta (2014) ran laboratory tests to determine how *J. virginiana* LFM influenced flammability and found a critical LFM threshold of 60%. Dudek (2020) built upon their findings and was able to predict *J. virginiana* LFM using soil water potential and vapor pressure deficit. Their model retroactively showed declines in LFM leading up to the Rhea fire which burned over 250,000 acres. Sharma et al. (2018) and Sharma et al. (2021) investigated fuel moisture in an Oklahoma tallgrass prairie plant community. In 2018, they used an artificial neural network model to predict LFM using NDVI, day-of-year, and canopy height and in 2020, they found that soil moisture (as fraction of available water content) was correlated to mixed fuel moisture and curing rate.

Currently, the Oklahoma Mesonet maintains a well-developed fire management application called OK-Fire. The Oklahoma Mesonet is a collaboration between

Oklahoma State University and the University of Oklahoma and has been in operation since 1994 (Mesonet 2022). The Oklahoma Mesonet includes 120 automated weather stations, at least one per county, which transmit meteorological and soil data every five minutes (Mesonet 2022). These data are publicly accessible on the Mesonet's website or mobile app. OK-Fire is used to inform burn bans, red flag warnings, fire management activities, and prescribed burning (Carlson et al. 2002, Mesonet 2022). The Oklahoma Fire Danger Model is OK-Fire's fire danger rating system adapted from the NFDRS and was one of the earliest mesoscale fire danger systems in the USA (Carlson et al. 2002, Mesonet 2022). It predicts fire danger using meteorological data from the Mesonet stations and satellite imagery (Carlson et al. 2002).

Woody and herbaceous LFM are estimated in OK-Fire/the Oklahoma Fire Danger Model using Visible Infrared Imaging Radiometer Suite satellite seven-day composites to calculate relative greenness (Mesonet 2022). Relative greenness is calculated from daily NDVI as:

$$\frac{NDVI - min}{max - min} \times 100$$

where *max* is the ten-year historical maximum NDVI and *min* is the ten-year historical minimum NDVI for each 500-meter pixel (Carlson 2022). Since its release there was desire to improve the Oklahoma Fire Danger Model estimates of LFM (Carlson et al. 2002). There are currently no public studies validating OK-Fire estimates of LFM.

As of 2003, Ceccato et al. (2003) reported that NDVI was the most used vegetation index for approximating LFM. That said, NDVI is one of the earliest, and subsequently most popular vegetation indices and due to its accessibility and popularity

there is risk of misuse (Huang et al. 2020). NDVI is related to plant chlorophyll content and is thereby indirectly related to plant water content and then, only weakly so (Ceccato et al. 2003, Jones and Vaughan 2010, Roberto et al. 2012).

As such, many studies have shown NDVI to be a weak or lesser indicator of plant water content. For example, WI and NDWI were found to be more sensitive to changes in the relative water content of California chaparral species than NDVI in Serrano et al. (2000). Likewise, Dennison et al. (2006) found that NDWI was superior to NDVI for monitoring LFM, and Jia et al. (2018) found the same. Conversely, Roberts et al. (2006) and Peterson et al. (2008) found VARI bested other vegetation indices including NDVI and NDWI. Similarly, Schneider et al. (2008) found that relative greenness derived from VARI was more correlated to LFM than NDVI-derived. Other vegetation indices supported over NDVI include the Normalized Difference Infrared Index (NDII, (Hardisky et al. 1983)) and the Moisture Stress Index (MSI, (Hunt and Rock 1989)) (Baloun 2006, Caccamo et al. 2012). When comparing five popular vegetation indices, Myoung et al. (2018) found that LFM was best predicted by the Enhanced Vegetation Index (EVI, (Huete et al. 1997)), but that estimates improved when EVI was used along with daily minimum temperature. Relatedly, Costa-Saura et al. (2021) found that the Normalized Difference Moisture Index (normalized MSI) consistently outperformed twelve other vegetation indices, and when combined with 30- and 60-day average temperature and windspeed was a good estimate of LFM. These studies highlight the need to reevaluate the use of NDVI for approximating LFM.

Ultimately, climate predictions for Oklahoma and the Southern Great Plains warrant planning for a future of increased fire danger. A vital preparation is improving

upon our fire danger rating systems. To do so, we must validate current estimates of LFM and investigate the pyro-ecophysiology of Oklahoma plants. To my knowledge, there are no studies of in-situ LFM for the broader plant communities of Oklahoma or validating OK-Fire LFM estimates. While OK-Fire is an advanced fire danger rating system, it is possible that LFM may be misrepresented by relative greenness calculated from NDVI.

CHAPTER II

USING HYPERSPECTRAL, LEAF-LEVEL REFLECTANCE TO ESTIMATE LIVE FUEL MOISTURE CONTENT

INTRODUCTION

Climate change models predict the south-central United States/Southern Great Plains will be impacted by intense droughts and increased wildfire risk (An et al. 2015, Scasta et al. 2016). Already, throughout the Southern Great Plains, acreage burned and number of large fires have increased (Donovan et al. 2017). In this region, and others, accurate and accessible fire danger rating systems can be vital to preservation of life and property.

An important variable in fire danger models is live fuel moisture content (LFM), the proportion of water in living, nondormant vegetation. Unlike dead fuels, which have a direct relationship with meteorological conditions, live fuels have dynamic and diverse relationships with environmental conditions (Pyne et al. 1996). Water movement into and out of living plants occurs through the soil-plant-atmosphere-continuum (SPAC). Plants uptake water from the soil, transport water throughout their body, and lose water to the atmosphere through transpiration. Differences in the potential energy of water throughout

the SPAC dictate the direction of water movement. Water flows from less negative to more negative water potentials (Ψ). Plant Ψ becomes more negative as tension within vascular tissue (xylem) increases because of soil water deficit and/or increasingly hot/dry atmospheric conditions (Brady and Weil 2002, Taiz et al. 2015). During water stress plants can decrease water loss (further Ψ decline) by reducing transpiration rates, but this also reduces photosynthesis. As water deficits and stress increase, LFM declines (Nelson Jr 2001) and recent studies using NASA's The ECOsystem and Spaceborne Thermal Radiometer Experiment on Space Station in both California and Australia found that plant water stress was predictive of wildfire occurrence and severity (Masara et al. 2022, Pascolini-Campbell et al. 2022).

The relationships between environmental conditions and plant water stress/status are variable. Plants have different strategies for avoiding or managing water stress. A popular example of a physiological adaptation to reduce water loss is photosynthetic pathway. Rooting depth, then, would be a morphological strategy for avoiding water stress. There are many other, diverse, approaches that plants use to avoid or resist water stress (Al-Tawaha et al. 2017, Seleiman et al. 2021). As such, several studies have shown moisture content varies even between co-occurring species (Sobrado 1986, Pellizzaro et al. 2007, Pivovaroff et al. 2019, Costa-Saura et al. 2021, Brown et al. 2022). Nonetheless, accurate estimation of LFM is important for fire danger rating, as high LFM decreases available fuels, rates of spread, and intensity. (Pyne et al. 1996, Nelson Jr 2001, Ceccato et al. 2003). It is therefore an important area of research to better understand differences in LFM between species.

Collection of in-situ LFM data is resource intensive and is therefore often estimated via remote sensing proxies. Satellite or airborne remote sensing estimation benefits from usually being more affordable, spatially expansive, faster, and non-destructive when compared to field collection. Owing to these advantages, many studies have estimated plant water content from remote sensing successfully (Peñuelas et al. 1997, Serrano et al. 2000, Chuvieco et al. 2004, Dennison et al. 2006, Hao and Qu 2007, García et al. 2008, Peterson et al. 2008, Nolan et al. 2016, Jia et al. 2018). Vegetation indices (VIs) are used in remote sensing to estimate plant traits from reflectance using regions of the electromagnetic spectrum sensitive to plant traits/status/properties. Early, popular vegetation indices (VIs) created to measure plant water content include Hunt and Rock's Moisture Stress Index (MSI), Gao's Normalized Difference Water Index (NDWI), and Peñuelas et al.'s Water Index (WI) (Hunt and Rock 1989, Gao 1996, Peñuelas et al. 1997). These and other VIs suggested for the approximation of plant water content have been summarized in Roberto et al. (2012) and a compilation of studies which have used remote sensing for LFM estimation is available in Yebra et al. (2013).

Studies of the effectiveness of remote sensing estimation of LFM in Oklahoma plant communities have been limited. In Dudek's (2020) study which utilized a hyperspectral radiometer, NDWI was a better estimate of LFM in *Juniperus virginiana* in the state than The Normalized Difference Vegetation Index (NDVI, (Rouse et al. 1974)). In 2018, Sharma et al. included NDVI, measured using a hand-held multispectral radiometer, in their artificial neural network model for predicting LFM in an Oklahoma tallgrass prairie plant community. However, in 2021, at the same location, Sharma et al. found NDVI to be less accurate for mixed fuel moisture estimation when compared to

soil moisture. Currently, the Oklahoma Fire Danger Model, Oklahoma's most robust fire danger rating system, estimates LFM using NDVI−derived relative greenness from Visible Infrared Imaging Radiometer Suite satellite composites (Mesonet 2022).

According to Ceccato et al. (2003), NDVI is/was the most commonly used VI for estimating LFM. Yet, in several studies, NDVI has been shown to be an inferior indicator of plant water content/LFM when compared to other VIs. WI and NDWI were found to be more sensitive to changes in relative water content than NDVI in Serrano et al. (2000) and similarly, Dennison et al. (2006) found that NDWI was superior to NDVI for monitoring LFM. Roberts et al. (2006) found that The Visible Atmospherically Resistant Index (VARI, (Gitelson et al. 2002)) outperformed nine other VIs, including NDVI. Peterson et al. (2008) found the same (seven VIs tested) and Schneider et al. (2008) found that relative greenness derived from VARI was more correlated to LFM than NDVI-derived. Caccamo et al. (2012) found that NDIIb6 (adapted from NDII by Hardisky et al. 1983) and VARI were better estimates of LFM than NDVI and NDWI. Given this evidence, the use of NDVI for estimating LFM in Oklahoma should be validated.

The aim of this study was to assess the use of hyperspectral leaf-level reflectance for estimating LFM in Oklahoma dominant plant species. We tested three hypotheses: 1) that LFM is representative of plant water status and stress, 2) that changes in LFM alter hyperspectral leaf-level reflectance, and 3) that the relationship between LFM and leaf-level reflectance differs among plant species. We predicted that LFM would be correlated to leaf water potential and that hyperspectral leaf-level reflectance can be used to estimate LFM. Additional objectives of this study were 1) to identify wavelengths of

importance for estimating LFM and 2) compare vegetation indices for approximating LFM. Using identified wavelengths of importance we created a vegetation index for estimating LFM which we evaluated along with other vegetation indices, from literature, suggested for approximating LFM.

METHODS

Sites and species

To broadly represent the vegetation of Oklahoma we selected two or three of the dominant species of the most broadly distributed vegetation types in the state (Fig. 2.1, Table 2.1). The largest vegetation communities by area from east to west are oak-hickory-pine forests (or oak-hickory and oak-pine forests), post oak-blackjack oak forest (i.e., Cross Timbers), tallgrass prairie, mixedgrass prairie, and shortgrass prairie. Dominant species were selected according to Duck and Fletcher (1943) as reported by Tyrl et al. (2007). The species selected included four herbaceous, perennial grasses (*Andropogon gerardii* Vitman, *Bouteloua gracilis* (Kunth) Lag. ex Griffiths, *Panicum virgatum* L., and *Schizachyrium scoparium* (Michx.) Nash) and three trees (*Juniperus virginiana* L., *Pinus echinata* Mill., and *Quercus stellata* Wangenh.). See Table 2.1 for species (specific epithets and common names) per plant community and codes. We conducted greenhouse water stress experiments in the hopes of recording the full range of possible LFM values. This is important when using machine learning models that do not extrapolate well.

The experiments took place in the Oklahoma State University Department of Natural Resource Ecology and Management's greenhouse located in Stillwater, OK,

USA. During the periods prior to the water stress experiment, plants were watered and fertilized as needed. A potting soil mixture was used (a 1:1 mixture of Jolly Gardener Pro-line C20 and Hope Agri Products, Inc. Hapi-Gro organic compost). The experiments were conducted in two phases: grasses in summer 2021 and trees in summer 2022. Given our interest in fire danger, collection of plant Ψ occurred at, or after, 10:15 AM Central Time (U.S.) and collection leaf-level reflectance and LFM began at, or after, 11:00 AM Central Time (U.S.). Midday collections were chosen to coincide with the warmest, driest conditions of the day. Plant Ψ was measured first, typically taking one hour, followed by simultaneous collection of LFM and leaf-level reflectance.

Grasses

Seeds of *A. gerardii, B. gracilis, P. virgatum,* and *S. scoparium* were purchased from Prairie Moon Nursery (Winona, Minnesota, USA). Seed was sown in April 2021 in planting trays. Once grasses reached the three-leaf (blade) stage, they were transplanted to ~6283 cm^3 pots (~20 cm diameter, ~20 cm depth). The water stress experiment began in August 2021 when plants had reached reproductive maturity. Plants were divided into three groups: a smaller control group of four plants per species watered to field capacity twice weekly, a moderate drought group of twelve plants with weekly water reduced by approximately 25%, and a severe drought group of twelve plants watered to field capacity at the start of the experiment and never watered again. To mitigate the impact of defoliation from collection, each treatment group was subdivided into three groups, which were collected from on alternating days. Collections occurred daily from August 3, 2021 to September 17, 2021 (44 collections total).

Trees

Trees *J. virginiana, P. echinata,* and *Q. stellata* were purchased as one-year, bareroot seedlings of from the Oklahoma State Nursery in April 2021. They were then transplanted into ~12,566 cm^3 pots (~20 cm diameter, ~40 cm depth). The water stress experiment began in May 2022 when saplings were approximately two years old. Plants were divided into three groups: a small control group watered to field capacity three times per week, a moderate drought group with weekly water reduced by approximately 25% per week, and a severe drought group watered to field capacity at the start of the experiment and never watered again (Table 2.2). To mitigate the impact of defoliation from collection, each treatment group was subdivided into three groups corresponding to day-of-week. Collections occurred three times per week from May 11, 2022 to August 1, 2022 (36 collections total). In the severe drought group, *P. echinata* exhibited a faster rate of health decline (low LFM, low Ψ) from water stress, than *J. virginiana* and *Q. stellata*. To prolong collection of the severe treatment *P. echinata* saplings, the group received additional water after collection on May 20, 2022 and were not watered again. Only those individuals which recovered continued to be sampled (15 of the original 20 individuals).

Collection of leaf water potential (Ψ)

To relate LFM to true plant water status we measured leaf water potential (Ψ, as pressure in MPa) using Scholander pressure chambers. Collection of Ψ occurred at or after 10:15 AM Central Time (U.S.) for grasses and at or after 11 AM Central Time (U.S.) for trees. Measurements typically took one hour, after which LFM was measured,

typically also taking one hour. Species measurements for Ψ and LFM occurred in the same order (including individuals). Samples were taken from cut twigs of *P. echinata* and *J. virginiana* and leaves from *Q. stellata* and grasses. Grass Ψ was measured using PMS Instrument Company's Model 600 pressure chamber with a maximum pressure of 4 MPa and tree Ψ was measured using Model 1505D with a maximum pressure of 10 MPa (PMS Instrument Company 2023). Species were collected from in the same order, daily, to reduce impacts from the timing of measurements (diurnal Ψ fluctuations). We removed data where maximum pressure was reached, 4.0 MPa for grasses and 10.0 MPa for trees, which did limit the number of data points at lower LFM.

Collection of leaf spectra and LFM

Leaf-level hyperspectral data were collected using the field portable hyperspectral spectroradiometer ASD FieldSpec3, plant probe attachment, and the software RS^3, all from Malvern Panalytical Ltd (2023). The FieldSpec3 samples 2,151 spectral bands from 350−2500 nanometers (nm) wavelengths with spectral resolution of 3 nm at 700 nm, and 10 nm at 1400 and 2100 nm. Leaf-level reflectance was recorded as outlined by Burnett et al. (2021), except for our use of a one-to-one ratio of leaf spectra to LFM (trait). One-to-one collections were used to minimize damage/undue stress to resampled individuals. Spectra were processed and downloaded using Malvern Panalytical's free software ViewSpec Pro™ (Malvern Panalytical Ltd 2014). Jump correction, a pre-processing step that corrects jumps between spectroradiometer channels, was performed using ViewSpec's "Splice Correction" tool. The spectra were then exported as .txt files for analysis in RStudio (R, from RStudio Team (2022)).

For each individual, a set of leaves (or leaf for *Q. stellata*) were taken for spectra and a set of leaves were taken for LFM. The sets were collected from the same, mid-canopy branch/section of each plant. This approach was used to minimize evapotranspiration, via heat from the plant probe, and under the assumption that water content within the same region of the plant body is relatively equalized. Once removed, samples were stored in sealed plastic bags out of direct sunlight. Leaf spectra and weights were taken within one to five minutes from clipping.

All weights were measured using the same scale (Ohaus® Scout™ SPX series portable electronic balance with 0.001-gram readability). Once fresh, i.e., wet, mass was recorded, samples were transferred to an oven and dried at 60°C for at least 48 hours. At the start of the study, we confirmed that after 48 hours there were no significant changes in samples' masses. Dry mass was then recorded and LFM was calculated as:

$$LFM\ (\%) = \frac{fresh\ mass - dry\ mass}{dry\ mass} \times 100$$

Leaf water potential (Ψ) modeling

To determine the correlation between LFM and plant water status, we analyzed the relationship between LFM and Ψ using simple linear and second order polynomial models in R. First, we plotted the relationship between LFM and Ψ for each species using the R packages "ggplot" and "ggpmisc" (Wickham 2016, Aphalo 2022). Next, we created a linear mixed effects model including species, Ψ, and individual as a random effect using the R package "nlme" (Pinheiro et al. 2023). We included individual as a random effect because we resampled the same individuals over time. Additionally, dates with relative humidity measured as greater than or equal to 65% relative humidity (recorded

using a handheld weather meter) were excluded from analysis as these high humidity conditions were inconsistent with the water stress conditions plants were under (low soil moisture) and caused reduced transpiration (high Ψ).

Partial least squares regression (PLSR) modeling

As described in Burnett et al. (2021), PLSR modeling is well-suited for estimating plant traits from hyperspectral data due to its ability to mitigate issues related to collinearity between many predictors. For this reason, we created PLSR models in R to estimate LFM (dependent/response variable) from leaf-level reflectance. Reflectance at wavelengths 500-2400 nm were our independent/predictor variables which were reduced to a smaller number of components (latent variables). PLSR modeling was accomplished using the R packages "pls" and "spectratrait" (Liland et al. 2022, Terrestrial Ecosystem Science and Technology Group 2022). Our code was modelled after the spectratrait vignettes (example code) available from the Terrestrial Ecosystem Science and Technology Group. PLSR models were created for individual species, vegetation type (woody or herbaceous), and for all species combined. For each model 80% of the data was used for model calibration and 20% was withheld for validation. Data splitting was accomplished using the spectratrait function "create_data_split" which randomly selects rows for either the calibration or validation datasets. When splitting, we grouped data by species and date for multiple-species models and by date for single-species models.

For component selection, we used the spectratrait function "find_optimal_components" and method "firstMin" which uses permutation to select the optimal number of model components as the first statistically significant minimum value

of predicted residual error sum of squares (Serbin et al. 2022). Additional component selection parameters were as follows: maximum number of components was set to 20, 80 data segments were used for leave-one-out cross-validation, 70% of data were preserved, and 50 iterations were conducted. The optimal number of components calculated using these methods was then used for model creation and training.

Models were created with the pls package function "plsr" using only the calibration dataset as well as leave-one-out validation. The models were then tested using the withheld validation dataset. Variable importance projections (VIPs) were calculated using the spectratrait function "VIP". VIP values were used to identify wavelengths of importance for predicting LFM. Model uncertainty was estimated via jack-knifing using the pls package "jackknife" function. Root mean square error of prediction (RMSEP) and the coefficient of determination (R^2) were used to evaluate model performance.

Vegetation index modeling

In R, VIs suggested in reviewed literature for use in LFM estimation (or plant stress in the case of the Normalized Difference Red-edge Index, NDRE (Gitelson and Merzlyak 1994)) were calculated according to the following equations:

$$MSI = \frac{R_{1600}}{R_{820}} \text{ (Hunt and Rock 1989)}$$

$$NDII = \frac{R_{820} - R_{1650}}{R_{820} + R_{1650}} \text{ (Hardisky et al. 1983)}$$

$$NDRE = \frac{R_{750} - R_{705}}{R_{750} + R_{705}} \text{ (Gitelson and Merzlyak 1994)}$$

$$NDVI = \frac{R_{NIR} - R_{red}}{R_{NIR} + R_{red}} \text{ (Rouse et al. 1974)}$$

$$NDWI = \frac{R_{860} - R_{1240}}{R_{860} + R_{1240}} \text{ (Gao 1996)}$$

$$VIgreen = \frac{R_{green} - R_{red}}{R_{green} + R_{red}} \text{ (Gitelson et al. 2002)}$$

$$WI = \frac{R_{900}}{R_{970}} \text{ (Peñuelas et al. 1997)}$$

Where R_X is reflectance, R, at wavelength, X nm. *Green, red,* and *NIR* are calculated from averages across corresponding regions (*green*= 500−600 nm, *red*=600−700 nm, *NIR*=780−1400 nm). VI models were created and evaluated using the R packages "nlme", "bbmle", and "modelsummary" (Arel-Bundock 2022, Bolker et al. 2022, Pinheiro et al. 2023). We created linear mixed effects models including species, VI, and individual as a random effect using the nlme package. We included individual as a random effect because we resampled the same individuals over time. Model performance was then evaluated and compared using Akaike information criterion (AIC), R^2, t-value (estimate ÷ standard error), and p-value.

RESULTS

Leaf water potential (Ψ)

The relationship between plant water status/content and plant Ψ, is generally nonlinear, and has traditionally been displayed using pressure-volume curves often using relative water content (Turner 1988). Relative water content is similar to LFM but is calculated relative to full turgor weight (Turner 1988). We found the relationship between Ψ and LFM was generally nonlinear, resembling the relationship between Ψ and relative water content (Figs. 2.2 & 2.3). Absolute Ψ (|Ψ|) was moderately, nonlinearly, negatively correlated to LFM in all herbaceous/grasses and *J. virginiana*/ER (avg.

adjusted R^2= 0.51, Fig. 2.2 & 2.3). |Ψ| was strongly, linearly, negatively correlated to *Q. stellata* (PO) LFM (R^2= 0.63, Fig. 2.3). A cluster of moderate LFM collections with low |Ψ|, had great influence on the polynomial model for *P. echinata* (SP) (Fig. 2.3). As a result, the line of best fit poorly represents the suspected decay-like relationship and likely decreased the coefficient of correlation (adjusted R^2= 0.38). Ultimately, our polynomial linear mixed effects model

$$lme\ (LFM \sim species\ +\ |\Psi|\ +\ |\Psi|^2, random = \sim 1|Individual)$$

was able to predict observed LFM (adjusted R^2= 0.69, Fig. 2.4) and Ψ had greater t-values than all other predictors except the intercept (Table 2.3).

PLSR models

When all species, woody and herbaceous, were combined, the PLSR model was able to predict withheld LFM from the validation dataset with accuracy (R^2= 0.81, RMSEP= 30.96%, Fig. 2.5). The greatest VIPs were in the shortwave infrared regions of 1865−1890 nm and 1395−1410 nm and the red-edge region of 700−705nm (Fig. 2.5). The herbaceous/grass PLSR model was also able to predict LFM from the validation dataset (R^2= 0.80, RMSEP= 37.69%). In this model, the greatest VIPs were in the red-edge regions of 675−685 nm and 700−705 nm, and shortwave infrared region of 1875−1880 nm. When all trees were combined, PLSR model predictions were strongly correlated to observations with low error (R^2= 0.88, RMSEP= 18.18%) and the wavelengths of greatest VIP were shortwave infrared, around 1390−1415 nm and 1875−1880 nm. In each of these models, model predictions were best below ~200% LFM (Figs. 2.5, S2.1). For observed vs predicted and VIP plots for the herbaceous and woody models see supplemental figures (S2.1, S2.2).

The results for all models, including single-species models, are summarized in Table 2.4 and single-species model VIP plots are shown in Fig. 2.6. In deciduous and herbaceous species (grasses and *Q. stellata*/PO) the VIP plots are similar with three peaks at ~680−710 nm (red-edge), ~1400 nm, and ~1880 nm. In most these species, except *P. virgatum* (SG), there is a fourth peak at ~2000 nm (shortwave infrared). *J. virginiana* (ER) is missing the red-edge (~680−710 nm) peak present in all other species but retains the ~1400 nm, ~1880 nm, and ~2000 nm peaks. *P. echinata* (SP) has a similar, overall structure to other species, but all peaks except for ~680−710 nm are reduced and the ~2000 nm peak is absent. The number of components selected for single-species models varied greatly, the lowest being six (*J. virginiana,* ER) and greatest was 16 (*Q. stellata*, PO). RMSEP also significantly varied with the lowest being 6.34% (*Q. stellata*, PO) and highest being 53.12% (*A. gerardii*, BB). R^2 values varied to a lesser extent with all models having significant coefficients (lowest 0.73 in *A. gerardii*, BB and highest 0.97 in *Q. stellata*, PO). The greatest RMSEP values were found in *A. gerardii*, *P. virgatum,* and *S. scoparium* (BB, SG, and LB); these species also had the widest ranges of recorded LFM values (Fig. S2.3). When comparing RMSEP to standard deviation of LFM, by which RMSEP could be standardized, we see good agreement (Table 2.4).

Ultimately, when all species were combined, the PLSR model preformed similarly to the functional group and single-species models. The all-species model accuracy (R^2=0.81 and RMSEP=30.96%) is comparable to the herbaceous functional group model (R^2=0.8 and RMSEP=37.69%) and the average single species model (R^2=0.85 and RMSEP=25.66%). The woody species model was generally more accurate than the others (R^2=0.88 and RMSEP=18.18), potentially due to differences in standard

deviation (Table 2.4). When comparing the VIP plots of herbaceous grasses, the relationship between reflectance and LFM is generally consistent with peaks at ~700 nm, ~1400 nm, and ~1800 nm (Fig. 2.6). In fact, the relationship is moderately conserved between all species, except *J. virginiana* (ER), in which the red-edge region (~700 nm) was unimportant.

Vegetation index models

The relationship between VI and LFM was generally nonlinear (ex. Fig. S2.4). So, we created two linear mixed effects models for each VI with the following structure:

$$lme\ (LFM \sim species\ +\ VI, random = \sim 1|Individual)$$

$$lme\ (LFM \sim species\ +\ VI\ +\ VI^2, random = \sim 1|Individual)$$

The nonlinear relationship exhibited by our data is consistent with other studies of VIs (Bowyer and Danson 2004, Roberts et al. 2006) and is consistent with our Ψ results. After identifying the red-edge region as a region of importance for almost all our species of interest (Fig. 2.6), we created the LFM red-edge index (LFMREI):

$$LFMREI = \frac{mean(R_{710}{:}\,R_{730}) - mean(R_{670}{:}\,R_{690})}{mean(R_{710}{:}\,R_{730}) + mean(R_{670}{:}\,R_{690})}\ or\ LFMREI = \frac{\sim R_{720} - \sim R_{680}}{\sim R_{720} - \sim R_{680}}$$

We then evaluated performance of LFMREI and other VIs proposed for the estimation of LFM, as well as NDRE, a popular red-edge index comparable to LFMREI. We decided on LFMREI, using the red-edge region, for applications beyond leaf-level spectroscopy.

The AIC model comparison results are shown in Tables S2.1-S2.3. AIC supported the use of WI, linearly or nonlinearly, over all other VIs when all species were combined and for woody species. The curvilinear WI model followed by the curvilinear VIgreen model were the top selected models by AIC for herbaceous species. Following VIgreen

was LFMREI in herbaceous species and following WI was NDWI in woody species. NDVI was ranked lower than six other VIs for herbaceous species and eight others for the full-species and woody datasets. LFMREI was less supported than WI, VIgreen, and NDWI for all species, and was less supported than all other VIs except NDVI for woody species. The model summary for the top model:

$$lme\ (LFM \sim species\ +\ WI\ +\ WI^2, random = \sim 1|Individual)$$

is shown in Table 2.5. Most of the variation in LFM is explained by species (largest effects, t-values) and, as a result, the t-value of WI is non-significant ($p > 0.05$). At the functional group level WI becomes significant, and AIC increases (Table 2.6).

DISCUSSION

LFM was related to, and able to be predicted from, Ψ and leaf-level reflectance. These results support our hypotheses that LFM is related to true plant water status (measured as Ψ) and that variations in plant water status alter leaf-level reflectance. Our findings support the use of leaf-level hyperspectral reflectance to predict LFM using PLSR models or for the calculation of vegetation indices.

Our PLSR models were able to estimate withheld LFM values in all individual species, functional groups, and for all species combined. In different ecoregions the critical threshold for fire activity, in relation to LFM, varies and may be as low as 67% or as great as 167% (Arganaraz et al. 2016, Nolan et al. 2016). Therefore, accurate estimation at and around these values is important for fire danger applications. At approximately 50% LFM vegetation transitions from live fuel to dead/dormant fuel (National Wildfire Coordinating 2021). Model performance was generally best between

50−200% LFM (Figs. 2.5 and S2.1). Which implies model performance is greatest when LFM estimates, as related to fire danger, are most important.

Our PLSR model results do not support our hypothesis that the relationship between leaf-level reflectance and LFM would differ among species. The all-species PLSR model's performance was comparable to the single-species and functional group models; and the VIP plots indicate that regions of greatest important were fairly conserved across vegetation types and species (apart from *J. virginiana*). These results are promising for up-scaling estimation of LFM, by implying there may not be a need to distinguish between species or plant community. These findings support the Mesonet's current practice of estimating LFM as woody or herbaceous, without finer-level distinction (Carlson et al. 2002, Carlson 2022, Mesonet 2022).

Similarly, the initial results of our AIC model comparison of VIs support the use of WI regardless of functional group. However, upon further analysis VIgreen may be better for LFM estimation in herbaceous species. When model summary statistics are compared, VIgreen had greater t-values and significance, and when comparing model predictions versus observations, VIgreen estimates were more closely related to actual values (Table 2.7, Fig. S2.5). That said, our VI analysis results support the distinction between herbaceous and woody vegetation when approximating LFM that is currently used by the Mesonet.

It was surprising that WI was the most supported VI in this study when considering the PLSR model VIPs (Fig. 2.6). WI calculated as the ratio of reflectance at 900 nm over 970 nm, a region of the electromagnetic spectrum of little comparative

importance in our VIPs. Given the complexity of the PLSR models, it is difficult to compare these results to the simple linear VI models used. This difference may account for the failure of our index, LFMREI, for predicting LFM despite being created from regions of identified importance. Ultimately, LFMREI, our created index, was not the most predictive VI. However, LFMREI was more supported by AIC than NDVI for all-species and in each functional group (Tables S2.1−S2.3). LFMREI performed better than most indices (NDWI, NDRE, NDVI, NDII, and MSI) for the estimation of herbaceous LFM, but was a poorer estimate of woody species LFM than most VIs. For all species, LFMREI performance was comparable to most VIs. Our results supporting the use of WI, VIgreen, and NDWI are consistent with other studies that found WI, NDWI, and VIgreen/VARI to be useful estimates of LFM/water content (Serrano et al. 2000, Dennison et al. 2006, Roberts et al. 2006, Peterson et al. 2008, Schneider et al. 2008, Dudek 2020). In this study, because leaf-level reflectance was collected with a plant probe without atmospheric influence, and bands < 500 nm were not analyzed, VIgreen is virtually synonymous to VARI (Gitelson et al. 2002) which is typically calculated as:

$$\frac{R_{green} - R_{red}}{R_{green} + R_{red} - R_{blue}}$$

Recurring important regions of the electromagnetic spectrum associated with LFM were the red-edge region of the spectrum at ~680−750 nm (Horler et al. 1983), the boundary between the near-infrared (NIR) and shortwave infrared (SWIR) regions at ~1390−1420 nm, and the SWIR regions of ~1880 and ~2000 nm. The relationship between SWIR (1400−2500 nm) and plant water content is well known; these wavelengths are strongly absorbed by water (Horvath 1993, Jones and Vaughan 2010).

However, regions strongly absorbed by water, like these, are not useful for satellite remote sensing due to high absorption by water within the atmosphere resulting in low transmittance (Horvath 1993). In this study, the known water absorption peaks of the NIR and SWIR regions at 975 nm, 1175 nm, 1450 nm, and 1950 nm were not among the recurring VIP regions (Roberto et al. 2012). Rather, it seems that the greatest VIPs occurred in transitory zones: the red-edge and the transitions between the less absorptive wavelengths ~1350 nm and ~1850 nm and the highly absorptive wavelengths around 1400 nm and 1900 nm (Nagler et al. 2012). The red-edge is the transition from visible wavelengths (~400−700 nm) to NIR wavelengths (~700−1400 nm). This region is related to leaf chlorophyll content and plant health (Horler et al. 1983, Slonecker 2012). The importance of the red-edge in this study may be promising for future extrapolation to satellite imaging because the ~1400 nm and ~1880 nm regions have been identified as being highly impacted by atmospheric absorption and therefore are impractical for applications beyond leaf-level sensing (Thenkabail et al. 2004). A limitation of this study is that hyperspectral leaf-level reflectance does not account for the complexities of satellite sensing— most especially the influence of canopy.

Our hypothesis that LFM is related to true plant water status, was supported by our analysis of Ψ and LFM. Midday |Ψ| was moderately (min. R^2=0.41) to strongly (max. R^2=0.68) correlated to all species LFM and our polynomial linear mixed effects model was able to predict LFM from species and |Ψ| (R^2=0.69, Fig. 2.4). The nonlinear relationship between Ψ and LFM is consistent with what is seen in pressure volume curves and was also observed by Nolan et al. (2018), Pivovaroff et al. (2019), and Nolan et al. (2020). It is interesting, then, that a curvilinear relationship was not observed in *Q*.

stellata (PO). This may be due, in part, to the small range in LFM values collected in this species and/or due to rooting depth constrictions due to pot size (Fig. S2.3). The relationship between Ψ and LFM was similar to that of VI and LFM with the exception of *Q. stellata* (PO) (Figs. 2.2, 2.3, and S2.4).

In conclusion, LFM is a reliable estimate of true plant water status and hyperspectral leaf-level reflectance can be used to accurately estimate LFM in a variety of plant species either with PLSR models or simpler VI models. We found that the relationships between LFM, Ψ, and leaf-level reflectance were relatively conserved among species, but that estimates may be improved by distinguishing between woody and herbaceous vegetation types. We identified the red-edge as an important region of the electromagnetic spectrum for the estimation of LFM that could be used in satellite estimation of LFM. We identified the Water Index (WI) as a good approximation of LFM in all species, especially woody. Though, VIgreen may be a better suited index for the estimation of herbaceous LFM. For Oklahoma, our findings suggest that the use of NDVI-derived relative greenness for estimating LFM may need to be revaluated. It is our hope that these insights can help improve estimation of LFM and can contribute to the protection and preservation of lives and natural resources.

TABLES AND FIGURES

Table 2.1 Most widespread plant communities in Oklahoma (Fig. 2.1) and the dominant species selected for use in this study per community. Species specific epithets, common names, and codes.

Plant community	**Species sampled**	**Common name**	**Code**
Tallgrass prairie	*Andropogon gerardii*	big bluestem	BB
	Schizachyrium scoparium	little bluestem	LB
Shortgrass prairie	*Bouteloua gracilis*	blue grama	BG
	S. scoparium	little bluestem	LB
Mixedgrass prairie	*B. gracilis*	blue grama	BG
	Juniperus virginiana	eastern redcedar	ER
	S. scoparium	little bluestem	LB
Cross Timbers	*J. virginiana*	eastern redcedar	ER
(Post oak-blackjack oak)	*Panicum virgatum*	switchgrass	SG
	Quercus stellata	post oak	PO
Oak-hickory-pine forest	*J. virginiana*	eastern redcedar	ER
(or oak-hickory and oak-pine)	*Pinus echinata*	shortleaf pine	SP
	Q. stellata	post oak	PO

Table 2.2 Number of individuals per experimental group in the greenhouse tree water stress experiment. Fewer individuals of *Q. stellata* (PO) survived transplant.

Species	**Severe**	**Moderate**	**Control**
J. virginiana (ER)	24	23	6
Q. stellata (PO)	14	14	5
P. echinata (SP)	20	20	7

Table 2.3 Model summary of LFM ~ Species + |Ψ| + |Ψ|², random=~1|Individual. All t-values are significant, $p < 0.05$. Root-mean-square-error (RMSE) is in units of LFM% and is less than one standard deviation (60.9%). For species codes see Table 2.1.

	Value	**Std. Error**	**DF**	**t-value**	**p-value**
Species BB (Intercept)	291.978	6.763	753	43.174	<0.0001
Species BG	-59.827	7.591	194	-7.882	<0.0001
Species ER	-43.769	7.219	194	-6.063	<0.0001
Species LB	-37.652	7.963	194	-4.728	<0.0001
Species PO	-68.789	7.745	194	-8.881	<0.0001
Species SG	-16.284	7.885	194	-2.065	0.040
Species SP	-21.819	7.390	194	-2.953	0.004
Ψ	-54.936	2.949	753	-18.628	<0.0001
Ψ²	4.293	0.348	753	12.325	<0.0001

AIC	**Log-likelihood**	**Adjusted R²**	**RMSE**	**# obs.**
9753.299	-4865.65	0.69	35.01927	956

Table 2.4 Model results for all PLSR models. # comp. is components used for modeling determined by component selection. The coefficient of determination (R^2) and root mean square error of prediction (RMSEP) are shown for model validation (val.) results. LFM standard deviation (SD) by species. Regions of the electromagnetic spectrum with the greatest VIP are given in the last column.

Model	**# comp.**	**R^2 (val.)**	**RMSEP (val.)**	**SD**	**Regions of greatest VIP (~nm)**
A. gerardii (BB)	7	0.73	53.12	99.75	1390−1405, 680−685
B. gracilis (BG)	11	0.81	23.12	48.06	1870−1895, 2005−2015
J. virginiana (ER)	6	0.83	18.97	43.64	1390−1415, 1880−1885
P. virgatum (SG)	15	0.86	33.19	91.71	700−725, 500−505
P. echinata (SP)	9	0.85	18.87	45.82	700−725, 1395−1405
Q. stellata (PO)	16	0.97	6.34	31.56	1885−1900, 1980−1995
S. scoparium (LB)	11	0.88	25.99	77.83	670−715, 1400−1405
Sp. model avg.[1]	~11	0.85	25.66	62.62	NA
Herbaceous/grass (BB, BG, LB, SG)	15	0.80	37.69	81.82	675−685, 700−705, 1875−1880
Woody/tree (ER, PO, SP)	13	0.88	18.18	50.82	1390−1415, 1875−1880
All species	18	0.81	30.96	NA	1865−1890, 1395−1410, 700−705

[1] The single-species model averages are calculated from model validation statistics.

Table 2.5 Model summary for all-species (herbaceous and woody) AIC top-rated model LFM ~ Species + WI + WI^2 with individual as a random effect. For species codes see Table 2.1.

	Value	**Std. Error**	**DF**	**t-value**	**p-value**
Species ER (Intercept)	-2182.44	1157.312	1844	-1.88578	0.0595
Species PO	46.9366	5.5836	236	8.406225	<0.0001
Species SP	22.7212	4.7622	236	4.771124	<0.0001
Species LB	112.0815	5.7691	236	19.42785	<0.0001
Species BG	89.2045	5.5889	236	15.96088	<0.0001
Species SG	126.398	5.6034	236	22.55732	<0.0001
Species BB	137.0451	5.6537	236	24.23992	<0.0001
WI	1821.98	2273.68	1844	0.801335	0.423
WI^2	349.3395	1116.177	1844	0.312978	0.7543
AIC		**# obs.**		**RMSE**	
21692.65		2089		40.363 %	

Table 2.6 Model results for a) herbaceous and b) woody species AIC top-rated models. In each, individual was included as a random effect. For species codes see Table 2.1.

a) herbaceous LFM ~ Species + WI + WI^2		
	t-value	**p-value**
Intercept (Species LB)	8.371133	<0.0001
Species BG	-3.70567	0.0003
Species SG	1.238945	0.218
Species BB	2.80091	0.006
WI	-8.88541	<0.0001
WI^2	9.436834	<0.0001
AIC	**# obs.**	**RMSE**
10545.77	975	50.73 %
b) woody LFM ~ Species + WI + WI^2		
	t-value	**p-value**
Intercept (Species ER)	-11.5985	<0.0001
Species PO	8.275119	<0.0001
Species SP	7.575723	<0.0001
WI	10.97512	<0.0001
WI^2	-10.2868	<0.0001
AIC	**# obs.**	**RMSE**
10264.34	1114	21.14 %

Table 2.7 Model summary comparison for herbaceous species LFM modeled using WI or VIgreen (each with individual as a random effect). For species codes see Table 2.1.

	LFM ~ Species + WI + WI^2		LFM ~ Species + VIgreen+$VIgreen^2$	
	t-value	**p-value**	**t-value**	**p-value**
Species BB (Intercept)	8.38059	<0.0001	17.2622	<0.0001
Species BG	-6.6166	<0.0001	-4.9671	<0.0001
Species LB	-2.8009	0.006	-4.2385	<0.0001
Species SG	-1.6046	0.1115	-2.2123	0.029
VI	-8.8854	<0.0001	16.5445	<0.0001
VI^2	9.43683	<0.0001	8.85937	<0.0001
AIC	10545.8		10566.6	
RMSE	50.730 %		51.217 %	

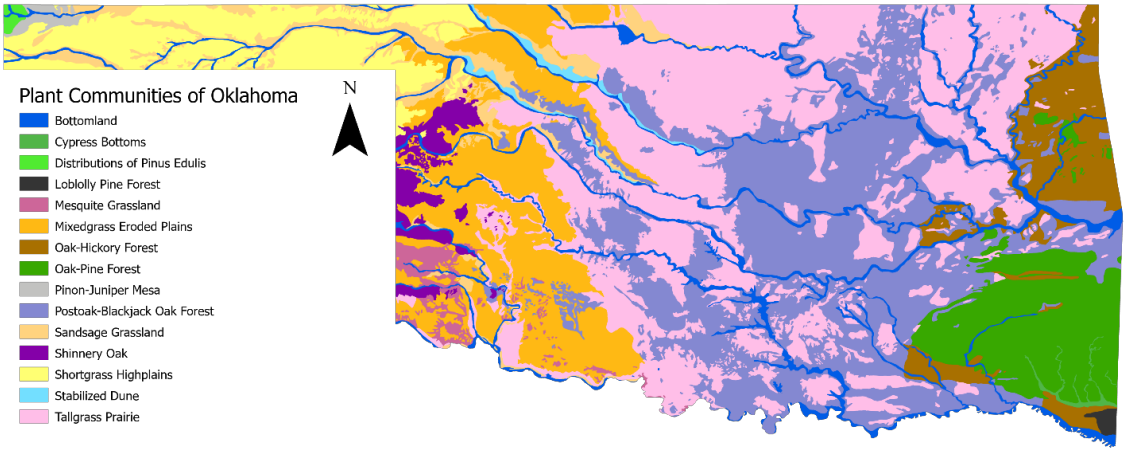

Figure 2.1 Vegetation of Oklahoma by Duck and Fletcher (1943) digitized by the Oklahoma Biological Survey/Hoagland and Johnson (1996).

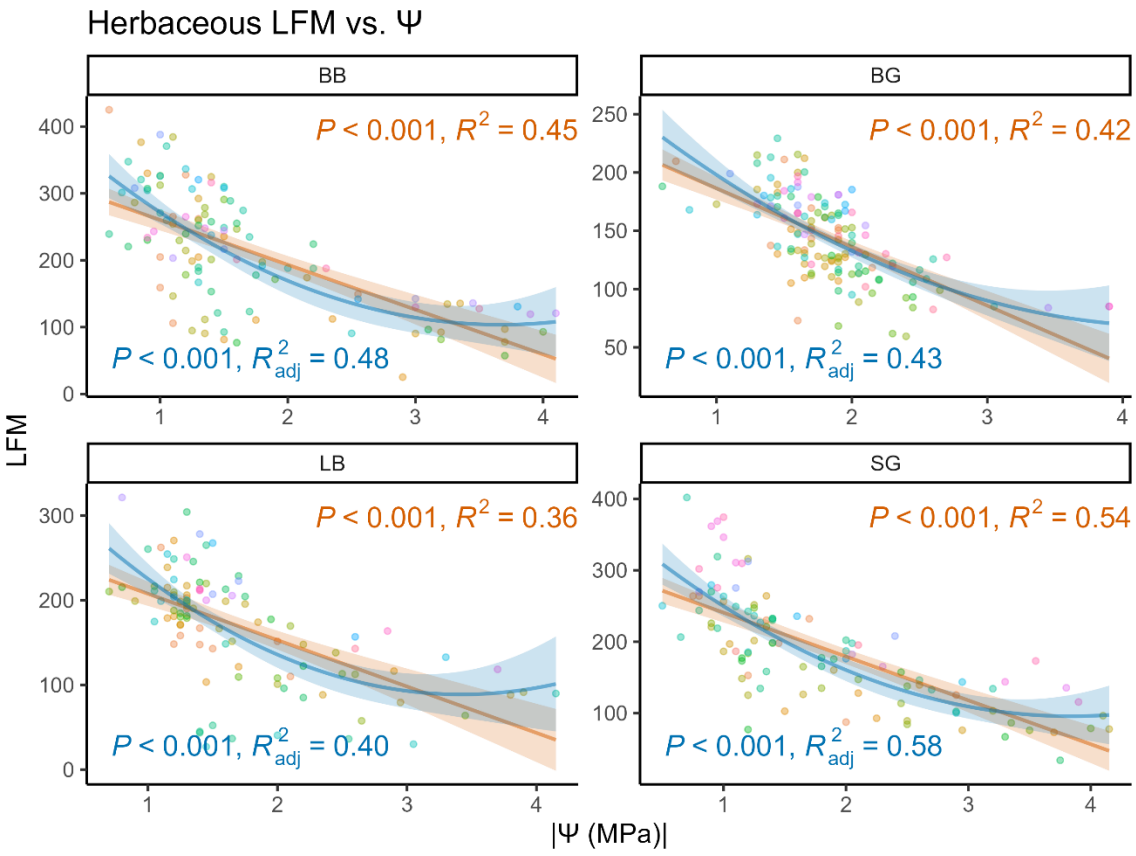

Figure 2.2 Plots of Ψ vs LFM in grasses. The second order polynomial model (blue) fits all species moderately well with an average adjusted R^2=0.47. Orange (line and text) represents the linear model. For species codes see Table 2.1. Different colors represent different individuals.

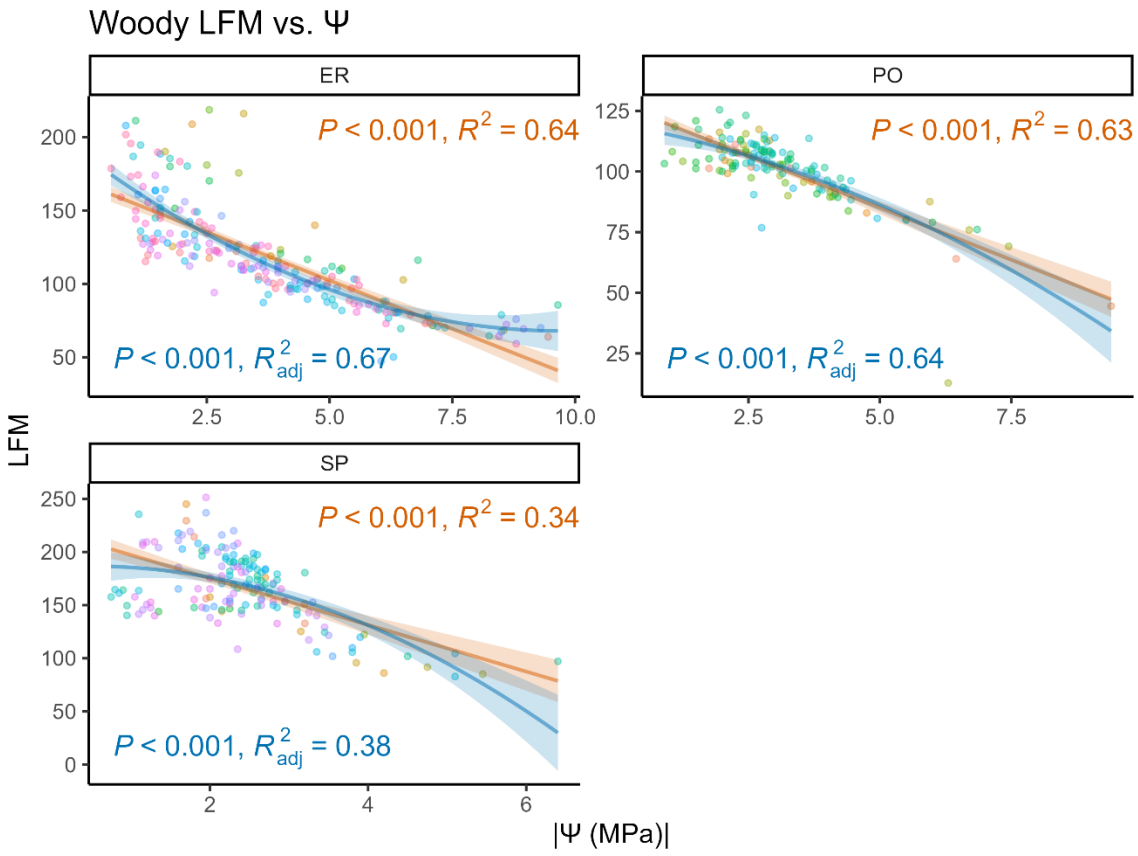

Figure 2.3 Plots of Ψ vs LFM for woody trees. The linear model (orange) fits PO well (R^2=0.63), fits ER moderately, and poorly fits SP. The second order polynomial model (blue) fits ER well (adjusted R^2=0.67) but not PO. In SP, the second order polynomial model (blue) is influenced by a cluster of moderate LFM values with low Ψ. For species codes see Table 2.1.

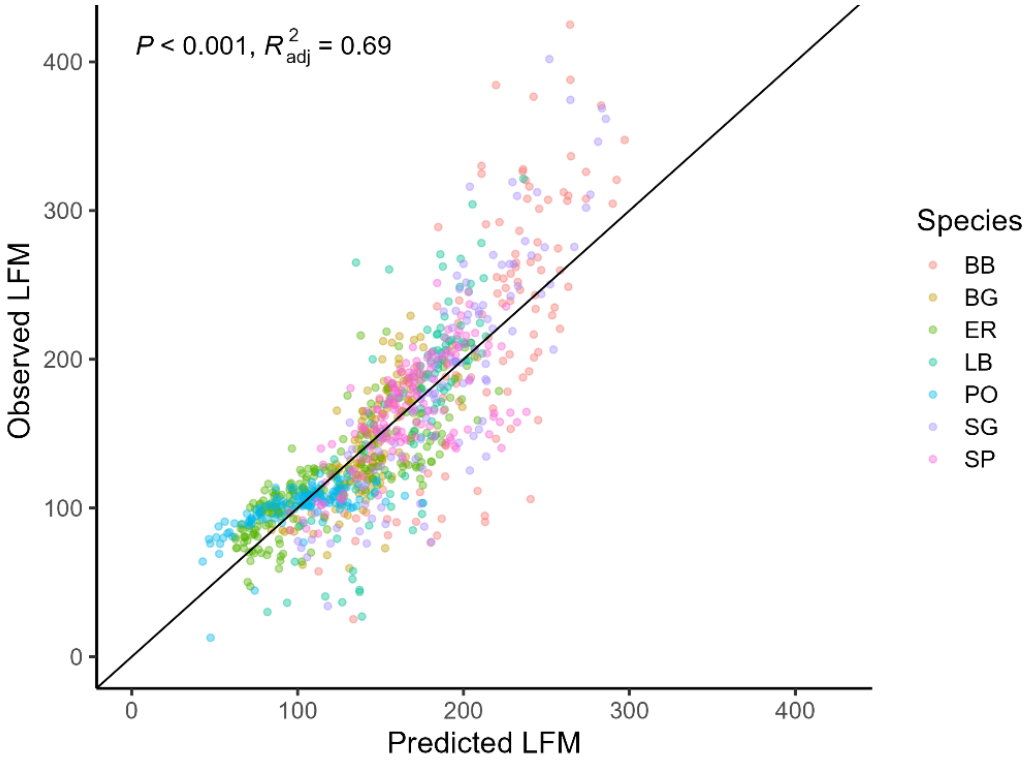

Figure 2.4 Model predictions vs observed LFM values for the LFM ~ Species + |Ψ| + |Ψ|² model with individual as a random effect. Model predictions tend to have increased error for tallgrasses (BB and SG) and/or LFM > 200%. For species codes see Table 2.1.

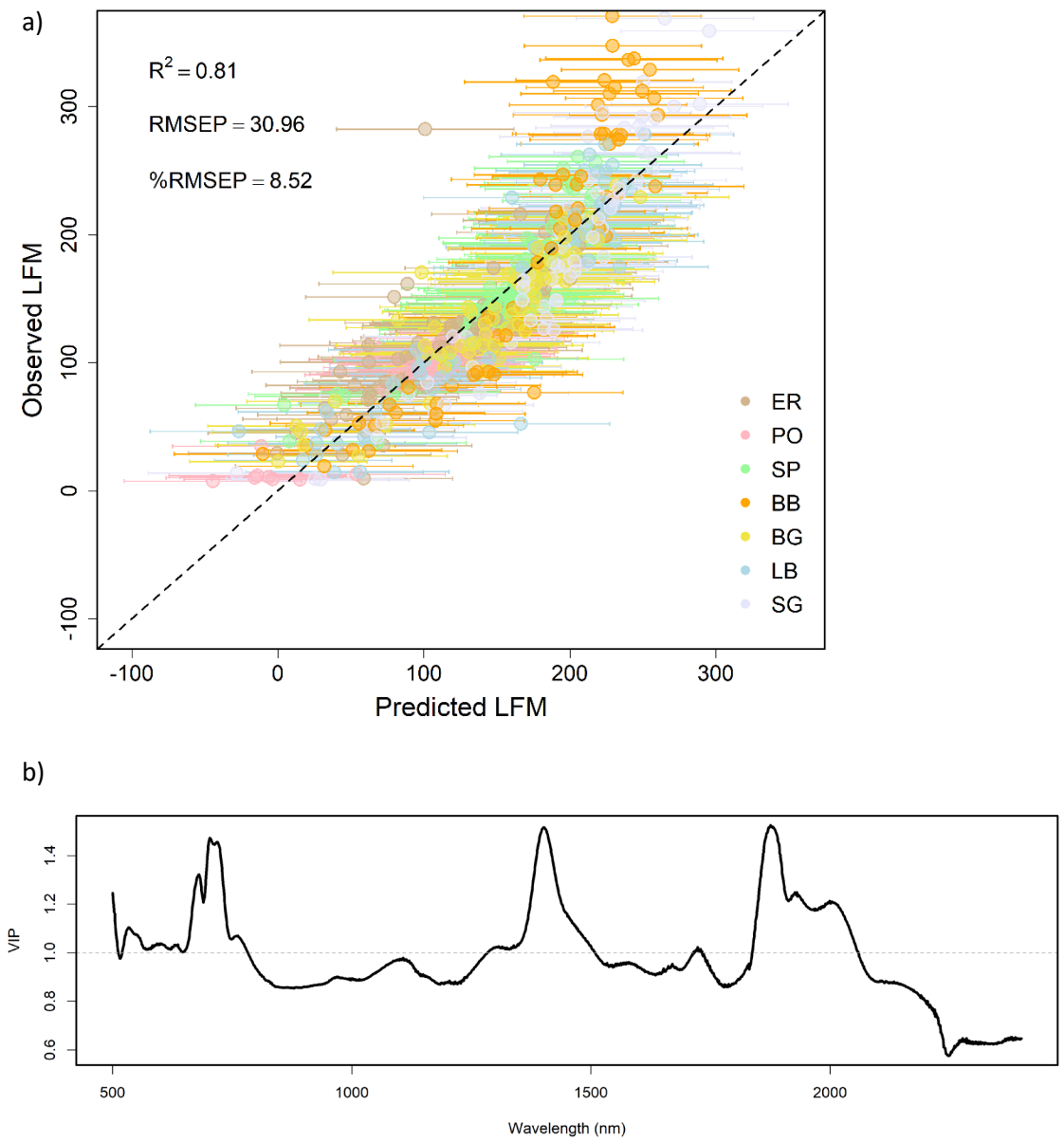

Figure 2.5 a) All-species PLSR model predicted LFM vs. observed LFM. The black, dashed line is the 1:1 line. Error bars represent the 95% uncertainty estimates from jackknifing. %RMSEP is RMSEP standardized by the range of LFM values. For species codes see Table 2.1. b) Variable importance projections (VIP) for the all-species PLSR model. Higher values are of greater importance to the model. Values greater than 1 are generally considered valuable.

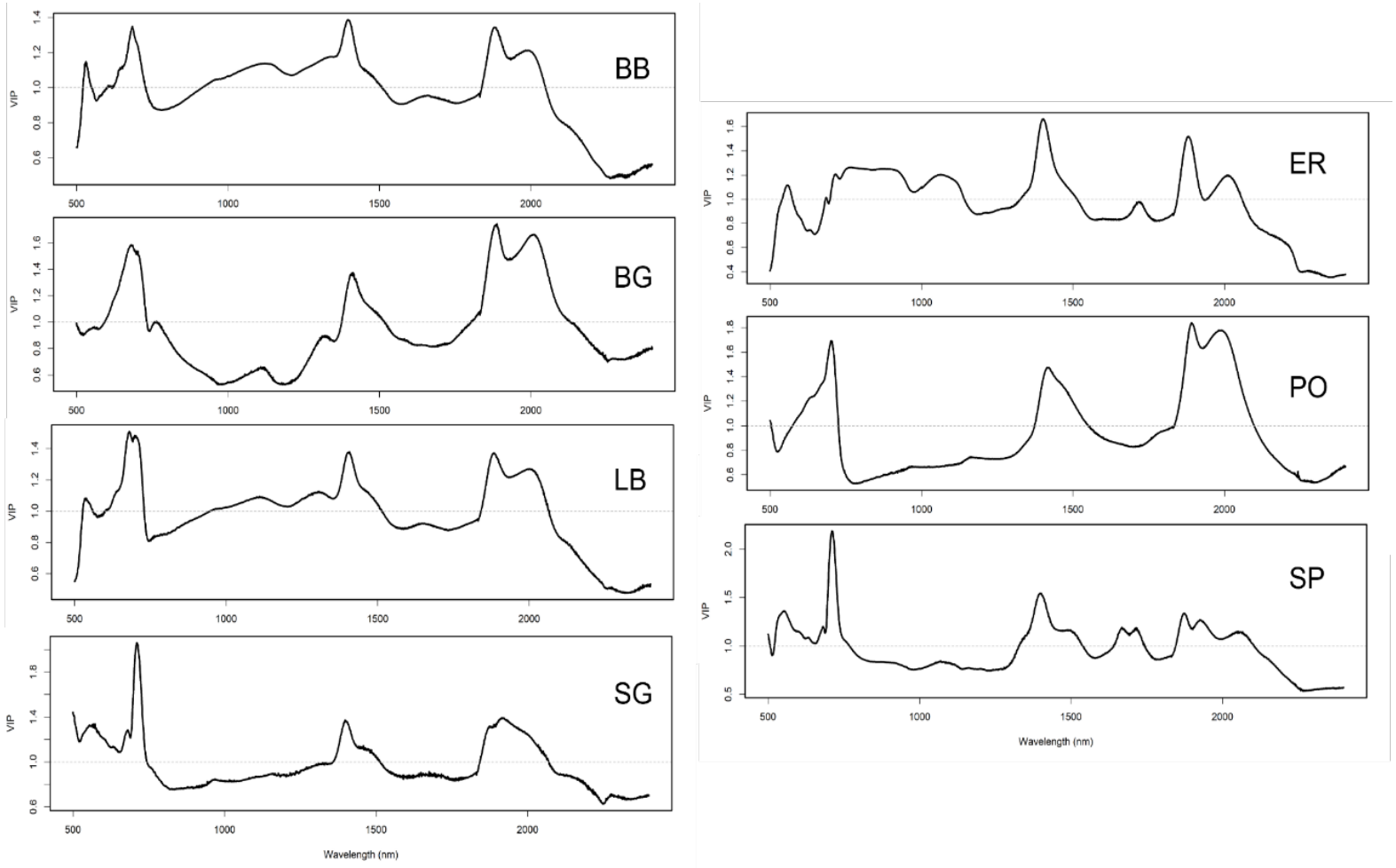

Figure 2.6 Variable importance projections (VIP) for single-species PLSR models. Higher values are of greater importance to the model. Values greater than 1 are generally considered valuable. See Table 2.1 for species codes.

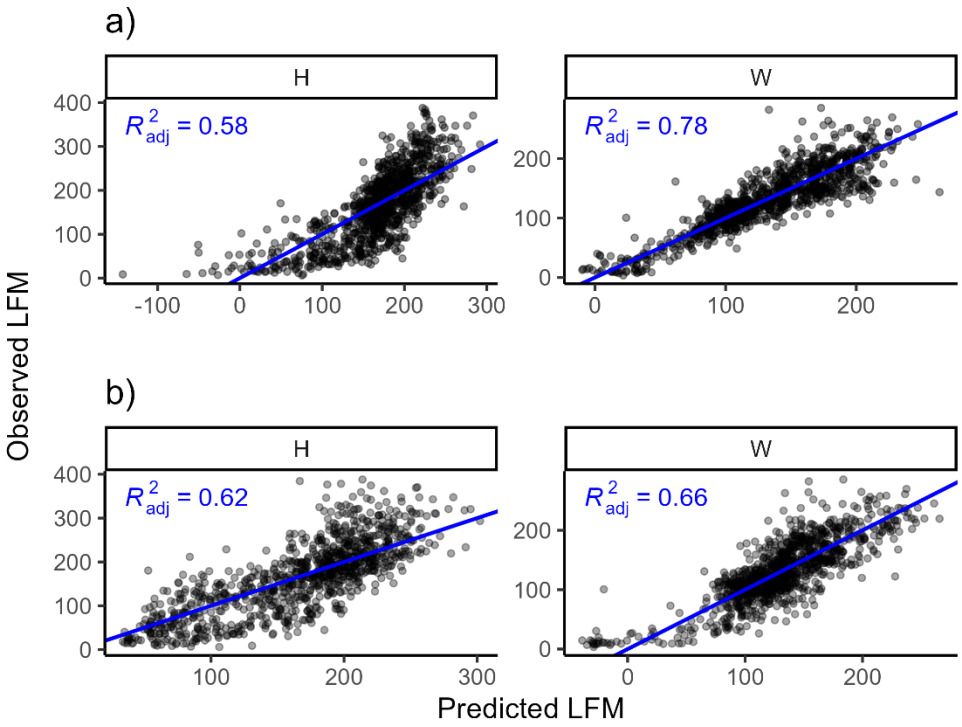

Figure 2.7 Model predicted vs observed LFM for herbaceous (H) and woody (W) species. Model from species and a) WI+WI² b) VIgreen+VIgreen² (each with individual as a random effect).

CHAPTER III

USING MESOSCALE METEROLOGICAL AND SOIL MOISTURE DATA TO ESTIMATE LIVE FUEL MOISTURE CONTENT

INTRODUCTION

In the south-central/Southern Great Plains region of the United States climate change will likely intensify droughts (Cook et al. 2015, Gensini et al. 2023) and heatwaves (Meehl and Tebaldi 2004, Kloesel et al. 2018) producing more frequent wildfire conditions. An et al.'s (2015) wildfire risk simulation predicts that within the contiguous USA, the south-central region will be most at-risk. Under future drought conditions in the Southern Great Plains, Scasta et al. (2016) predict increases in area burned, fire season length, and severe fire probability. Similarly, when compared to the previous decade, Donovan et al. (2017b, a) reported significant increases in the number of large wildfires, acres burned, and wildfire likelihood throughout the Southern Great Plains and found fire seasons may be changing (seasonality or length). If these trends continue, reliable fire danger rating systems will be imperative for public safety, preparedness, and preservation.

In a review of users' needs for operational fire danger rating systems Carlson and Burgan (2003) identified the following important features: forecasting capabilities, mesoscale estimates, timely updates, and accessibility. Fortunately, Oklahoma maintains a robust fire danger rating system, OK-Fire, an application of the Oklahoma Mesonet. OK-Fire provides fire weather forecasts, smoke dispersion modeling, a fire prescription planner, and Oklahoma Fire Danger Model estimates (Mesonet 2022). The Oklahoma Fire Danger Model is adapted from the National Fire Danger Rating System and uses mesoscale data from the network of Mesonet weather towers (Carlson et al. 2002). Fire weather conditions are publicly accessible and updated every fifteen minutes (Mesonet 2022). However, OK-Fire estimates of live fuel moisture content have not been validated in-situ and when OK-Fire was released there were hopes to improve live fuel moisture estimation (Carlson et al. 2002).

Live fuel moisture content (LFM) is the proportion of water in living, nondormant vegetation. In wildfires, live vegetation with high LFM acts as a heat sink. Elevated LFM increases time to ignition, slows rates of spread, and reduces fire intensity (Pyne et al. 1996, Nelson Jr 2001, Ceccato et al. 2003). Water content and status vary between species; and are related plant morphological and physiological diversity and adaptations to water stress. For example, plants with deeper roots and/or stomatal control are better able to withstand and recover from drought (Pinheiro et al. 2005). Other than plant physiological and morphological differences, atmospheric moisture demand and soil moisture are the main influences affecting plant water status (Brady and Weil 2002, Taiz et al. 2015). The movement of water from the soil, through plants, and into the atmosphere is called the soil-plant-atmosphere continuum or SPAC (Brady and Weil

2002, Taiz et al. 2015). Climate change has already altered, and is expected to continue to alter, demands on the SPAC, by increasing atmospheric moisture demand and decreasing available soil moisture (Jung et al. 2010, Field et al. 2014, Novick et al. 2016).

Despite its known role in fire behavior, the best approach for LFM estimation is not agreed upon. This is due, in part, to LFM variation between vegetation types (functional groups, forms, and species) and locations. Several studies have shown variations in moisture content among co-occurring species (Sobrado 1986, Pellizzaro et al. 2007b, Pivovaroff et al. 2019, Costa-Saura et al. 2021, Brown et al. 2022) and intraspecies variation between locations (Smith et al. 1995, Touchette 2006, Wright et al. 2015). Furthermore, LFM data are relatively limited. In fact, the National Fuel Moisture Database contains no records for the state of Oklahoma (National Fuel Moisture Database 2022). Data are likely restricted because in-situ LFM collection is time and resource intensive. For this reason, LFM is often approximated from remote sensing or meteorological proxies.

Several remote sensing vegetation indices (VIs) or satellite bands have been proposed for the estimation of LFM/plant water status. Roberto et al. (2012) contains a list of VIs for estimating plant water status and Yebra et al. (2013) reviewed the use of remote sensing for LFM estimation. OK-Fire estimates LFM from satellite imagery as relative greenness calculated from the Normalized Difference Vegetation Index (NDVI, Rouse et al. (1974)) (Mesonet 2022). NDVI was, at one point, the most used VI in the estimation of LFM (Ceccato et al. 2003). Yet, in many studies NDVI has been shown to be a poor or inferior indicator of plant water content (Serrano et al. 2000, Baloun 2006, Dennison et al. 2006, Roberts et al. 2006, Hao and Qu 2007, Dennison et al. 2008,

Peterson et al. 2008, Schneider et al. 2008, Dennison and Moritz 2009, Caccamo et al. 2012, Qi et al. 2012, Jia et al. 2018, Myoung et al. 2018, Costa-Saura et al. 2021).

Benefits of approximating LFM from meteorological data, as opposed to remote sensing, include forecasting capabilities, increased temporal resolution, and collection regardless of atmospheric conditions like cloud cover. Two popular examples of LFM estimation from meteorological indices are The US National Fire Danger Rating System (NFDRS) and The Canadian Forest Fire Danger Rating System (CFFDRS). NFDRS has included an approximation of LFM in each of its four iterations, but currently uses the Growing Season Index to estimate LFM from photoperiod, vapor pressure deficit, and minimum temperature (Jolly et al. 2005, Jolly 2018). CFFDRS, which is also used in other countries, estimates LFM from location and day-of-year (Van Wagner 1987, Van Nest and Alexander 1999). But external studies have shown that LFM can be predicted from the CFFDRS's Buildup Index and Drought Code; which are calculated using temperature, rainfall, humidity (used in the Buildup Index only), and day-length (i.e., photoperiod) (Viegas et al. 2001, Castro et al. 2003, Pellizzaro et al. 2007a, Ruffault et al. 2018).

Because plants can respond to water deficit by reducing transpirational water losses, changes in plant water content are not always immediate or linear. For this reason, LFM cannot be easily estimated from meteorological conditions alone, unlike dead fuels (Pyne et al. 1996). One approach to account for lagged LFM response to environment is to include compounding effects. For example, the Buildup Index is calculated using present day weather conditions and the previous days' Buildup Index (Van Wagner 1987, Van Nest and Alexander 1999). The Keetch-Byram Drought Index (KBDI, (Keetch and

Byram 1968)), a soil moisture index commonly used in fire danger rating, also uses a cumulative factor; and KBDI has been linked to LFM (Dimitrakopoulos and Bemmerzouk 2003, Ganatsas et al. 2011, Ruffault et al. 2018).

There have been limited studies of LFM in Oklahoma. Dudek (2020) created a model for predicting *Juniperus virginiana* LFM from soil water potential and vapor pressure deficit (VPD). In tallgrass prairie, Sharma et al. (2018) included day-of-year, canopy height, and NDVI in their model for predicting LFM, but at the same location Sharma et al. (2021) found NDVI failed to detect rapid curing (declining LFM) when compared to fraction available water content (FAW). FAW is a soil moisture measurement that approximates site-normalized plant available water (Ochsner 2019). FAW may be a better measurement of plant water status than other soil moisture measures because it is soil-specific, and plant water relations have been found to vary between soil types (Smith et al. 1995). For growing season wildfires in Oklahoma, Kruger et al. (2015, 2016, 2017) found FAW was related to both wildfire size and large wildfire probability. They speculated that these relationships were the result of changing LFM.

The objectives of this study were to 1) assess the use of meteorological and soil moisture data for the estimation of LFM in Oklahoma plant communities, 2) validate the accuracy of the Oklahoma Mesonet's LFM predictions, 3) investigate LFM relations in Oklahoma's dominant plant species, and 4) improve predictions using our findings. We tested two hypotheses 1) through the soil-plant-atmosphere-continuum changes in atmospheric moisture demand and soil moisture are major drivers for changes in LFM and 2) variation in plant physiology and morphology produce variations in LFM and its

relation to environmental conditions. We predicted that LFM could be estimated from environmental proxies and that LFM, as well as its relationship to environment, would be species dependent.

METHODS

Sites and species

The five most widespread plant communities in Oklahoma from east to west are oak-hickory-pine forest (or oak-hickory and oak-pine forests), post-oak-blackjack-oak forest (i.e., Cross Timbers), tallgrass prairie, mixedgrass (eroded plains) prairie, and shortgrass (highplains) prairie (Duck and Fletcher 1943, Hoagland and Johnson 1996). We surveyed in each of these five plant communities in Osage, Texas, Washita, Cherokee, and Payne counties the field site locations are shown and described in Fig. 2.1. At each of our sites we collected 2−5 of the dominant species according to the vegetation type descriptions of Duck and Fletcher (1943) recounted by Tyrl et al. (2007). Species collected included herbaceous-perennial grasses (*Andropogon gerardii* Vitman, *Bouteloua gracilis* (Kunth) Lag. ex Griffiths, *Panicum virgatum* L., and *Schizachyrium scoparium* (Michx.) Nash), evergreen conifers (*Juniperus virginiana* L., *Pinus echinata* Mill.), and deciduous hardwoods (*Carya tomentosa* (Poir.) Nutt., *Quercus marilandica* Münchh., *Quercus stellata* Wangenh., and *Quercus velutina* Lam.). The plant communities these species are dominant in/representative of are in Table 3.1.

For each species, 20 random individuals were selected, marked, and georeferenced at each site. Individuals were then resampled over time. At three of our sites (oak-hickory-pine, mixedgrass prairie, and shortgrass prairie) some individuals were

randomly replaced after losses from fire. We began year-round collection of evergreen conifers *J. virginiana* in March 2021 and *P. echinata* in December 2021. Deciduous trees and grasses were collected during the growing season from green-up/leaf-flush (April/May) until senescence in fall (September). Collections concluded in September 2022. Collections by site are shown in Table S3.1.

Collection of LFM

The most hazardous fire weather conditions occur in the afternoon when temperatures are greatest and humidity lowest. To correspond with these conditions, collections began at or after 11:00 AM Central Time (U.S.). For each individual, leaves were collected from the same branch or section of the plant from mid-canopy for calculation of LFM. Once removed, samples were stored in sealed bags out of direct sunlight and wet/fresh mass was measured within 1−10 minutes of clipping. All weights were measured using the same scale (Ohaus® Scout™ SPX series portable electronic balance with 0.001-gram readability). After fresh mass was recorded, samples were dried in an oven at 60°C for at least 48 hours. At the start of the study, we confirmed that after 48 hours there were no significant changes in samples' masses. LFM was then calculated as:

$$LFM\ (\%) = \frac{fresh\ mass - dry\ mass}{dry\ mass} \times 100$$

Environmental data

Photoperiod was determined using site latitude and the function "daylength" from the package "geosphere" in RStudio (R) (Hijmans et al. 2022, RStudio Team 2022).

Photoperiod was included to represent day-length (hours of daylight) which influences photosynthetic activity as well as phenology and is related to season (Jackson 2009, Bauerle et al. 2012).

Meteorological and soil moisture data were retrieved from the Oklahoma Mesonet, a joint project between Oklahoma State University and the University of Oklahoma (Mesonet 2022). The Mesonet includes an automated network of 120 weather stations across the state, with at least one station per county (Mesonet 2022). These stations transmit data every five minutes and are available at www.mesonet.org (Mesonet 2022). Daily records directly downloaded were maximum temperature (°F), minimum temperature (°F), vapor pressure deficit (millibars), and rainfall amount (inches).

The Mesonet measures soil moisture at depths of 5, 25, and 60 cm as calibrated change in temperature (°C) after heat pulse (Mesonet 2022). Depths available vary from site to site. At our tallgrass prairie, shortgrass prairie, and Cross Timbers sites all three sensor depths were available. At our mixedgrass prairie site 5 and 25 cm depths were available. At our oak-hickory-pine forest site only a 5 cm depth was available. The delta-temperature data were used to calculate soil volumetric water content (θ) in MATLAB (2022) using code provided by the Oklahoma State University Soil Physics lab (Ochsner 2022). Soil volumetric water content is the ratio of volume water to volume soil. Soil volumetric water content was then used in combination with site soil properties (provided by Krueger 2022) to calculate FAW.

$$FAW = \frac{\theta_{current} - \theta_{wilting\ point}}{\theta_{field\ capacity} - \theta_{wilting\ point}}$$

Where $\theta_{current}$ is the daily average volumetric water content from the Mesonet at a given depth and $\theta_{wilting\ point}$ and $\theta_{field\ capacity}$ are volumetric water contents at permanent wilting point and field capacity for each site at that given depth.

Considering our study species consisted of deeply rooted trees and perennial grasses, it was unlikely that moisture at 5 cm would be representative of soil moisture across the rooting zone. Therefore, in addition to using FAW at 5 cm depth (the common available depth between sites) we also calculated depth-weighted averages of FAW (avg. FAW) across available soil moisture sensor depths.

When only 5 cm is available:

$$avg.\ FAW = 5\text{-}cm\ FAW$$

When 5 and 25 cm are available:

$$avg.\ FAW = 0.25(5\text{-}cm\ FAW) + 0.75(25\text{-}cm\ FAW)$$

When 5, 25, and 60 cm are available:

$$avg.\ FAW = 0.125(5\text{-}cm\ FAW) + 0.375(25\text{-}cm\ FAW) + 0.5(60\text{-}cm\ FAW)$$

The depth-weighted average equations were from Krueger et al. (2016) and/or Ochsner (2022). While using avg. FAW could reduce accuracy at the few sites like our oak-hickory-pine location, where only one, 5-cm sensor is available, it increases predictive power at all others. As of March 2023, the Mesonet reported that 120 sites had 5-cm sensors, 110 had 25-cm, and 85 had 60-cm (Melvin 2023). Given our objective of accurate LFM prediction across the state, we decided to include avg. FAW in this study.

As mentioned earlier, plant responses to water inputs or declines are lagged. Without model estimates from previous, we decided to use moving averages of meteorological and soil moisture variables at temporal scales of one week (7 days) and one month (30 days) in lieu of a cumulative effect like in the Buildup Index and KBDI. A cumulative effect could be considered in future applications.

Modeling

Modeling and model evaluation were accomplished using the R packages "bbmle" and "modelsummary" (Arel-Bundock 2022, Bolker et al. 2022). Photoperiod, meteorological, and soil moisture variables were centered and scaled before analysis and a variable correlation matrix was created. For each collection date per species, a species' mean LFM and upper and lower 95% confidence intervals (CI) were calculated. When selecting explanatory variables, we decided to use species or other functional groupings as opposed to site. Site was excluded to avoid covariation between site, species, and/or climate. By including species/functional group in our model we account for plant community, as the combination of species at a site, and variation between co-occurring species. Other studies of plant moisture content have found that within site variation was greater than between site variation (Scarff et al. 2021, Brown et al. 2022).

Variable selection was conducted using manual stepwise regression where models were evaluated and compared using Akaike information criterion (AIC), the coefficient of determination (R^2), t-value (estimate ÷ standard error), and p-value. Based on the results of the correlation matrix (Table 3.2), we selected the following variables for modeling: photoperiod, VPD, rainfall, and FAW. Photoperiod and temperature minimum

were highly correlated. Since photoperiod in this study accounts for season and is essential to plant phenology and physiology, temperature minimum (which is used in the Growing Season Index) was excluded (Jolly et al. 2005, Jolly 2018). VPD was strongly correlated to temperature maximum. In this study no variable other than VPD accounts for humidity, and VPD is also related to temperature. As such, VPD was selected instead of temperature maximum. Lastly, 5-cm FAW, which was correlated to avg. FAW, was only used to compare to avg. FAW and the two were never included in the same model. Of note, avg. FAW is near our |0.60| correlation threshold (-0.56) likely due to evapotranspiration influencing soil water balance and the intrinsic relationship between soil moisture and atmospheric moisture through the SPAC (Ochsner 2019). However, given our interest in plant ecophysiology, and the importance of both atmospheric and soil moisture to plant water status, we decided to retain both variables.

After our selection of the above environmental variables, we created models predicting LFM from species, photoperiod, and one of the selected environmental variables at a specific temporal scale (1-, 7-, or 30-day). We then compared these "univariate" (single environmental variable) models using AIC (Table 3.3). Our objectives were to select each environmental variable at the most explanatory temporal scale and to identify which of these variables are most predictive of LFM. The model using 1-day VPD was most supported by AIC, indicating that of the compared variables VPD on the date of collection was most related to LFM. When comparing avg. FAW to 5-cm FAW, avg. FAW was a better predictor of mean LFM. Lastly, rainfall and avg. FAW at the seven-day temporal scale were also selected for use in the global (full) model in this manner by AIC (Table 3.3). Using another correlation matrix, we found no

correlation greater than |0.6| between these variables (1-day VPD, 7-day avg. FAW, 7-day rainfall, and 1-day photoperiod). The global (full) model was then created as:

$$mean\ LFM \sim species/functional\ group + photoperiod + VPD + rainfall_7 + avg.FAW_7$$

Where either species or functional group were used and where *rainfall*$_7$ and *avg.* FAW_7 are seven-day moving averages. We tested the following functional groups: 1) woody or herbaceous 2) seasonal-vegetation type (grass, deciduous tree, evergreen tree), and 3) FxnGroup which was informed by growth form (woody or herbaceous), phenology (deciduous or evergreen), and LFM. Similar and dissimilar LFM between species was analyzed using ANOVA and Tukey tests and the R package "multcompView" (Fig. 2.2) (Graves et al. 2019). The FxnGroups created in this manner were as follows: shortgrass (*B. gracilis*/BG), mixedgrass (*S. scoparium*/LB), tallgrass (*A. gerardii*/BB and *P. virgatum*/SG), deciduous trees (*Quercus* species/PO/BJ/BO and *C. tomentosa*/MH), cedar (*J. virginiana*/ER), and pine (*P. echinata*/SP).

After model selection, we compared model predicted LFM to observed mean LFM. We then related each environmental variable to mean LFM per species per site. Lastly, we obtained archived LFM estimates for woody and herbaceous plants from the Oklahoma Mesonet which we compared to our observed values. Plots were created using the R packages "ggplot", "ggpmisc", and "gridExtra" (Auguie 2015, Wickham 2016, Aphalo 2022).

RESULTS

The global model (1) using FxnGroup as the categorical variable was selected by AIC over the same model using species (AIC 1168.2 vs 1170.4). When categorized at larger scales (grass, deciduous tree, evergreen) or vegetation type (woody or herbaceous) model performance declined (R^2 for both models was less than 0.24). The most influential variables (greatest t-values) in all models were species and/or functional group (ex. Table 3.5). In the global (full) model (1) containing VPD, avg. FAW, and rainfall, the t-value of VPD was small (t-value=0.215, estimate=0.76, standard error=3.538) and the p-value was non-significance (0.83). This is despite the global (full) model (1) being selected by AIC and VPD being the most explanatory standalone environmental variable (Tables 3.3 & 3.4). When excluding seven-day avg. FAW, the absolute t-value of VPD increases from |0.215| to |-2.036| (estimate=-6.361, standard error=3.125) and VPD becomes statistically significant (p= 0.044). This is likely due to overlap in explanation by VPD and avg. FAW, as a result of their correlation mentioned earlier. These results indicate that VPD and avg. FAW should not be included in the same model due to correlation. Therefore, despite having a lower AIC, the best supported model is model 2 which excludes avg. FAW ($mean\ LFM \sim FxnGroup + photoperiod + VPD + rainfall_7$) and was able to predict observed LFM (R^2= 0.51, Fig. 2.3).

The relationship between environmental variables and LFM varied within and between species. The most correlated variables per species per site are summarized in Table 3.6. From this analysis, VPD, seven-day avg. FAW, and photoperiod are the most strongly related variables to LFM. Seven-day rainfall exhibited the weakest relationships with LFM in herbaceous (avg. R^2=0.18) and woody (avg. R^2= 0.17) species and was only

significantly (p= 0.03) related to *Q. stellata* LFM in the Cross Timbers (Figs S2.3 & S2.4). Photoperiod was uncorrelated to LFM in mixed and shortgrass prairies but was strongly correlated to tallgrasses and tallgrass prairie LFM (avg. R^2=0.67, Fig. 2.4). Photoperiod was positively correlated to deciduous LFM except *Q. stellata*, was uncorrelated to *P. echinata* LFM, and was the only variable correlated to *J. virginiana* LFM (avg. R^2=0.56, Fig. 2.5). VPD was strongly correlated to herbaceous LFM in mixedgrass prairie (avg. R^2=0.80) but weakly in other grasslands (Fig. 2.6). Woody species' LFM was strongly correlated to VPD in all species except *J. virginiana* (avg. R^2 excluding *J. virginiana* = 0.71, Fig. 2.7). VPD was negatively or not related to LFM in all species except *P. echinata*, which exhibited strong, positive correlation. Seven-day avg. FAW was strongly related to LFM in tallgrasses and tallgrass prairie (avg. R^2=0.90) but was weakly related to LFM in short and mixedgrass prairies (avg. R^2=0.25, Fig. 2.8). Seven-day avg. FAW was strongly correlated to LFM in oak-hickory-pine forest species except *J. virginiana* (avg. R^2=0.91) but was uncorrelated to *J. virginiana* LFM (avg. R^2=0.06) and Cross Timbers trees' LFM (avg. R^2=0.45, Fig. 2.9). *P. echinata* LFM was negatively related to avg. FAW, opposite to all other correlated species. We suspect that the opposite, counterintuitive relationships between *P. echinata* LFM and VPD as well as avg. FAW is related to a wildfire that burned in and around the collection site during our study period. The high temperatures likely caused trees to shed leaves and/or foliage may have been directly burned. This loss of foliage resulted in the collection of newer, younger leaves (flush/cohort). These results indicate that LFM is difficult to estimate after fire, and that our results regrading *P. echinata* should be considered in this context.

When comparing our observed woody and herbaceous mean LFM data to OK-Fire predicted woody and herbaceous LFM (derived from satellite relative greenness), the OK-Fire estimates weakly (R^2=0.37 & 0.14) reflected our in-situ collections (Fig. 2.10).

DISCUSSION

Our results support our hypothesis that changes in moisture availability (measured as VPD, avg. FAW, and rainfall) within the SPAC are related to changes in LFM. Using environmental data (photoperiod, VPD, and rainfall) and functional group, we were able to estimate LFM (R^2 = 0.51). These estimates seem to be an improvement over the relative greenness-derived predictions of OK-Fire (Fig. 2.10).

Our prediction that LFM, and its relationship with environmental conditions, would be species dependent was not fully supported. In the case of tallgrasses (*A. gerardii* and *P. virgatum*) and deciduous trees (*Quercus* species and *C. tomentosa*), LFM was not significantly different between species based on the results of our ANOVA and Tukey tests (Fig. 2.2). And, when creating models, the use of functional group was more supported by AIC as opposed to species. Yet, our results suggest that LFM varies at scales finer than vegetation type (woody or herbaceous) or taxonomic family (ex. *Poaceae*). Additionally, in three of our four species collected in more than one plant community (*B. gracilis, S. scoparium,* and *Q. stellata*) we found that correlation to environmental variables differed, indicating that the relationship between LFM and environment in these species is location dependent. Lastly, the high t-values and effect sizes of species/functional groups in all models indicates that the largest influence on LFM is plant species/functional group. These results support our hypothesis that the

relationship between LFM and environmental conditions are variable among species, likely due to differences in physiology and morphology. Our findings are consistent with other studies that have found variations between species' LFM, but less so in more closely related species (Viegas et al. 2001, Behm et al. 2004, Ruffault et al. 2018, Costa-Saura et al. 2021). Our functional grouping is akin to previous studies' pyro-ecophysiological groupings (Pellizzaro et al. 2007a, Pellizzaro et al. 2007b). Ultimately, our results fall somewhere between studies that have found plant water relations differ at finer scales like species (Pivovaroff et al. 2019, Scarff et al. 2021) and those that have been able to successfully predict LFM based on vegetation type alone (Dimitrakopoulos and Bemmerzouk 2003, Chuvieco et al. 2004, Roberts et al. 2006, García et al. 2008, Jurdao et al. 2012, Helman et al. 2015, Brown et al. 2022). This study adds evidence in support of variable LFM relations among co-occurring species and within species.

Our species and site-specific analysis of environmental variables indicated that photoperiod, avg. FAW, and VPD are the most correlated to LFM. In our model for predicting LFM, photoperiod acted as an estimate of plant phenology and season. Photoperiods' importance, then, is consistent with phenological studies that have shown autumn senescence and spring budburst/release from dormancy are both influenced by photoperiod (Heide 1993, Caffarra et al. 2011, Liang 2019). Additionally, in a study of *Adenostoma fasciculatum* fuel moisture Capps et al. (2021) found day-length to be the most influential predictor of new-growth LFM. Photoperiod is also linked to temperature, as seen in our correlation matrix (Table 3.2), and is related to transpiration rates through photosynthesis. The relationship between FAW and LFM seen in figures 2.8 and 2.9 corroborate the findings of Sharma et al. (2021) and Kruger et al. (2015, 2016, 2017). As

well as other studies in which soil moisture was related to LFM (Qi et al. 2012, Jia et al. 2019, Lu and Wei 2021, Vinodkumar et al. 2021). It is interesting, that avg. FAW was strongly correlated to species LFM at our oak-hickory-pine site despite the limited depth (5-cm); this could indicate that estimates for sites with fewer sensors are still accurate (Fig. 2.3). The importance of VPD to plant water status is in accord with the known influence of atmospheric moisture demand on plant water status (Zhang et al. 2017, Grossiord et al. 2020, López et al. 2021). VPD's relationship to LFM was also shown by Dudek (2020), and several studies have related VPD to wildfire danger (Sedano and Randerson 2014, Seager et al. 2015, Mueller et al. 2020). AIC selection of seven-day temporal scales for rainfall and avg. FAW support the Mesonet's current use of seven-day composites when calculating relative greenness. These findings are consistent with literature describing the lagged response time of LFM (Viegas et al. 2001, Dennison et al. 2008, Dennison and Moritz 2009, Jurdao et al. 2012, Ruffault et al. 2018, Capps et al. 2021).

VPD was negatively or unrelated to LFM in all species except *P. echinata*, which exhibited strong, positive correlation. This seems counterintuitive because as evaporative demand increases, water stress increases and LFM should decrease. Furthermore, *P. echinata* LFM exhibited a counterintuitive, negative relationship with FAW, opposite to all other correlated species. These behaviors of *P. echinata* make it a species of concern when predicting LFM after fire, as mentioned previously. In *J. virginiana* LFM was only related to photoperiod, suggesting that the main influence acting on *J. virginiana* LFM is day-length, possibly due to seasonality or photosynthetic rates. Our analysis of environmental variables and LFM per species, per site, found no significantly, correlated

environmental variables in shortgrass prairie species. This is likely do to very low variation in LFM in this plant community. Our driest site, this location was experiencing drought throughout our entire study period, resulting in very little fluctuation in LFM. As such, we theorize this lack of variation in LFM resulted in weak relationships between LFM and environmental conditions, resulting in decreased accuracy in predictions.

Our model seemingly struggled to predict high LFM during spring green-up/leaf-flush and *S. scoparium* LFM, in general (Fig. 2.3). Luckily, during green-up/leaf-flush moisture is high and fire danger will typically be low. As mentioned, spring budburst is influenced by both photoperiod and temperature, so if one was interested in being better able to predict spring leaf-flush it could possibly be accomplished by including temperature in lieu of VPD. We speculate that the high error when predicting *S. scoparium* LFM could be the result of sampling across the widest range of environmental conditions, from nearly the driest portion of Oklahoma, where annual precipitation is less than 50 cm, to some of the wettest where annual precipitation is greater than 100 cm (Oklahoma Climatological Survey 2021).

Considering the multi-step process to calculate avg. FAW, sensor depth availability, and the correlation between avg. FAW and VPD, we recommend the use of functional group, photoperiod, VPD, and seven-day rainfall for estimating LFM in Oklahoma plant communities. Our model (2), without FAW, had comparable AIC (AIC=1180.2) to the global model (AIC=1168.2) which suffered from multicollinearity. In this model soil moisture is assumed to be most influenced by rainfall. We realize that this does not account for other soil water inputs like initial soil moisture, but this model is more statistically reliable and, for application purposes, requires less inputs and

computations. Lastly, if vegetation type and latitude (for photoperiod calculation) are known, all other variables are available through the Mesonet directly and can be forecasted because they are meteorologically based. This model is very similar to the CFFDRS's Buildup Index/Drought Code and with the addition of priors, could be used as an estimate of live and dead fuel moisture.

In conclusion, we found that LFM differs between co-occurring species, varies within vegetation types, is influenced by season/phenology, and is related to changes in moisture demands throughout the SPAC. By accounting for each of these factors, we were able to estimate LFM (R^2=0.51, RMSE=30.42) and our estimates seem to be an improvement over relative-greenness predictions from the Oklahoma Mesonet. This study now adds to the growing body of research of plant ecophysiology as it relates to fire science. It is our hope that our results, and other advancements in the study of pyro-ecophysiology, can improve fire danger rating systems.

TABLES AND FIGURES

Table 3.1 Surveyed species (common names and specific epithets), species two-letter codes, and the plant communities they were sampled in.

Species common name, specific epithet	**Code**	**Plant communities (site code)**
Big bluestem, *Andropogon gerardii* Vitman	BB	Tallgrass prairie (tgpp)
Blue grama, *Bouteloua gracilis*	BG	Mixedgrass prairie (klem)
		Shortgrass prairie (opti)
Little bluestem, *Schizachyrium scoparium*	LB	Mixedgrass prairie (klem)
		Shortgrass prairie (opti)
		Tallgrass prairie (tgpp)
Switchgrass, *Panicum virgatum* L.	SG	Cross Timbers (cter)
Blackjack oak, *Quercus marilandica*	BJ	Cross Timbers (cter)
Black oak, *Quercus velutina*	BO	Oak-hickory-pine forest (cook)
Mockernut hickory, *Carya tomentosa*	MH	Oak-hickory-pine forest (cook)
Eastern redcedar, *Juniperus virginiana*	ER	Oak-hickory-pine forest (cook)
		Cross Timbers (cter)
		Mixedgrass prairie (klem)
Post oak, *Quercus stellata*	PO	Oak-hickory-pine forest (cook)
		Cross Timbers (cter)
Shortleaf pine, *Pinus echinata*	SP	Oak-hickory-pine forest (cook)

Table 3.2 Environmental variable correlation matrix. Variables were analyzed at the daily scale. avg. FAW= depth weighted average FAW across available site depths. *correlation > |0.60|.

	Photoperiod	Temp (max)	Temp (min)	VPD	Rainfall	5-cm FAW	Avg. FAW
Photoperiod	1	—	—	—	—	—	—
Temp (max)	0.478	1	—	—	—	—	—
Temp (min)	0.649*	0.881*	1	—	—	—	—
VPD	0.17	0.718*	0.496	1	—	—	—
Rainfall	0.054	0.223	0.161	-0.052	1	—	—
5-cm FAW	-0.126	-0.487	-0.364	-0.531	-0.147	1	—
Avg. FAW	0.034	-0.445	-0.3	-0.559	-0.149	0.813*	1

Table 3.3 Single environmental variable model AIC comparison at all temporal scales (single-day, 7-day average, and 30-day average). Avg. FAW is depth weighted average FAW. The general equation used was mean LFM ~ species + photoperiod + environmental variable.

Environmental variable	**ΔAIC**	**DF**	**Weight**
VPD	0	13	0.966
7-day avg. FAW	7.9	13	0.0185
30-day VPD	8.8	13	0.0119
7-day rainfall	12.8	13	0.0016
7-day VPD	13.8	13	<0.001
Avg. FAW	14.4	13	<0.001
30-day avg. FAW	17.6	13	<0.001
30-day 5-cm FAW	18.4	13	<0.001
7-day 5-cm FAW	21.5	13	<0.001
30-day rainfall	22.6	13	<0.001
Rainfall	24	13	<0.001
5-cm FAW	25.3	13	<0.001

Table 3.4 AIC model comparison. FxnGroup is described in methods and shown in Fig. 2.2. Avg. FAW_7 and $Rainfall_7$ are the seven-day moving averages. The global model containing photoperiod, VPD, avg. FAW_7, and $Rainfall_7$ was most supported by AIC.

Model		ΔAIC	DF	Weight
FxnGroup + Photoperiod + VPD + Avg. FAW_7 + $Rainfall_7$	1	0	11	0.744
FxnGroup + Photoperiod + VPD + $Rainfall_7$	2	11.9	10	0.002
FxnGroup + Photoperiod + VPD+ Avg. FAW_7	3	15.4	10	<0.001
FxnGroup + Photoperiod + Avg. FAW_7 + $Rainfall_7$	4	30.8	10	<0.001

Table 3.5 Model summary comparison of the global model (FxnGroup+Photoperiod+VPD+7-day avg. FAW+7-day rainfall) and the model without FAW (FxnGroup+ Photoperiod+VPD+7-day rainfall) RMSE of 28.7% and 30.42% LFM are less than one standard deviation (43.5%). Species codes in Table 3.1.

Model	Global (1)		w/o FAW (2)	
	t-value	**p-value**	**t-value**	**p-value**
Intercept (FxnGroup BG)	7.811	< 0.001	6.897	< 0.001
Photoperiod	3.319	0.001	4.125	< 0.001
FxnGroup Deciduous (BJ/BO/PO/MH)	3.573	0.001	3.895	< 0.001
FxnGroup ER	3.544	0.001	4.129	< 0.001
FxnGroup LB	3.626	< 0.001	3.72	< 0.001
FxnGroup SP	7.553	< 0.001	7.619	< 0.001
FxnGroup Tallgrass (BB/SG)	5.997	< 0.001	6.497	< 0.001
VPD	0.215	0.83	-2.036	0.044
7-day avg. FAW	3.679	< 0.001	—	—
7-day rainfall	2.69	0.008	3.134	0.002
# obs.	**R^2**	**RMSE**	**R^2**	**RMSE**
120	0.57	28.7 %	0.51	30.42 %

Table 3.6 Most correlated environmental variable to mean LFM by species and plant community. Avg. FAW is 7-day depth-weighted average FAW.

Species (code)	Plant community (code)	Variable	R^2 (*p<0.05)
Andropogon gerardii (BB)	Tallgrass prairie (tgpp)	Avg. FAW	0.95*
Bouteloua gracilis (BG)	Mixedgrass prairie (klem)	VPD	0.89*
	Shortgrass prairie (opti)	Avg. FAW	0.29
Schizachyrium scoparium (LB)	Mixedgrass prairie (klem)	VPD	0.71*
	Shortgrass prairie (opti)	Avg. FAW	0.17
	Tallgrass prairie (tgpp)	Avg. FAW	0.92*
Panicum virgatum (SG)	Cross Timbers (cter)	Avg. FAW	0.83*
Quercus marilandica (BJ)	Cross Timbers (cter)	VPD	0.59*
Quercus velutina (BO)	Oak-hickory-pine forest (cook)	Photoperiod	0.99
Carya tomentosa (MH)	Oak-hickory-pine forest	Photoperiod	0.96*
Juniperus virginiana (ER)	Oak-hickory-pine forest (cook)	Photoperiod	0.68*
	Cross Timbers (cter)	Photoperiod	0.57*
	Mixedgrass prairie (klem)	Photoperiod	0.42*
Quercus stellata (PO)	Oak-hickory-pine forest (cook)	Avg. FAW	0.88*
	Cross Timbers (cter)	VPD	0.44*
Pinus echinata (SP)	Oak-hickory-pine forest (cook)	Avg. FAW	0.86*

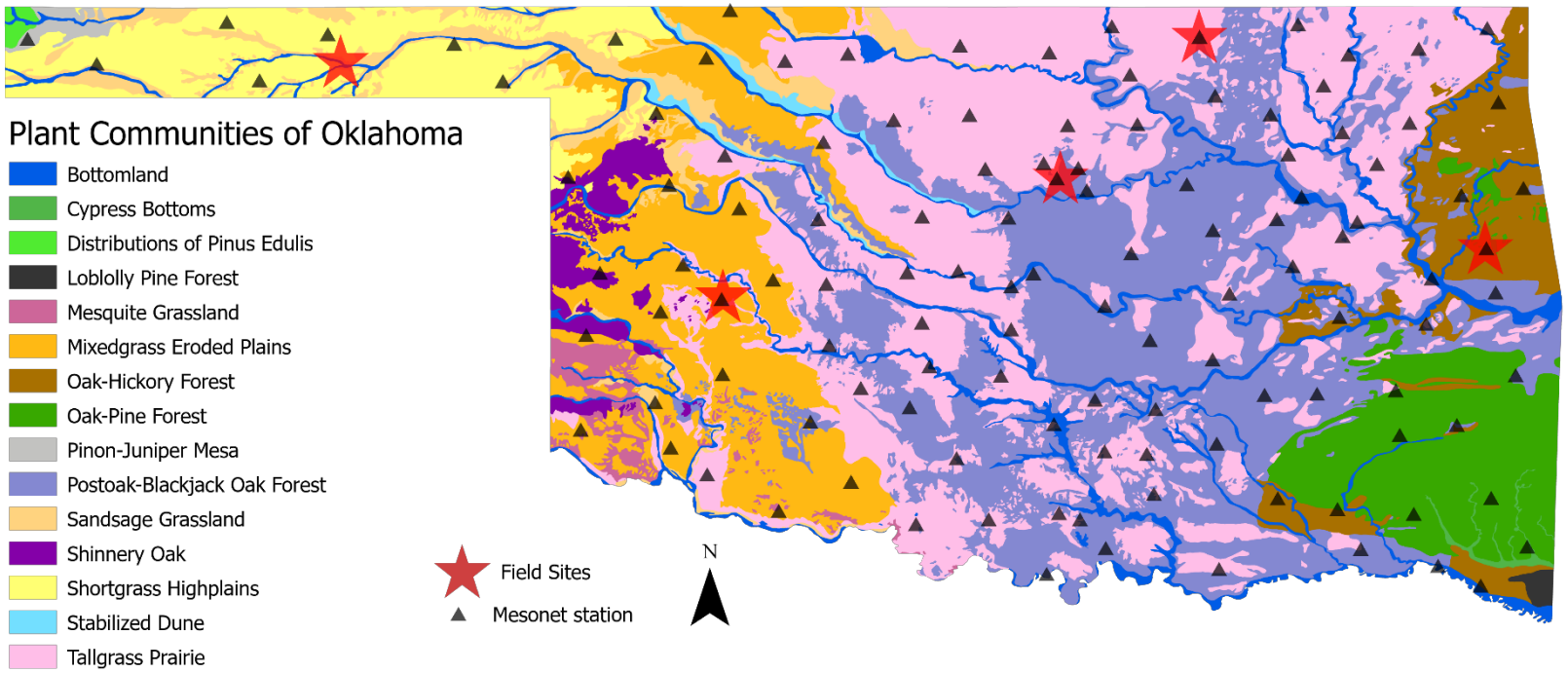

Figure 3.1 Plant communities of Oklahoma described by Duck and Fletcher (1943) were digitized by the Oklahoma Biological Survey and Hoagland and Johnson (1996). Black triangles are the Oklahoma Mesonet weather towers. Our field sites (red stars) from west to east: Optima Wildlife Mgmt. Area/opti, Oklahoma State University Klemme Research Station/klem, Oklahoma State University Cross Timbers Experimental Range/cter, Joseph H. Williams Tallgrass Prairie Preserve/tgpp, and Cookson Hills Wildlife Management Area/cook. According to this map opti occurs within sandsage grassland, but the site was dominated by *B. gracilis*, *S. scoparium, Buchloe dactyloides*, and *Yucca* spp. and as such was classified as shortgrass prairie (see Fig. S3.2).

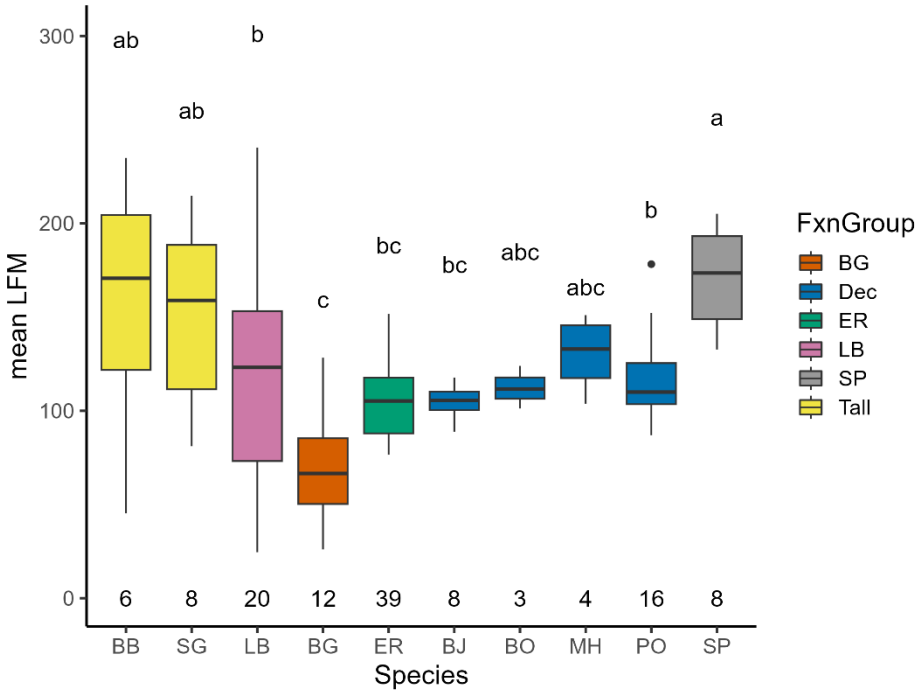

Figure 3.2 Mean LFM by species compared using ANOVA and Tukey tests. Different letters signify significant differences in means. Lower numbers are number of observations. Dec= deciduous hardwoods and Tall= tallgrasses. Species codes found in Table 3.1.

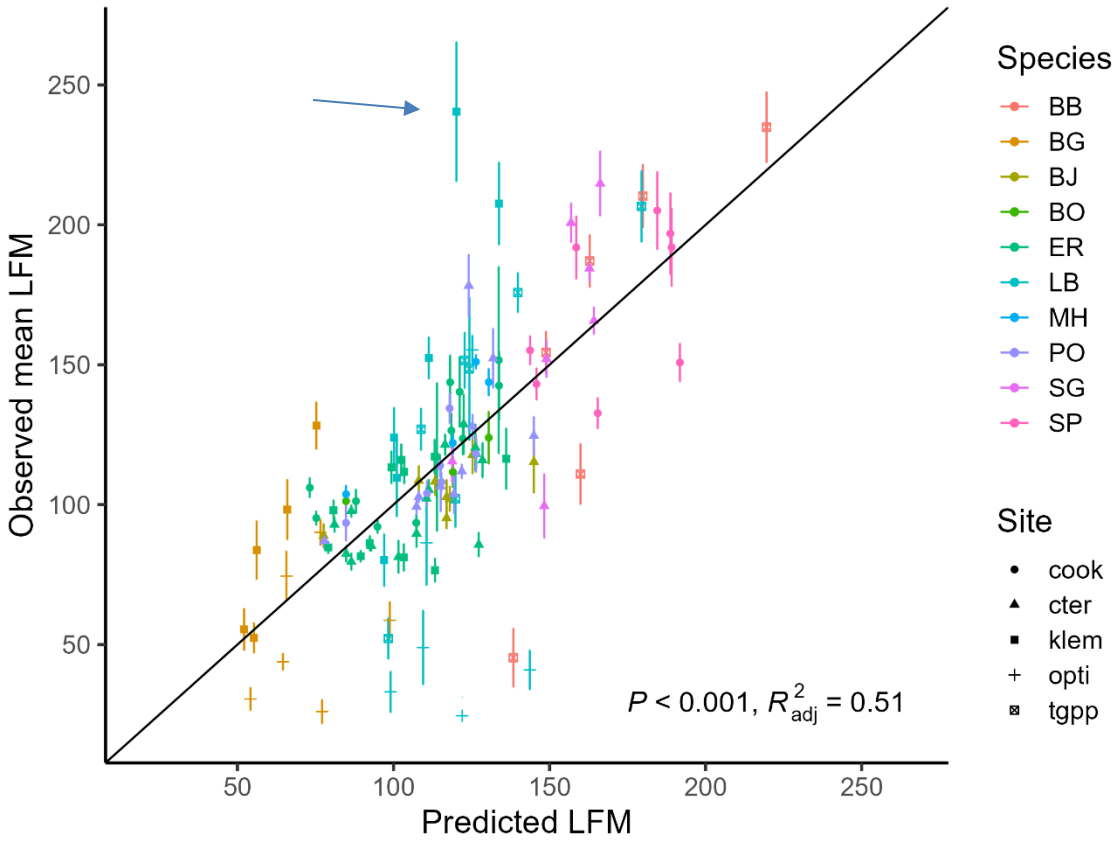

Figure 3.3 Predicted vs observed mean LFM for the model excluding FAW (model 2). The black line is the 1:1 observed:predicted line. Error bars represent the 95% CI for mean LFM per species per day. The point indicated by the arrow is spring green-up/leaf-flush in 2021. Site/species are listed in Table 3.1.

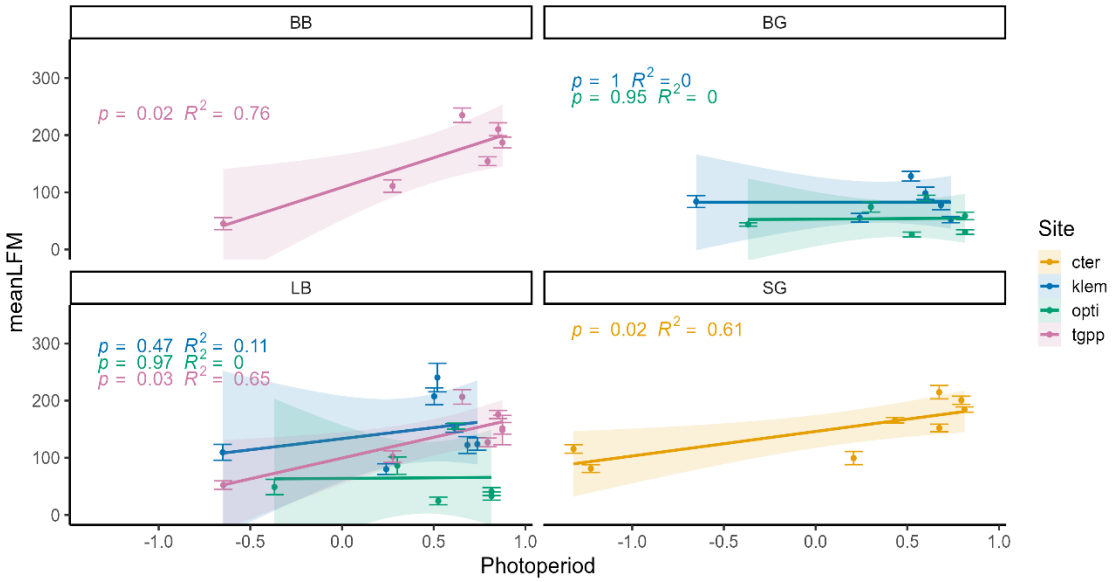

Figure 3.4 Daily photoperiod (centered and scaled) vs herbaceous mean LFM. Error bars are the 95% CI for mean LFM and shading is the 95% model CI. There is strong positive correlation to tallgrasses (BB*, SG*) and LB* at the tallgrass prairie preserve (pink). Site/species are listed in Table 3.1. *p≤0.05

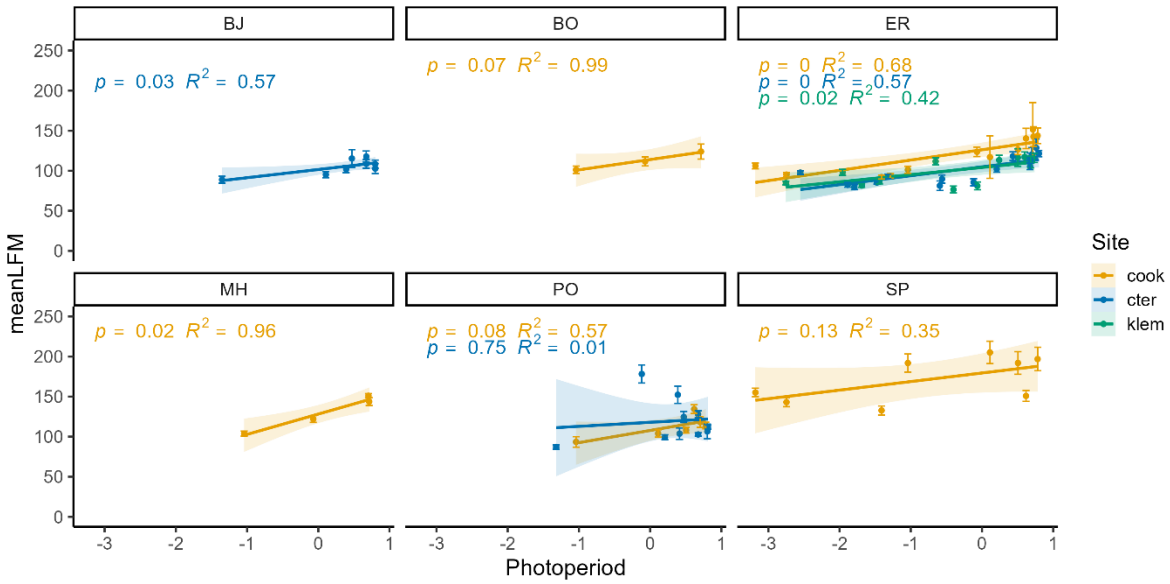

Figure 3.5 Daily photoperiod (centered and scaled) vs woody mean LFM. Error bars are the 95% CI for mean LFM and shading is the 95% model CI. There is strong positive correlation to deciduous trees (BO, MH*, PO) in oak-hickory-pine (yellow), moderate positive correlation to BJ*, moderate positive correlation to SP, and moderate-strong correlation in ER*. Site/species are listed in Table 3.1. *p≤0.05

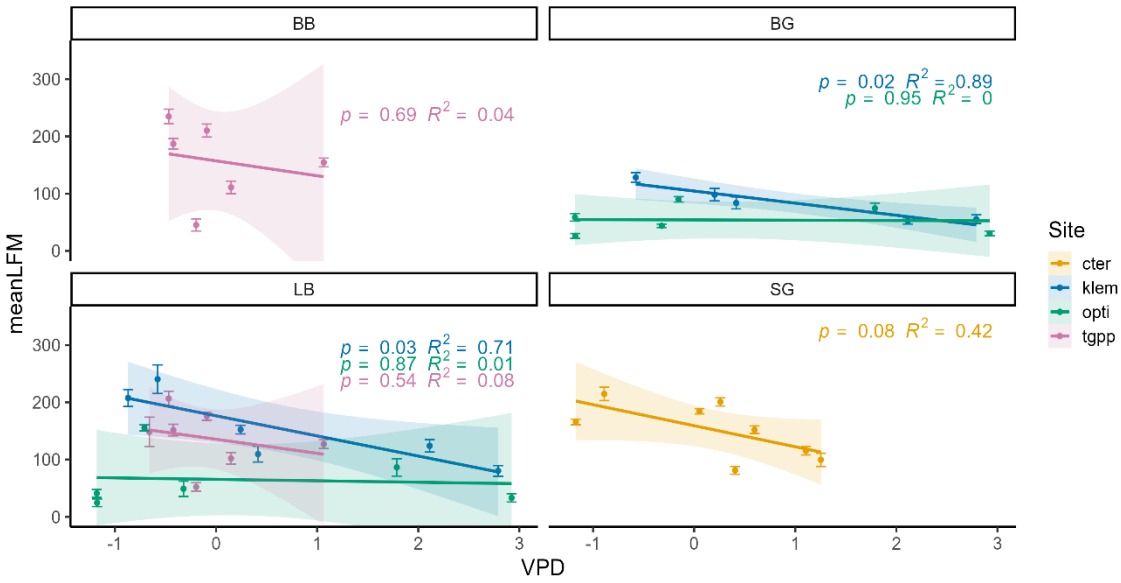

Figure 3.6 Daily VPD (centered and scaled) vs herbaceous mean LFM. Error bars are the 95% CI for mean LFM and shading is the 95% model CI. There is strong negative correlation with mixedgrass prairie* (blue) and moderate correlation with SG. Site/species are listed in Table 3.1. *p≤0.05

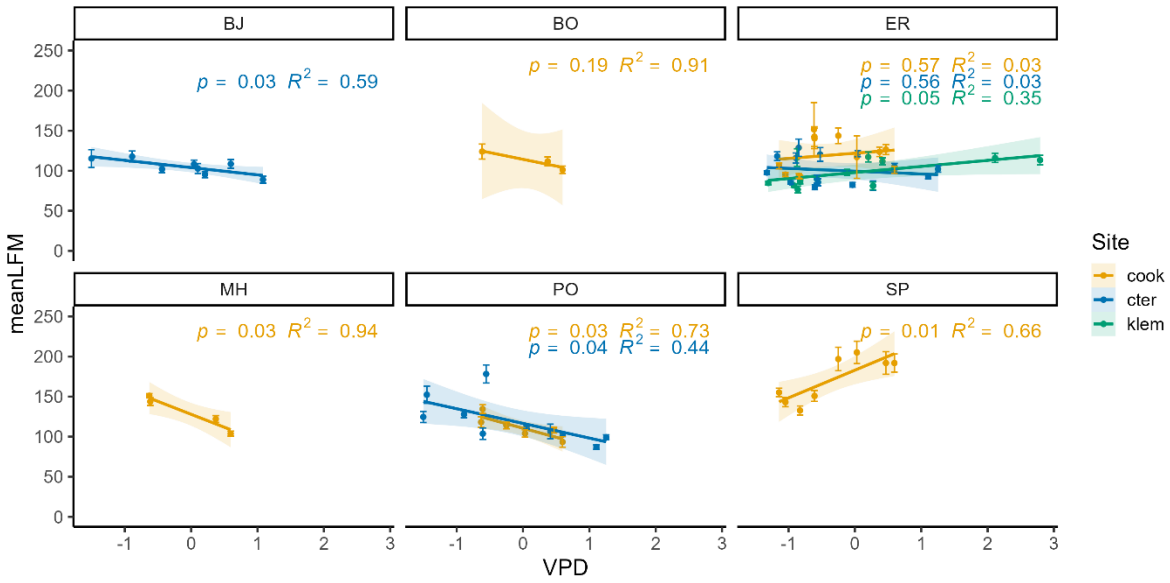

Figure 3.7 Daily VPD (centered and scaled) vs woody mean LFM. Error bars are the 95% CI for mean LFM and shading is the 95% model CI. There is strong negative correlation to all deciduous trees (BO, MH*, PO*) in oak-hickory-pine (yellow), moderate negative correlation to oaks (BJ*, PO*) in the Cross Timbers (blue), weak positive correlation to encroached ER (green), and strong positive correlation to SP*. Site/species are listed in Table 3.1. *p≤0.05

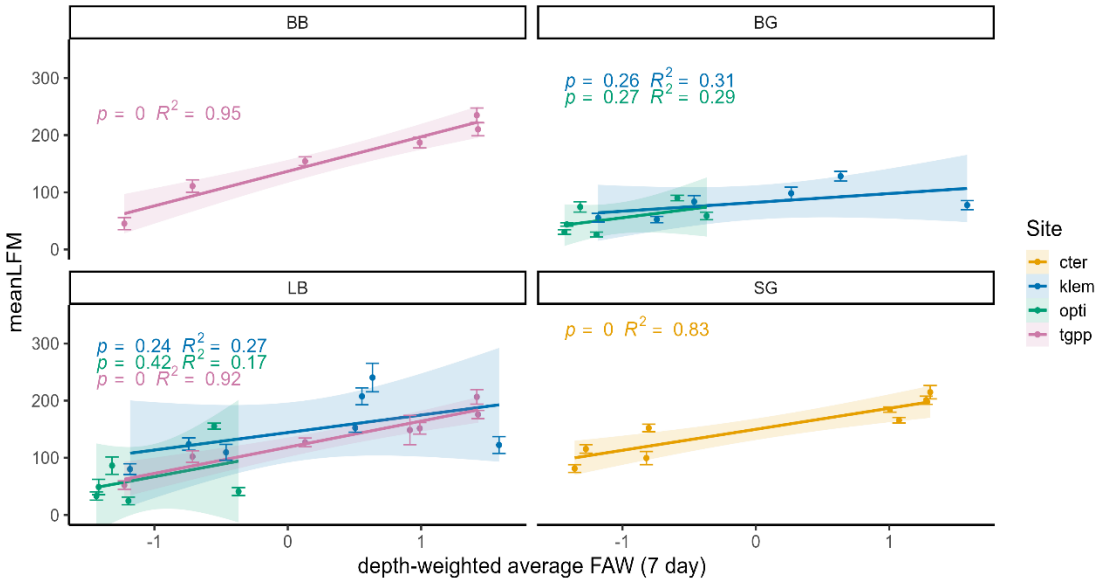

Figure 3.8 Depth-weighted mean FAW 7-day average (centered and scaled) vs herbaceous mean LFM. Error bars are the 95% CI for mean LFM and shading is the 95% model CI. There is strong positive correlation to tallgrasses (BB*, SG*) and LB* at the tallgrass prairie preserve (pink). Site/species are listed in Table 3.1. *p≤0.05

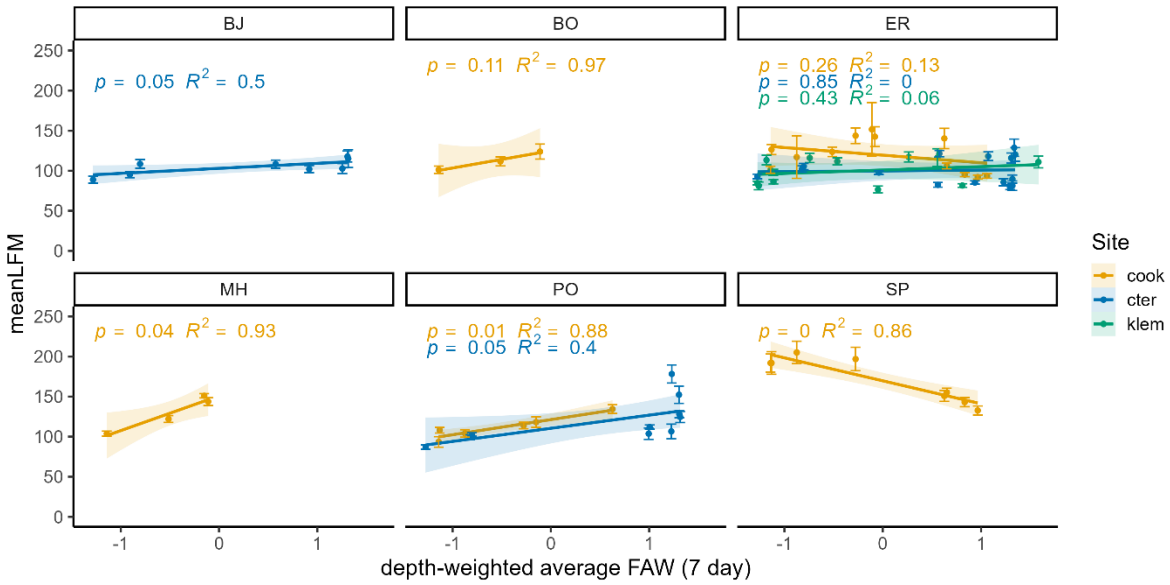

Figure 3.9 Depth-weighted mean FAW 7-day average (centered and scaled) vs woody mean LFM. Error bars are the 95% CI for mean LFM and shading represents the 95% model CI. There is strong positive correlation with deciduous trees (BO, MH*, PO*) in oak-hickory-pine (yellow), moderate positive correlation to oaks (BJ*, PO*) in Cross Timbers (blue), and strong negative correlation to SP*. Site/species are listed in Table 3.1. *p≤0.05

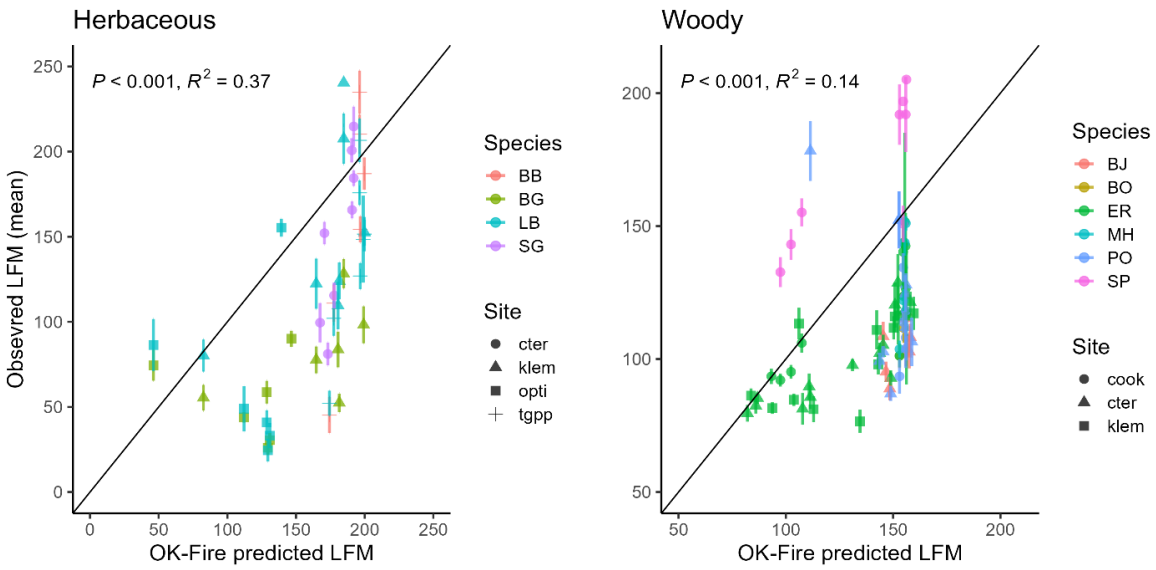

Figure 3.10 Mesonet/OK-Fire relative greenness estimates for a) herbaceous and b) woody species vs observed mean LFM. Error bars are the 95% CI for LFM mean. Site/species are listed in Table 3.1.

REFRENCES

Al-Tawaha, A. R., M. A. Turk, Y. M. Abu-Zaitoon, S. H. Aladaileh, I. M. Al-Rawashdeh, S. Alnaimat, A. R. M. Al-Tawaha, M. H. Alu'datt, and M. Wedyan. 2017. Plants adaptation to drought environment. *Bulgarian Journal of Agricultural Science* **23**:381-388.

Alba, C., H. Skálová, K. F. McGregor, C. D'Antonio, P. Pyšek, and J. Morgan. 2015. Native and exotic plant species respond differently to wildfire and prescribed fire as revealed by meta-analysis. *Journal of Vegetation Science* **26**:102-113.

An, H., J. Gan, and S. J. Cho. 2015. Assessing climate change impacts on wildfire risk in the United States. *Forests* **6**:3197-3211.

Aphalo, P. J. 2023. ggpmisc: miscellaneous extensions to 'ggplot2'. Available at https://docs.r4photobiology.info/ggpmisc/, https://github.com/aphalo/ggpmisc.

Arel-Bundock, V. 2022. modelsummary: data and model summaries in R. *Journal of Statistical Software* **103**:1-23.

Arganaraz, J. P., M. A. Landi, S. J. Bravo, G. I. Gavier-Pizarro, C. M. Scavuzzo, and L. M. Bellis. 2016. Estimation of live fuel moisture content from MODIS images for fire danger assessment in Southern Gran Chaco. *IEEE Journal of Selected Topics in Applied Earth Observations and Remote Sensing* **9**:5339-5349.

Auguie, B. and A. Antonov. 2015. gridExtra: miscellaneous functions for "grid" graphics. Available at https://cran.r-project.org/web/packages/gridExtra/index.html.

Baloun, K. R. 2006. Assessing moisture content change in chaparral using spectral mixture analysis. Unpublished master's thesis. California State University.

Behm, A. L., M. L. Duryea, A. J. Long, and W. C. Zipperer. 2004. Flammability of native understory species in pine flatwood and hardwood hammock ecosystems and implications for the wildland-urban interface. *International Journal of Wildland Fire* **13**:355-365.

Bidwell, T. G., D. M. Engle, M. E. Moseley, and R. E. Masters. 2016. Invasion of Oklahoma rangelands and forests by eastern redcedar and ashe juniper. Oklahoma Cooperative Extension Service, Division of Agricultural Sciences and Natural Resources, Oklahoma State University. Circular E-947.

Bolker, B., R Development Core Team, and I. Giné-Vázquez. 2022. Tools for general maximum likelihood estimation. Available at https://github.com/bbolker/bbmle.

Bowyer, P., and F. M. Danson. 2004. Sensitivity of spectral reflectance to variation in live fuel moisture content at leaf and canopy level. *Remote Sensing of Environment* **92**:297-308.

Bradshaw, L. S., J. E. Deeming, R. E. Burgan, and J. D. Cohen. 1984. The 1978 National Fire-Danger Rating System: technical documentation. U.S. Department of Agriculture, Forest Service, Intermountain Forest and Range Experiment Station. General Technical Report INT-169. (Ogden, UT)

Brady, N. C., and R. R. Weil. 2002. The nature and properties of soils. (Ed S. Helba) pp 228-234. Prentice Hall.

Brown, T. P., Z. H. Hoylman, E. Conrad, Z. Holden, K. Jencso, and W. M. Jolly. 2022. Decoupling between soil moisture and biomass drives seasonal variations in live fuel moisture across co-occurring plant functional types. *Fire Ecology* **18:**14.

Burgan, Robert E. 1988. 1988 Revisions to the 1978 National Fire-Danger Rating System. U.S. Department of Agriculture, Forest Service, Southeastern Forest Experiment Station. Research Paper SE-273. (Asheville, NC)

Burke, M., A. Driscoll, S. Heft-Neal, J. Xue, J. Burney, and M. Wara. 2021. The changing risk and burden of wildfire in the United States. *Proceedings of the National Academy of Sciences of the USA* **118**:e2011048118.

Burnett, A. C., J. Anderson, K. J. Davidson, K. S. Ely, J. Lamour, Q. Li, B. D. Morrison, D. Yang, A. Rogers, and S. P. Serbin. 2021. A best-practice guide to predicting plant traits from leaf-level hyperspectral data using partial least squares regression. *Journal of Experimental Botany* **72**:6175-6189.

Butler, C., S. Marsh, J. W. Domitrovich, and J. Helmkamp. 2017. Wildland firefighter deaths in the United States: a comparison of existing surveillance systems. *Journal of Occupational and Environmental Hygiene* **14**:258-270.

Caccamo, G., L. A. Chisholm, R. A. Bradstock, M. L. Puotinen, and B. G. Pippen. 2012. Monitoring live fuel moisture content of heathland, shrubland and sclerophyll forest in south-eastern Australia using MODIS data. *International Journal of Wildland Fire* **21**: 257-269.

Caffarra, A., A. Donnelly, I. Chuine, and M. B. Jones. 2011. Modelling the timing of *Betula pubescens* budburst. I. Temperature and photoperiod: a conceptual model. *Climate Research* **46**:147-157.

Capps, S. B., W. Zhuang, R. Liu, T. Rolinski, and X. Qu. 2021. Modelling chamise fuel moisture content across California: a machine learning approach. *International Journal of Wildland Fire* **31**:136-148.

Carlson, J. D. 2022. Personal communication.

Carlson, J. D., R. E. Burgan, D. M. Engle, and J. R. Greenfield. 2002. The Oklahoma Fire Danger Model: An operational tool for mesoscale fire danger rating in Oklahoma. *International Journal of Wildland Fire* **11**:183-191.

Carlson, J. D., and R. E. Burgan. 2003. Review of users' needs in operational fire danger estimation: the Oklahoma example. *International Journal of Remote Sensing* **24**:1601-1620.

Castro, F. X., A. Tudela, and M. T. Sebastià. 2003. Modeling moisture content in shrubs to predict fire risk in Catalonia (Spain). *Agricultural and Forest Meteorology* **116**:49-59.

Ceccato, P., B. Leblon, E. Chuvieco, S. Flasse, and J. D. Carlson. 2003. Estimation of live fuel moisture content. In 'Wildland fire danger estimation and mapping'. (Ed E. Chuvieco) pp 63-90. World Scientific Publishing Company.

Chen, H., J. M. Samet, P. A. Bromberg, and H. Tong. 2021. Cardiovascular health impacts of wildfire smoke exposure. *Particle and Fibre Toxicology* **18**:2.

Chen, H., and S. Wang. 2022. Accelerated transition between dry and wet periods in a warming climate. *Geophysical Research Letters* **49**:e2022GL099766.

Christian, J., K. Christian, and J. B. Basara. 2015. Drought and pluvial dipole events within the Great Plains of the United States. *Journal of Applied Meteorology and Climatology* **54**:1886-1898.

Chuvieco, E., D. Cocero, D. Riaño, P. Martin, J. Martínez-Vega, J. de la Riva, and F. Pérez. 2004. Combining NDVI and surface temperature for the estimation of live fuel moisture content in forest fire danger rating. *Remote Sensing of Environment* **92**:322-331.

Chuvieco, E., I. González, F. Verdú, I. Aguado, and M. Yebra. 2009. Prediction of fire occurrence from live fuel moisture content measurements in a Mediterranean ecosystem. *International Journal of Wildland Fire* **18**:430–441.

Coates, P. S., M. A. Ricca, B. G. Prochazka, M. L. Brooks, K. E. Doherty, T. Kroger, E. J. Blomberg, C. A. Hagen, and M. L. Casazza. 2016. Wildfire, climate, and invasive grass interactions negatively impact an indicator species by reshaping sagebrush ecosystems. *Proceedings of the National Academy of Sciences of the USA* **113**:12745-12750.

Cook, B. I., T. R. Ault, and J. E. Smerdon. 2015. Unprecedented 21st century drought risk in the American Southwest and Central Plains. *Science Advances* **1**:e1400082.

Costa-Saura, J. M., Á. Balaguer-Beser, L. A. Ruiz, J. E. Pardo-Pascual, and J. L. Soriano-Sancho. 2021. Empirical models for spatio-temporal live fuel moisture content estimation in mixed Mediterranean vegetation areas using Sentinel-2 indices and meteorological data. *Remote Sensing* **13**:3726.

Countryman, C. M. 1974. Moisture in living fuels affects fire behavior. *Fire Management* **35**:10-14.

Dale, L. 2010. The true cost of wildfire in the Western U.S.. The Western Forestry Leadership Coalition. (Lakewood, CO, USA)

Day, N. J., K. E. Dunfield, J. F. Johnstone, M. C. Mack, M. R. Turetsky, X. J. Walker, A. L. White, and J. L. Baltzer. 2019. Wildfire severity reduces richness and alters composition of soil fungal communities in boreal forests of western Canada. *Global Change Biology* **25**:2310-2324.

Deeming, J. E., J. W. Lancaster, M. A. Fosberg, R. W. Furman, and M. J. Schroeder. 1972. National Fire-Danger Rating System. Rocky Mountain Forest and Range Experiment Station, Forest Service, U.S. Dept. of Agriculture. Research Paper RM-84. (Fort Collins, CO)

Dennison, P. E., and M. A. Moritz. 2009. Critical live fuel moisture in chaparral ecosystems: a threshold for fire activity and its relationship to antecedent precipitation. *International Journal of Wildland Fire* **18**:1021-1027.

Dennison, P. E., M. A. Moritz, and R. S. Taylor. 2008. Evaluating predictive models of critical live fuel moisture in the Santa Monica Mountains, California. *International Journal of Wildland Fire* **17**:18-27.

Dennison, P. E., D. A. Roberts, S. H. Peterson, and J. Rechel. 2006. Use of Normalized Difference Water Index for monitoring live fuel moisture. *International Journal of Remote Sensing* **26**:1035-1042.

Dickens, S. J. M., and E. B. Allen. 2013. Exotic plant invasion alters chaparral ecosystem resistance and resilience pre- and post-wildfire. *Biological Invasions* **16**:1119-1130.

Dillis, C., V. Butsic, D. Moanga, P. Parker-Shames, A. Wartenberg, and T. E. Grantham. 2022. The threat of wildfire is unique to cannabis among agricultural sectors in California. *Ecosphere* **13**:e4205.

Dimitrakopoulos, A. P., and A. M. Bemmerzouk. 2003. Predicting live herbaceous moisture content from a seasonal drought index. *International Journal of Biometeorology* **47**:73-79.

Dimitrakopoulos, A. P., and K. K. Papaioannou. 2001. Flammability Assessment of Mediterranean Forest Fuels. *Fire Technology* **37**:143-152.

Donovan, V. M., C. L. Wonkka, and D. Twidwell. 2017a. Supporting information for surging wildfire activity in a grassland biome. *Geophysical Research Letters*.

Donovan, V. M., C. L. Wonkka, and D. Twidwell. 2017b. Surging wildfire activity in a grassland biome. *Geophysical Research Letters* **44**:5986-5993.

Duck, L. G., and J. B. Fletcher. 1943. The game types of Oklahoma. Oklahoma Game and Fish Commission.

Dudek, J. 2020. A burning question: How much drought causes increased flammability in eastern redcedar? Unpublished master's thesis. Oklahoma State University.

Field, C. B., V.R. Barros, K.J. Mach, M.D. Mastrandrea, M. van Aalst, W.N. Adger, D.J. Arent, J. Barnett, R. Betts, T. E. Bilir, J. Birkmann, J. Carmin, D.D. Chadee, A.J. Challinor, M. Chatterjee, W. Cramer, D.J. Davidson, Y.O. Estrada, J.-P. Gattuso, Y. Hijioka, O. Hoegh-Guldberg, H.Q. Huang, G.E. Insarov, R.N. Jones, R.S. Kovats, P. Romero-Lankao, J.N. Larsen, I.J. Losada, J.A. Marengo, R.F. McLean, L.O. Mearns, R. Mechler, J.F. Morton, I. Niang, J. M. O. T. Oki, M. Opondo, E.S. Poloczanska, H.-O. Pörtner, M.H. Redsteer, A. Reisinger, A. Revi, D.N. Schmidt, M.R. Shaw, W. Solecki, D.A. Stone, J.M.R. Stone, K.M. Strzepek, A.G. Suarez, P. Tschakert, R. Valentini, S. Vicuña, A. Villamizar, K.E. Vincent, R. Warren, L.L. White, T.J. Wilbanks, P.P. Wong, and G. W. Yohe. 2014. Technical summary. In: Climate change 2014: impacts, adaptation, and vulnerability. Part A: global and sectoral aspects. Contribution of Working Group II to the Fifth Assessment Report of the Intergovernmental Panel on Climate Change.

Fares, S., S. Bajocco, L. Salvati, N. Camarretta, J.-L. Dupuy, G. Xanthopoulos, M. Guijarro, J. Madrigal, C. Hernando, and P. Corona. 2017. Characterizing potential wildland fire fuel in live vegetation in the Mediterranean region. *Annals of Forest Science* **74**:1.

Ganatsas, P., M. Antonis, and T. Marianthi. 2011. Development of an adapted empirical drought index to the Mediterranean conditions for use in forestry. *Agricultural and Forest Meteorology* **151**:241-250.

Gao, B.-C. 1996. NDWI A Normalized Difference Water Index for remote sensing of vegetation liquid water from space. *Remote Sensing of Environment* **58**:257-266.

García, M., E. Chuvieco, H. Nieto, and I. Aguado. 2008. Combining AVHRR and meteorological data for estimating live fuel moisture content. *Remote Sensing of Environment* **112**:3618-3627.

Gensini, V. A., A. M. Haberlie, and W. S. Ashley. 2023. Convection-permitting simulations of historical and possible future climate over the contiguous United States. *Climate Dynamics* **60**:109–126.

Gitelson, A., and M. N. Merzlyak. 1994. Quantitative estimation of chlorophyll-a using reflectance spectra: Experiments with autumn chestnut and maple leaves. *Journal of Photochemistry and Photobiology B: Biology* **22**:247-252.

Gitelson, A. A., Y. J. Kaufman, R. Stark, and D. Rundquist. 2002. Novel algorithms for remote estimation of vegetation fraction. *Remote Sensing of Environment* **80**:76-87.

Graves, S., H.-P. Piepho, and L. Selzer. 2019. Package 'multcompView'. Available at https://cran.r-project.org/web/packages/multcompView/index.html.

Grossiord, C., T. N. Buckley, L. A. Cernusak, K. A. Novick, B. Poulter, R. T. W. Siegwolf, J. S. Sperry, and N. G. McDowell. 2020. Plant responses to rising vapor pressure deficit. *New Phytologist* **226**:1550-1566.

Hao, X., and J. Qu. 2007. Retrieval of real-time live fuel moisture content using MODIS measurements. *Remote Sensing of Environment* **108**:130-137.

Hardisky, M. A., V. Klemas, and R. M. Smart. 1983. The influence of soil salinity, growth form, and leaf moisture on-the spectral radiance of *Spartina alterniflora* canopies. *Photogrammetric Engineering and Remote Sensing* **49**:77-83.

Hardy, C. C., and C. E. Hardy. 2007. Fire danger rating in the United States of America: an evolution since 1916. *International Journal of Wildland Fire* **16**:217-231.

Hays, R. 2017. Oklahoma State extension says over sixteen million dollars in losses to agriculture as a result of Northwest Oklahoma Fire Complex. Radio Oklahoma Network, Oklahoma Farm Report.

Heide, O. M. 1993. Dormancy release in beech buds (*Fagus sylvatica*) requires both chilling and long days. *Physiologia Plantarum* **89**:187-191.

Helman, D., I. Lensky, N. Tessler, and Y. Osem. 2015. A phenology-based method for monitoring woody and herbaceous vegetation in Mediterranean forests from NDVI time series. *Remote Sensing* **7**:12314-12335.

Hijmans, R. J., C. Karney, E. Williams, and C. Vennes. 2022. Package 'geosphere'. Available at https://cran.r-project.org/web/packages/geosphere/index.html.

Hoagland, B., and F. Johnson. 1996. The Game Types of Oklahoma. Oklahoma Biological Survey.

Horler, D. N. H., M. Dockray, and J. Barber. 1983. The red edge of plant leaf reflectance. *International Journal of Remote Sensing* **4**:273-288.

Horn, K. J., and S. B. St. Clair. 2016. Wildfire and exotic grass invasion alter plant productivity in response to climate variability in the Mojave Desert. *Landscape Ecology* **32**:635-646.

Horvath, H. 1993. Atmospheric light absorption—a review. *Atmospheric Environment* **27A**:293-317.

Huang, S., L. Tang, J. P. Hupy, Y. Wang, and G. Shao. 2020. A commentary review on the use of normalized difference vegetation index (NDVI) in the era of popular remote sensing. *Journal of Forestry Research* **32**:1-6.

Huete, A., H. Q. Liu, K. Batchily, and W. Van Leeuwen. 1997. A comparison of vegetation indices over a global set of TM images for EOS-MODIS. *Remote Sensing of Environment* **59**:440-451.

Hunt, E. R. J., and B. N. Rock. 1989. Detection of changes in leaf water content using near- and middle-infrared reflectances. *Remote Sensing of Environment* **30**:43-54.

Ingalsbee, T. 2010. Getting burned: a taxpayer's guide to wildfire suppression costs. Firefighters United for Safety, Ethics, & Ecology. (Eugene, OR, USA)

Intergovernmental Panel on Climate Change. 2014. Climate Change 2014: synthesis report. Contribution of Working Groups I, II and III to the Fifth Assessment Report of the Intergovernmental Panel on Climate Change.

Jia, S., S. H. Kim, S. V. Nghiem, W. Cho, and M. C. Kafatos. 2018. Estimating live fuel moisture in Southern California using remote sensing vegetation water content proxies. *2018 IEEE International Geoscience and Remote Sensing Symposium*, pp 5587-5890.

Jia, S., S. H. Kim, S. V. Nghiem, and M. Kafatos. 2019. Estimating live fuel moisture using SMAP L-Band radiometer soil moisture for Southern California, USA. *Remote Sensing* **11**:1575.

Jolly, W., and D. Johnson. 2018. Pyro-ecophysiology: shifting the paradigm of live wildland fuel research. *Fire* **1**:8.

Jolly, W. M. 2007. Sensitivity of a surface fire spread model and associated fire behaviour fuel models to changes in live fuel moisture. *International Journal of Wildland Fire* **16**:503-509.

Jolly, W. M. 2018. Overview of NFDRS 2016. National NFDRS 2016 rollout workshop. United States Department of Agriculture, Forest Service.

Jolly, W. M., R. Nemani, and S. W. Running. 2005. A generalized, bioclimatic index to predict foliar phenology in response to climate. *Global Change Biology* **11**:619-632.

Jones, H. G., and R. A. Vaughan. 2010. Remote sensing of vegetation: principles, techniques, and applications. Oxford University Press.

Jung, M., M. Reichstein, P. Ciais, S. I. Seneviratne, J. Sheffield, M. L. Goulden, G. Bonan, A. Cescatti, J. Chen, R. de Jeu, A. J. Dolman, W. Eugster, D. Gerten, D. Gianelle, N. Gobron, J. Heinke, J. Kimball, B. E. Law, L. Montagnani, Q. Mu, B. Mueller, K. Oleson, D. Papale, A. D. Richardson, O. Roupsard, S. Running, E. Tomelleri, N. Viovy, U. Weber, C. Williams, E. Wood, S. Zaehle, and K. Zhang. 2010. Recent decline in the global land evapotranspiration trend due to limited moisture supply. *Nature* **467**:951-954.

Jurdao, S., E. Chuvieco, and J. M. Arevalillo. 2012. Modelling fire ignition probability from satellite estimates of live fuel moisture content. *Fire Ecology* **8**:77-97.

Kauf, Z., A. Fangmeier, R. Rosavec, and Z. Spanjol. 2015. Seasonal and local differences in leaf litter flammability of six Mediterranean tree species. *Environmental Management* **55**:687-701.

Keetch, J. J., and G. M. Byram. 1968. A drought index for forest fire control. U.S. Department of Agriculture, Forest Service, Southeastern Forest Experiment Station. Research Paper SE-38. (Asheville, NC)

Kelly, L. T., K. M. Giljohann, A. Duane, N. Aquilue, S. Archibald, E. Batllori, A. F. Bennett, S. T. Buckland, Q. Canelles, M. F. Clarke, M. J. Fortin, V. Hermoso, S. Herrando, R. E. Keane, F. K. Lake, M. A. McCarthy, A. Moran-Ordonez, C. L. Parr, J. G. Pausas, T. D. Penman, A. Regos, L. Rumpff, J. L. Santos, A. L. Smith, A. D. Syphard, M. W. Tingley, and L. Brotons. 2020. Fire and biodiversity in the Anthropocene. *Science* **370**:929.

Klepper, B. 1968. Diurnal pattern of water potential in woody plants. *Plant Physiology* **43**:1931-1934.

Kloesel, K., B. Bartush, J. Banner, D. Brown, J. Lemery, X. Lin, C. Loeffler, G. McManus, E. Mullens, J. Nielsen-Gammon, M. Shafer, C. Sorenson, S. K. Sperry, D. R. Wildcat, and J. R. Ziolkowska. 2018. Southern Great Plains. In 'Impacts, risks, and adaptation in the United States: fourth national climate assessment'. (Eds R. D.R., C. W. Avery, D. R. Easterling, K. E. Kunkel, K. L. M. Lewis, T. K. Maycock, and B. C. Stewart) pp 987–1035. U.S. Global Change Research Program.

Köster, K., H. Aaltonen, F. Berninger, J. Heinonsalo, E. Köster, C. Ribeiro-Kumara, H. Sun, L. Tedersoo, X. Zhou, and J. Pumpanen. 2021. Impacts of wildfire on soil microbiome in Boreal environments. *Current Opinion in Environmental Science & Health* **22**:100258.

Krstic, M. P., D. L. Johnson, and M. J. Herderich. 2015. Review of smoke taint in wine: smoke-derived volatile phenols and their glycosidic metabolites in grapes and vines as biomarkers for smoke exposure and their role in the sensory perception of smoke taint. *Australian Journal of Grape and Wine Research* **21**:537-553.

Krueger, E. S. 2022. Personal communication.

Krueger, E. S., T. E. Ochsner, J. D. Carlson, D. M. Engle, D. Twidwell, and S. D. Fuhlendorf. 2016. Concurrent and antecedent soil moisture relate positively or negatively to probability of large wildfires depending on season. *International Journal of Wildland Fire* **25**:657-668.

Krueger, E. S., T. E. Ochsner, D. M. Engle, J. D. Carlson, D. Twidwell, and S. D. Fuhlendorf. 2015. Soil moisture affects growing-season wildfire size in the southern Great Plains. *Soil Science Society of America Journal* **79**:1567-1576.

Krueger, E. S., T. E. Ochsner, S. M. Quiring, D. M. Engle, J. D. Carlson, D. Twidwell, and S. D. Fuhlendorf. 2017. Measured soil moisture is a better predictor of large growing-season wildfires than the Keetch-Byram Drought Index. *Soil Science Society of America Journal* **81**:490-502.

Laughlin, D. C., and P. Z. Fulé. 2008. Wildland fire effects on understory plant communities in two fire-prone forests. *Canadian Journal of Forest Research* **38**:133-142.

Liang, L. 2019. A spatially explicit modeling analysis of adaptive variation in temperate tree phenology. *Agricultural and Forest Meteorology* **266-267**:73-86.

Liland, K. H., B.-H. Mevik, R. Wehrens, and P. Hiemstra. 2022. pls: partial least squares and principal component regression. Available at https://github.com/khliland/pls.

Lin, B., J. P. Stackhouse, W. Sun, Y. Hu, Z. Liu, and T.-F. Fan. 2013. Is Oklahoma getting drier? *Journal of Quantitative Spectroscopy and Radiative Transfer* **122**:208-213.

Lindley, T. T., J. L. Guyer, G. P. Murdoch, S. R. Nagle, K. Schneider, and G. Skwira. 2007. A meteorological composite of the 2005/06 wildfire outbreaks in the Southern Plains. *Seventh Symposium on Fire and Forest Meteorology*. American Meteorological Society.

Lindley, T. T., G. P. Murdoch, B. R. Smith, and K. M. V. Speybroeck. 2013. Environmental factors contributing to the emergence of Southern Great Plains Wildfire Outbreaks. *Tenth Symposium on Fire and Forest Meteorology*. American Meteorological Society.

Lindley, T. T., G. D. Skwira, G. P. Murdoch, and J. L. Guyer. 2011a. Preliminary meteorological analysis of the 2011 “Texas firestorms”. *9th Symposium on Fire and Forest Meteorology*. American Meteorological Society.

Lindley, T. T., D. A. Speheger, M. A. Day, G. P. Murdoch, B. R. Smith, N. J. Nauslar, and D. C. Daily. 2019. Megafires on the Southern Great Plains. *Journal of Operational Meteorology* **7**:164-179.

Lindley, T. T., J. D. Vitale, W. S. Burgett, and M.-J. Beierle. 2011b. Proximity meteorological observations for wind-driven grassland wildfire starts on the Southern High Plains. *Electronic Journal of Severe Storms Meteorology* **6**:1-27.

Loomis, R. M., P. J. Roussopoulos, and R. W. Blank. 1979. Summer moisture contents of understory vegetation in northeastern Minnesota. U.S. Dept. of Agriculture, Forest Service, North Central Forest Experiment Station. Research Paper NC-179. (St. Paul, MN)

López, J., D. A. Way, and W. Sadok. 2021. Systemic effects of rising atmospheric vapor pressure deficit on plant physiology and productivity. *Global Change Biology* **27**:1704-1720.

Lu, Y., and C. Wei. 2021. Evaluation of microwave soil moisture data for monitoring live fuel moisture content (LFMC) over the coterminous United States. *Science of The Total Environment* **771**:145410.

Malvern Panalytical Ltd. 2014. ViewSpec Pro. Available at https://www.malvernpanalytical.com/en/support/product-support/software/viewspecprosoftwareinstall.

Malvern Panalytical Ltd. 2023. Malvern Panalytical a Spectris company.

Masara, I. K., S. B. Murugesan, S. W. Myint, Y. Zhu, and J. B. Fisher. 2022. Wildfire dynamics from ECOSTRESS data and machine learning: The case of South-Eastern Australia's black summer. *Authorea*. Preprint.

MATLAB. 2022. version 9.13.0.2126072 (R2022b Update 3). The MathWorks Inc.

Meehl, G. A., and C. Tebaldi. 2004. More intense, more frequent, and longer lasting heat waves in the 21st Century. *Science* **305**:994-997.

Mesonet. 2022. The Oklahoma Mesonet. Available at https://mesonet.org/.

Monitoring Trends in Burn Severity. 2022. Monitoring Trends in Burn Severity (MTBS). Available at https://www.mtbs.gov/.

Mueller, S. E., A. E. Thode, E. Q. Margolis, L. L. Yocom, J. D. Young, and J. M. Iniguez. 2020. Climate relationships with increasing wildfire in the southwestern US from 1984 to 2015. *Forest Ecology and Management* **460**: 117861.

Myoung, B., S. Kim, S. Nghiem, S. Jia, K. Whitney, and M. Kafatos. 2018. Estimating live fuel moisture from MODIS satellite data for wildfire danger assessment in Southern California USA. *Remote Sensing* **10**:87.

Nagler, P. L., B. B. M. Sridhar, A. D. Olsson, W. J. D. v. Leeuwen, and E. P. Glenn. 2012. Hyperspectral remote sensing tools for quantifying plant litter and invasive species in arid ecosystems. In 'Hyperspectral remote sensing of vegetation'. (Eds P. S. Thenkabail, J. G. Lyon, and A. Huete). CRC Press.

Nagy, C. R., E. Fusco, B. Bradley, J. T. Abatzoglou, and J. Balch. 2018. Human-related ignitions increase the number of large wildfires across U.S. Ecoregions. *Fire* **1**:4.

Nanjappan, E., E. Sullo, S. Shrestha, S. Thomas, and E. Nouvet. 2021. Californian wildfires and associated human health outcomes: an epidemiological scoping review. *International Journal of Trend in Scientific Research and Development* **5**: 944-953.

National Fuel Moisture Database. 2009. National Fuel Moisture Database 2009 users guide. Eastern Great Basin Predictive Services. (Salt Lake City, UT)

National Fuel Moisture Database. 2022. National Fuel Moisture Database. USFS-WFAS. Available at https://www.wfas.net/index.php/national-fuel-moisture-database-moisture-drought-103.

National Wildfire Coordinating Group. 2023. Live fuel moisture content. Available at https://www.nwcg.gov/publications/pms437/fuel-moisture/live-fuel-moisture-content.

Nelson Jr, R. M. 2001. Water relations of forest fuels. In 'Forest fires: behavior and ecological effects'. (Eds E. A. Johnson and K. Miyanishi). Elsevier Inc.

Nolan, R. H., C. J. Blackman, V. R. de Dios, B. Choat, B. E. Medlyn, X. Li, R. A. Bradstock, and M. M. Boer. 2020. Linking forest flammability and plant vulnerability to drought. *Forests* **11**:779.

Nolan, R. H., M. M. Boer, V. Resco de Dios, G. Caccamo, and R. A. Bradstock. 2016. Large-scale, dynamic transformations in fuel moisture drive wildfire activity across southeastern Australia. *Geophysical Research Letters* **43**:4229-4238.

Nolan, R. H., J. Hedo, C. Arteaga, T. Sugai, and V. Resco De Dios. 2018. Physiological drought responses improve predictions of live fuel moisture dynamics in a Mediterranean forest. *Agricultural and Forest Meteorology* **263**:417-427.

Novick, K. A., D. L. Ficklin, P. C. Stoy, C. A. Williams, G. Bohrer, A. C. Oishi, S. A. Papuga, P. D. Blanken, A. Noormets, B. N. Sulman, R. L. Scott, L. Wang, and R. P. Phillips. 2016. The increasing importance of atmospheric demand for ecosystem water and carbon fluxes. *Nature Climate Change* **6**:1023-1027.

Ochsner, T. 2019. Rain or shine: an introduction to soil physical properties and processes. Oklahoma State University. Available at https://osf.io/z4rbt/.

Oklahoma Climatological Survey. 2021. Normal annual precipitation. Available at https://climate.ok.gov/index.php/climate/map/normal_annual_precipitation/oklahoma_climate.

Oswald, B. P., and The Association for Fire Ecology Board of Directors. 2007. San Diego declaration on climate change and fire management: ramifications for fuels management. In 'The fire environment—innovations, management, and policy'. (Comps B.W. Butler and W. Cook) Proceedings RMRS-P-46CD. U.S. Department of Agriculture, Forest Service, Rocky Mountain Research Station. (Fort Collins, CO)

Pascolini-Campbell, M., C. Lee, N. Stavros, and J. B. Fisher. 2022. ECOSTRESS reveals pre-fire vegetation controls on burn severity for Southern California wildfires of 2020. *Global Ecology and Biogeography* **31**:1976-1989.

Pellizzaro, G., C. Cesaraccio, P. Duce, A. Ventura, and P. Zara. 2007a. Relationships between seasonal patterns of live fuel moisture and meteorological drought indices for Mediterranean shrubland species. *International Journal of Wildland Fire* **16**:232-241.

Pellizzaro, G., P. Duce, A. Ventura, and P. Zara. 2007b. Seasonal variations of live moisture content and ignitability in shrubs of the Mediterranean Basin. *International Journal of Wildland Fire* **16**:633-641.

Peñuelas, J., I. Filella, C. Biel, L. Serrano, and R. Savé. 1992. The reflectance at the 950–970 nm region as an indicator of plant water status. *International Journal of Remote Sensing* **14**:1887-1905.

Peñuelas, J., J. Piñol, R. Ogaya, and I. Filella. 1997. Estimation of plant water concentration by the reflectance Water Index WI (R900/R970). *International Journal of Remote Sensing* **18**:2869-2875.

Peterson, S., D. Roberts, and P. Dennison. 2008. Mapping live fuel moisture with MODIS data: a multiple regression approach. *Remote Sensing of Environment* **112**:4272-4284.

Pinheiro, J., D. Bates, and R Core Team. 2023. nlme: linear and nonlinear mixed effects models. R package version 3.1-162. Available at https://CRAN.R-project.org/package=nlme.

Pivovaroff, A. L., N. Emery, M. R. Sharifi, M. Witter, J. E. Keeley, and P. W. Rundel. 2019. The effect of ecophysiological traits on live fuel moisture content. *Fire* **2**:28.

PMS Instrument Company. 2023. Available at https://www.pmsinstrument.com/.

Prestemon, J., E. J. Belval, S. H. Brown, J. Costanza, L. A. Joyce, S. Kay, M. Lichtenstein, J. T. Morisette, K. Riley, and K. C. Short. 2022. Climate risk exposure: an assessment of the federal government's financial risks to climate change. U.S. Office of Management and Budget.

Pyne, S. J., P. L. Andrews, and R. D. Laven. 1996. Introduction to wildland fire. John Wiley & Sons, Inc.

Pyne, S. J. 2017. The Great Plains: a fire survey. The University of Arizona Press.

Qi, Y., P. E. Dennison, J. Spencer, and D. Riaño. 2012. Monitoring live fuel moisture using soil moisture and remote sensing proxies. *Fire Ecology* **8**:71-87.

Qi, Y., W. M. Jolly, P. E. Dennison, and R. C. Kropp. 2016. Seasonal relationships between foliar moisture content, heat content and biochemistry of lodgepole line and big sagebrush foliage. *International Journal of Wildland Fire* **25**:574-578.

Radeloff, V. C., D. P. Helmers, H. A. Kramer, M. H. Mockrin, P. M. Alexandre, A. Bar-Massada, V. Butsic, T. J. Hawbaker, S. Martinuzzi, A. D. Syphard, and S. I. Stewart. 2018. Rapid growth of the US wildland-urban interface raises wildfire risk. *Proceedings of the National Academy of Science of the USA* **115**:3314-3319.

Reid, A. M., S. D. Fuhlendorf, and J. R. Weir. 2010. Weather variables affecting Oklahoma wildfires. *Rangeland Ecology & Management* **63**:599-603.

Reid, C. E., M. Brauer, F. H. Johnston, M. Jerrett, J. R. Balmes, and C. T. Elliott. 2016. Critical review of health impacts of wildfire smoke exposure. *Environmental Health Perspectives* **124**:1334-1343.

Resco de Dios, V. 2020. Plant-fire interactions: applying ecophysiology to wildfire management. Springer.

Roberto, C., B. Lorenzo, M. Michele, R. Micol, and P. Cinzia. 2012. Optical remote sensing of vegetation water content. In 'Hyperspectral remote sensing of vegetation'. (Eds P. S. Thenkabail, J. G. Lyon, and A. Huete). CRC Press.

Roberts, D. A., P. E. Dennison, S. Peterson, S. Sweeney, and J. Rechel. 2006. Evaluation of Airborne Visible/Infrared Imaging Spectrometer (AVIRIS) and Moderate Resolution Imaging Spectrometer (MODIS) measures of live fuel moisture and fuel condition in a shrubland ecosystem in southern California. *Journal of Geophysical Research: Biogeosciences* **111**: G04S02.

Rossa, C. G., R. Veloso, and P. M. Fernandes. 2016. A laboratory-based quantification of the effect of live fuel moisture content on fire spread rate. *International Journal of Wildland Fire* **25**:569-573.

Rouse, J. W. J., R. H. Haas, J. A. Well, and D. W. Deering. 1974. Monitoring vegetation systems in the Great Plains with ERTS. Conference paper. NASA. Goddard Space Flight Center 3d ERTS-1 Symp., Vol. 1, Sect. A.

RStudio Team. 2022. RStudio. Available at https://posit.co/download/rstudio-desktop/.

Ruffault, J., N. Martin-StPaul, F. Pimont, and J.-L. Dupuy. 2018. How well do meteorological drought indices predict live fuel moisture content (LFMC)? An assessment for wildfire research and operations in Mediterranean ecosystems. *Agricultural and Forest Meteorology* **262**:391-401.

Scarff, F. R., T. Lenz, A. E. Richards, A. E. Zanne, I. J. Wright, M. Westoby, and K. McCulloh. 2021. Effects of plant hydraulic traits on the flammability of live fine canopy fuels. *Functional Ecology* **35**:835-846.

Scasta, J. D., J. R. Weir, and M. C. Stambaugh. 2016. Droughts and wildfires in Western U.S. rangelands. *Rangelands* **38**:197-203.

Schlobohm, P., and J. Brain. 2002. Gaining an understanding of the National Fire Danger Rating System. National Wildfire Coordinating Group.

Schneider, P., D. A. Roberts, and P. C. Kyriakidis. 2008. A VARI-based relative greenness from MODIS data for computing the Fire Potential Index. *Remote Sensing of Environment* **112**:1151-1167.

Schoenberg, F. P., R. Peng, Z. Huang, and P. Rundel. 2003. Detection of non-linearities in the dependence of burn area on fuel age and climatic variables. *International Journal of Wildland Fire* **12**:1-6.

Seager, R., A. Hooks, A. P. Williams, B. Cook, J. Nakamura, and N. Henderson. 2015. Climatology, variability, and trends in the U.S. vapor pressure deficit, an important fire-related meteorological quantity. *Journal of Applied Meteorology and Climatology* **54**:1121-1141.

Sedano, F., and J. T. Randerson. 2014. Multi-scale influence of vapor pressure deficit on fire ignition and spread in boreal forest ecosystems. *Biogeosciences* **11**:3739-3755.

Seleiman, M. F., N. Al-Suhaibani, N. Ali, M. Akmal, M. Alotaibi, Y. Refay, T. Dindaroglu, H. H. Abdul-Wajid, and M. L. Battaglia. 2021. Drought stress impacts on plants and different approaches to alleviate its adverse effects. *Plants* **10**:259.

Serbin, S. P., J. Lamour, and J. Anderson. 2022. Spectra-trait PLSR example using leaf-level spectra and leaf mass per area (LMA) data from 36 species growing in *Rosa rugosa* invaded coastal grassland communities in Belgium. Available at https://rstudio-pubs-static.s3.amazonaws.com/721898_56039b1b9c1e4f2aa12f34c9816626af.html.

Serrano, L., S. L. Ustin, D. A. Roberts, J. A. Gamon, and J. Peñuelas. 2000. Deriving water content of chaparral vegetation from AVIRIS data. *Remote Sensing of Environment* **74**:570-581.

Shakesby, R., and S. Doerr. 2006. Wildfire as a hydrological and geomorphological agent. *Earth-Science Reviews* **74**:269-307.

Sharma, S., J. D. Carlson, E. S. Krueger, D. M. Engle, D. Twidwell, S. D. Fuhlendorf, A. Patrignani, L. Feng, and T. E. Ochsner. 2021. Soil moisture as an indicator of growing-season herbaceous fuel moisture and curing rate in grasslands. *International Journal of Wildland Fire* **30**:57-69.

Sharma, S., T. E. Ochsner, D. Twidwell, J. D. Carlson, E. S. Krueger, D. M. Engle, and S. D. Fuhlendorf. 2018. Nondestructive estimation of standing crop and fuel moisture content in tallgrass prairie. *Rangeland Ecology & Management* **71**:356-362.

Slonecker, E. T. 2012. Analysis of the effects of heavy metals on vegetation hyperspectral reflectance properties. In 'Hyperspectral remote sensing of vegetation'. (Eds P. S. Thenkabail, J. G. Lyon, and A. Huete). CRC Press.

Smith, H. G., G. J. Sheridan, P. N. J. Lane, P. Nyman, and S. Haydon. 2011. Wildfire effects on water quality in forest catchments: A review with implications for water supply. *Journal of Hydrology* **396**:170-192.

Smith, S. D., C. A. Herr, K. L. Learyt, and J. M. Piorkowski. 1995. Soil-plant water relations in a Mojave Desert mixed shrub community: a comparison of three geomorphic surfaces. *Journal of Arid Environments* **29**:339-351.

Snyder, R. L., D. Spano, P. Duce, D. Baldocchi, L. Xu, and K. T. Paw U. 2006. A fuel dryness index for grassland fire-danger assessment. *Agricultural and Forest Meteorology* **139**:1-11.

Sobrado, M. A. 1986. Aspects of tissue water relations and seasonal changes of leaf water potential components of evergreen and deciduous species coexisting in tropical dry forests. *Oecologia* **68**:413-416.

St. Denis, L. A., N. P. Mietkiewicz, K. C. Short, M. Buckland, and J. K. Balch. 2020. All-hazards dataset mined from the US National Incident Management System 1999–2014. *Scientific Data* **7**:64.

Starr, M., P. Harron, and O. Joshi. 2018. Forestry — important to Oklahoma's economy. Oklahoma Cooperative Extension Service, Division of Agricultural Sciences and Natural Resources, Oklahoma State University.

Taiz, L., E. Zeiger, I. M. Moller, and A. Murphy. 2015. Plant physiology and development. pp 116-117. SINAUER Associates Inc.

Tedim, F., V. Leone, M. Amraoui, C. Bouillon, M. Coughlan, G. Delogu, P. Fernandes, C. Ferreira, S. McCaffrey, T. McGee, J. Parente, D. Paton, M. Pereira, L. Ribeiro, D. Viegas, and G. Xanthopoulos. 2018. Defining extreme wildfire events: difficulties, challenges, and impacts. *Fire* **1**:9.

Texas Forest Service Communications. 2011. East Texas wildfires destroy $97 million worth of timber. Available at https://tfsweb.tamu.edu/Content/Article.aspx?id=27432.

Thenkabail, P. S., E. A. Enclona, M. S. Ashton, and B. Van Der Meer. 2004. Accuracy assessments of hyperspectral waveband performance for vegetation analysis applications. *Remote Sensing of Environment* **91**:354-376.

The North American Meat Institute. 2016. The economic impact of the meat industry 2016 data: Oklahoma. John Dunham & Associates.

Thomas, D., D. Butry, S. Gilbert, D. Webb, and J. Fung. 2017. The costs and losses of wildfires: a literature review. U.S. Department of Commerce, National Institute of Standards and Technology. NIST Special Publication 1215.

Touchette, B. W. 2006. Salt tolerance in a *Juncus roemerianus* brackish marsh: spatial variations in plant water relations. *Journal of Experimental Marine Biology and Ecology* **337**:1-12.

Turner, N. C. 1988. Measurement of plant water status by the pressure chamber technique. *Irrigation Science* **9**:289-308.

Tyrl, R. J., T. G. Bidwell, R. E. Masters, R. D. Elmore, and J. R. Weir. 2007. Oklahoma's native vegetation types. Natural Resource Ecology and Management, Oklahoma Cooperative Extension Service, Oklahoma State University.

U.S. Climate Change Science Program. 2008. The effects of climate change on agriculture, land resources, water resources, and biodiversity in the United States. U.S. Climate Change Science Program and the Subcommittee on Global Change Research.

U.S.D.I. National Park Service, Southern Plains Inventory and Monitoring Network. 2008. Southern Plains Network Vital Signs Monitoring Plan. Natural Resource Report NPS/SOPN/NRR-2008/028. (Fort Collins, CO)

U.S. Global Change Research Program. 2017. Climate science special report: fourth national climate assessment, volume 1. (Eds Wuebbles, D.J., D.W. Fahey, K.A. Hibbard, D.J. Dokken, B.C. Stewart, and T.K. Maycock). U.S. Global Change Research Program. (Washington, DC)

U.S. Global Change Research Program. 2018. Impacts, risks, and adaptation in the United States: fourth national climate assessment, volume II. (Eds Reidmiller, D.R., C.W. Avery, D.R. Easterling, K.E. Kunkel, K.L.M. Lewis, T.K. Maycock, and B.C. Stewart). U.S. Global Change Research Program. (Washington, DC)

United Nations Environment Programme. 2022. Emissions Gap Report 2022: The Closing Window — Climate crisis calls for rapid transformation of societies. 978-92-807-3979-4.

United States Environmental Protection Agency. 2016. What climate change means for Oklahoma.

United States Environmental Protection Agency. 2022a. Climate change indicators: wildfires. Available at https://www.epa.gov/climate-indicators/climate-change-indicators-wildfires.

United States Environmental Protection Agency. 2022b. ICLUS Data for the Southern Plains Region. Available at https://www.epa.gov/gcx/iclus-data-southern-plains-region.

Van Nest, T. A., and M. E. Alexander. 1999. Systems for rating fire danger and predicting fire behavior used in Canada. National Interagency Fire Behavior Workshop, March 1-5, 1999, Phoenix, Arizona.

Van Speybroeck, K. M., G. P. Murdoch, T. T. Lindley, and P. G. Witsaman. 2011. Early recognition of drought potential resulting in enhanced interagency collaboration during the 2010/11 Texas wildfire season. *Ninth Symposium on Fire and Forest Meteorology*. American Meteorological Society.

Van Speybroeck, K. M., A. R. Patrick, and M. C. Oaks. 2007. P2.23 climate variability and the Texas fire weather season of 2005-2006: an historic perspective of a statewide disaster. *19th Conference on Climate Variability and Change*. American Meteorological Society.

Van Wagner, C. E. 1987. Development and structure of the Canadian Forest Fire Weather Index System. Canadian Forestry Service. Forestry Technical Report 35. (Ottawa, ON)

Viegas, D. X., J. Piñol, M. T. Viegas, and R. Ogaya. 2001. Estimating live fine fuels moisture content using meteorologically-based indices. *International Journal of Wildland Fire* **10**:223-240.

Vukomanovic, J., and T. Steelman. 2019. A systematic review of relationships between mountain wildfire and ecosystem services. *Landscape Ecology* **34**:1179-1194.

Weir, J. R., A. M. Reid, and S. D. Fuhlendorf. 2017. Wildfires in Oklahoma. Oklahoma Cooperative Extension Service, Division of Agricultural Sciences and Natural Resources, Oklahoma State University.

Weir, J. R., and J. D. Scasta. 2014. Ignition and fire behaviour of *Juniperus virginiana* in response to live fuel moisture and fire temperature in the southern Great Plains. *International Journal of Wildland Fire* **23**:839-844.

Weise, D. R., X. Zhou, L. Sun, and S. Mahalingam. 2005. Fire spread in chaparral—'go or no-go?'. *International Journal of Wildland Fire* **14**:99-106.

Wickham H (2016). ggplot2: Elegant Graphics for Data Analysis. Springer-Verlag New York. ISBN 978-3-319-24277-4. Available at https://ggplot2.tidyverse.org.

Wright, A., S. A. Schnitzer, P. B. Reich, and R. Jones. 2015. Daily environmental conditions determine the competition–facilitation balance for plant water status. *Journal of Ecology* **103**:648-656.

Yebra, M., P. E. Dennison, E. Chuvieco, D. Riaño, P. Zylstra, E. R. Hunt, F. M. Danson, Y. Qi, and S. Jurdao. 2013. A global review of remote sensing of live fuel moisture content for fire danger assessment: Moving towards operational products. *Remote Sensing of Environment* **136**:455-468.

Yebra, M., G. Scortechini, A. Badi, M. E. Beget, M. M. Boer, R. Bradstock, E. Chuvieco, F. M. Danson, P. Dennison, V. Resco de Dios, C. M. Di Bella, G. Forsyth, P. Frost, M. Garcia, A. Hamdi, B. He, M. Jolly, T. Kraaij, M. P. Martin, F. Mouillot, G. Newnham, R. H. Nolan, G. Pellizzaro, Y. Qi, X. Quan, D. Riano, D. Roberts, M. Sow, and S. Ustin. 2019. Globe-LFMC, a global plant water status database for vegetation ecophysiology and wildfire applications. *Scientific Data* **6**:155.

Youssouf, H., C. Liousse, L. Roblou, E. M. Assamoi, R. O. Salonen, C. Maesano, S. Banerjee, and I. Annesi-Maesano. 2014. Non-accidental health impacts of wildfire smoke. *International Journal of Environmental Research and Public Health* **11**:11772-11804.

Zhang, D., Q. Du, Z. Zhang, X. Jiao, X. Song, and J. Li. 2017. Vapour pressure deficit control in relation to water transport and water productivity in greenhouse tomato production during summer. *Scientific Reports* **7**:43461.

APPENDICES

APPENDIX A

Supplemental Tables and Figures for Chapter II

Table S2.1 All-species (woody and herbaceous) model AIC comparison. The general equation for the models is LFM ~ species + VI (with or without + VI^2) and individual as a random effect. LFMREI our derived index and NDVI are shown in grey.

VI	Model	AIC	ΔAIC	Weight
WI	WI + WI^2	21692.7	0	1
WI	WI	21706.6	14	<0.001
VIgreen	VIgreen +$VIgreen^2$	21799.9	107.3	<0.001
NDWI	NDWI+$NDWI^2$	21845.3	152.6	<0.001
VIgreen	VIgreen	21949.5	256.9	<0.001
NDWI	NDWI	21968.3	275.6	<0.001
LFMREI	LFMREI + $LFMREI^2$	22053.6	361	<0.001
LFMREI	LFMREI	22096.6	403.9	<0.001
NDRE	NDRE+$NDRE^2$	22115.1	422.4	<0.001
NDRE	NDRE	22132	439.3	<0.001
MSI	MSI+MSI^2	22140.7	448.1	<0.001
NDII	NDII+$NDII^2$	22188.2	495.5	<0.001
NDII	NDII	22197.3	504.6	<0.001
NDVI	NDVI+$NDVI^2$	22223.6	530.9	<0.001
MSI	MSI	22229.9	537.2	<0.001
NDVI	NDVI	22270	577.4	<0.001

Table S2.2 Herbaceous species model AIC comparison of VIs. The general equation for the models is LFM ~ species + VI (with or without + VI^2) and individual as a random effect. LFMREI our derived index and NDVI are shown in grey.

VI	Model	AIC	ΔAIC	Weight
WI	WI + WI^2	10545.8	0	1
VIgreen	VIgreen +$VIgreen^2$	10566.6	20.8	<0.001
LFMREI	LFMREI + $LFMREI^2$	10640.8	95.1	<0.001
WI	WI	10645.9	100.1	<0.001
VIgreen	VIgreen	10650.7	105	<0.001
NDWI	NDWI+$NDWI^2$	10653.1	107.4	<0.001
LFMREI	LFMREI	10673.5	127.7	<0.001
NDRE	NDRE+$NDRE^2$	10683.7	138	<0.001
NDRE	NDRE	10693.3	147.5	<0.001
NDVI	NDVI+$NDVI^2$	10741.1	195.3	<0.001
NDVI	NDVI	10773.8	228	<0.001
NDWI	NDWI	10794.9	249.1	<0.001
NDII	NDII+$NDII^2$	10838.1	292.4	<0.001
MSI	MSI+MSI^2	10847.4	301.7	<0.001
NDII	NDII	10888.1	342.3	<0.001
MSI	MSI	10927.6	381.8	<0.001

Table S2.3 Woody species model AIC comparison for VIs. The general equation for the models is LFM ~ species + VI (with or without + VI^2) and individual as a random effect. LFMREI our derived index and NDVI are shown in grey.

VI	Model	AIC	ΔAIC	Weight
WI	$WI+WI^2$	10264.3	0	1
WI	WI	10378.5	114.2	<0.001
NDWI	$NDWI+NDWI^2$	10394.1	129.7	<0.001
NDWI	NDWI	10454	189.6	<0.001
MSI	$MSI+MSI^2$	10535.7	271.4	<0.001
MSI	MSI	10544.9	280.6	<0.001
NDII	$NDII+NDII^2$	10555.5	291.2	<0.001
NDII	NDII	10635.7	371.4	<0.001
VIgreen	$VIgreen+VIgreen^2$	10848.4	584	<0.001
VIgreen	VIgreen	10940.1	675.7	<0.001
NDRE	$NDRE+NDRE^2$	10981.3	717	<0.001
NDRE	NDRE	10996.2	731.9	<0.001
LFMREI	LFMREI + $LFMREI^2$	11000	735.7	<0.001
NDVI	$NDVI+NDVI^2$	11022.7	758.4	<0.001
LFMREI	LFMREI	11039.8	775.4	<0.001
NDVI	NDVI	11050.6	786.2	<0.001

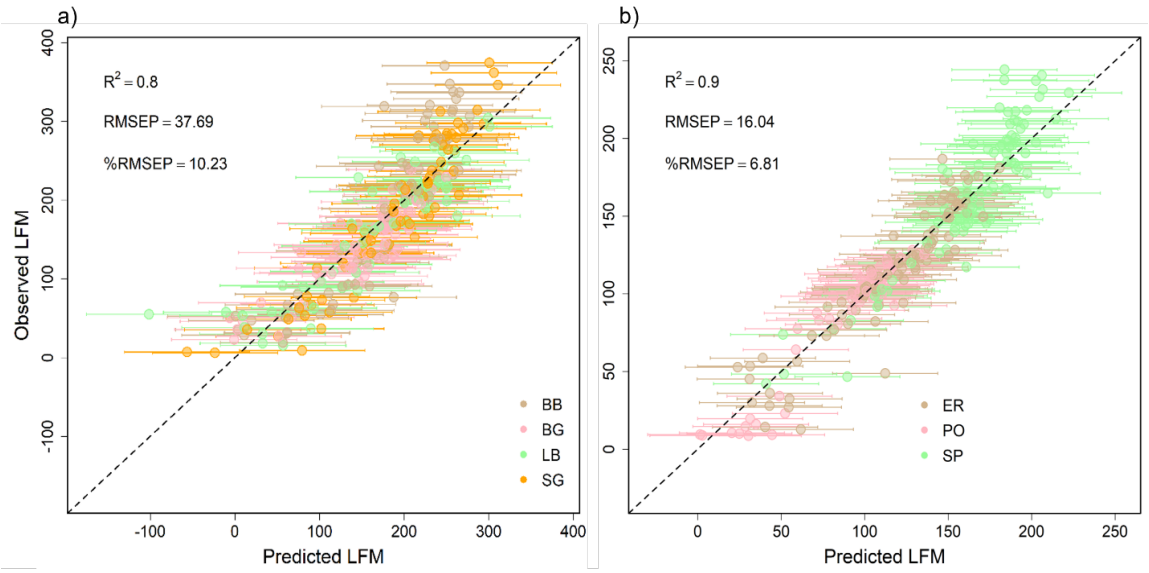

Figure S2.1 a) herbaceous and b) woody PLSR model predicted LFM vs. observed LFM. The black, dashed line is the 1:1 line. Error bars represent the 95% uncertainty estimates from jackknifing. %RMSEP is RMSEP standardized by the range of LFM values. See Table 2.1 for species codes.

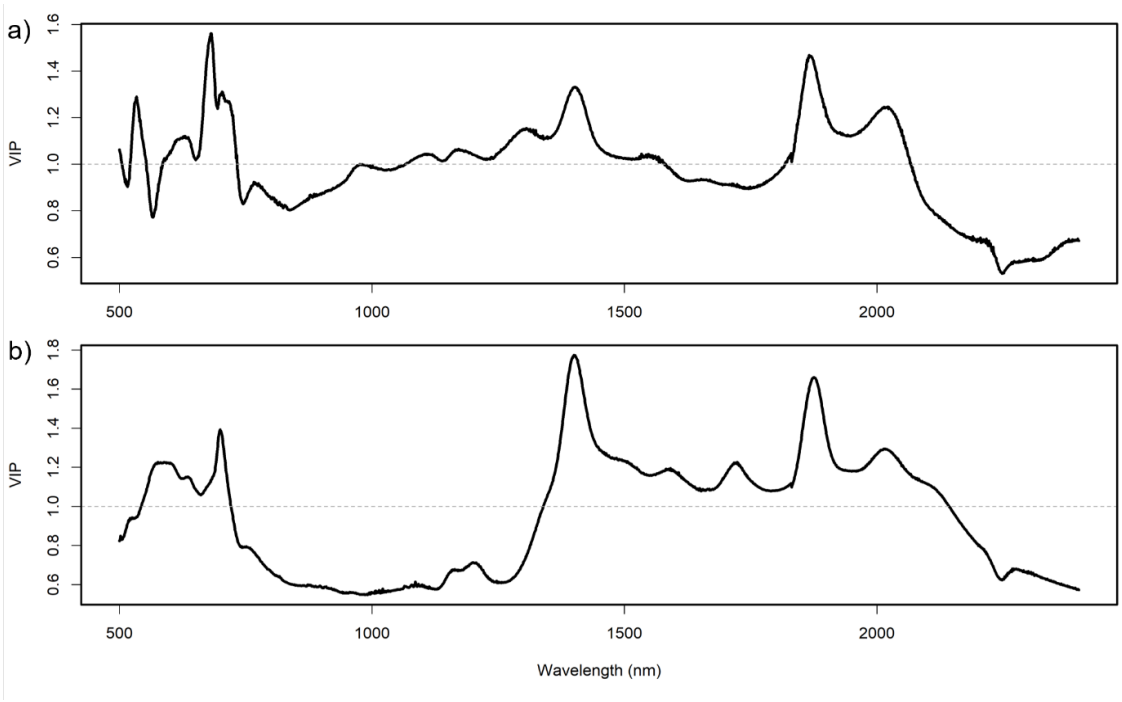

Figure S2.2 Variable importance projections (VIP) for a) herbaceous and b) woody PLSR models. Higher values are of greater importance to the model. Values greater than 1 are generally considered valuable.

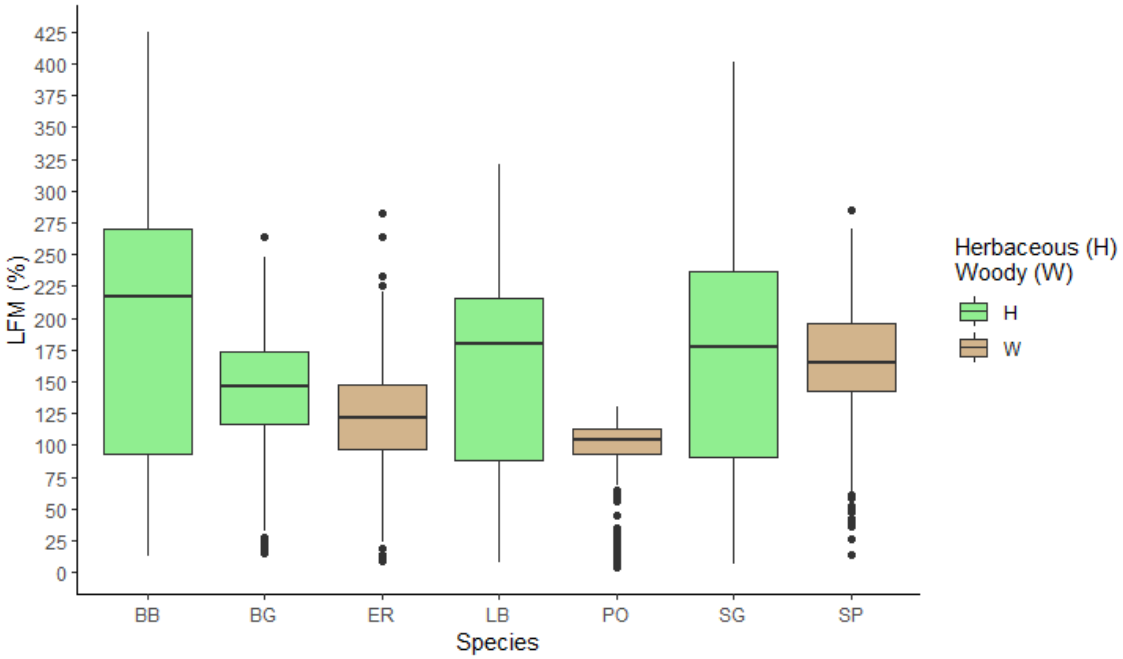

Figure S2.3 LFM range per species, herbaceous species in green and woody in tan. For species codes see Table 2.1.

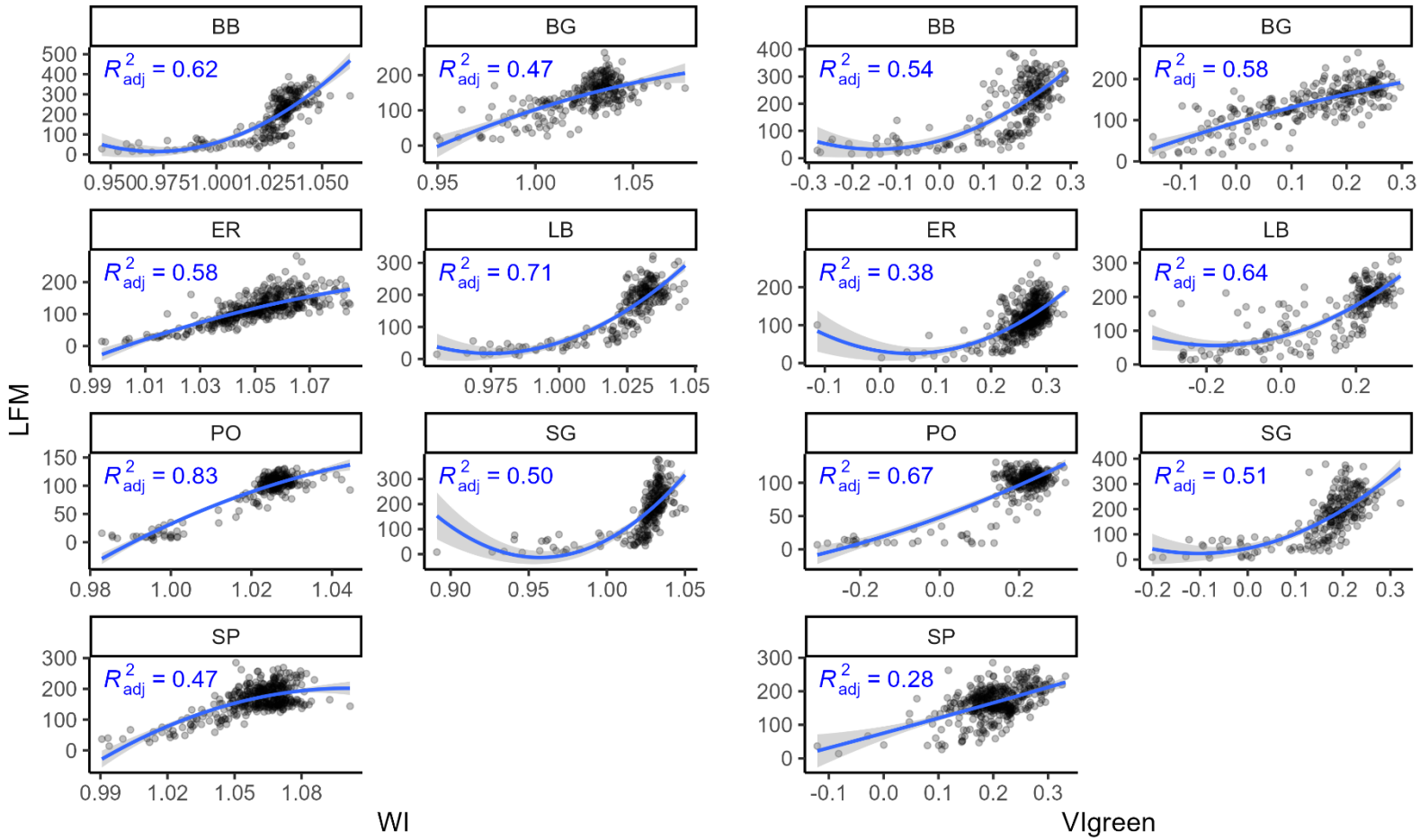

Figure S2.4 WI and VIgreen vs. LFM per species. Blue lines are the polynomial (VI + VI²) relationship. See Table 2.1 for species codes.

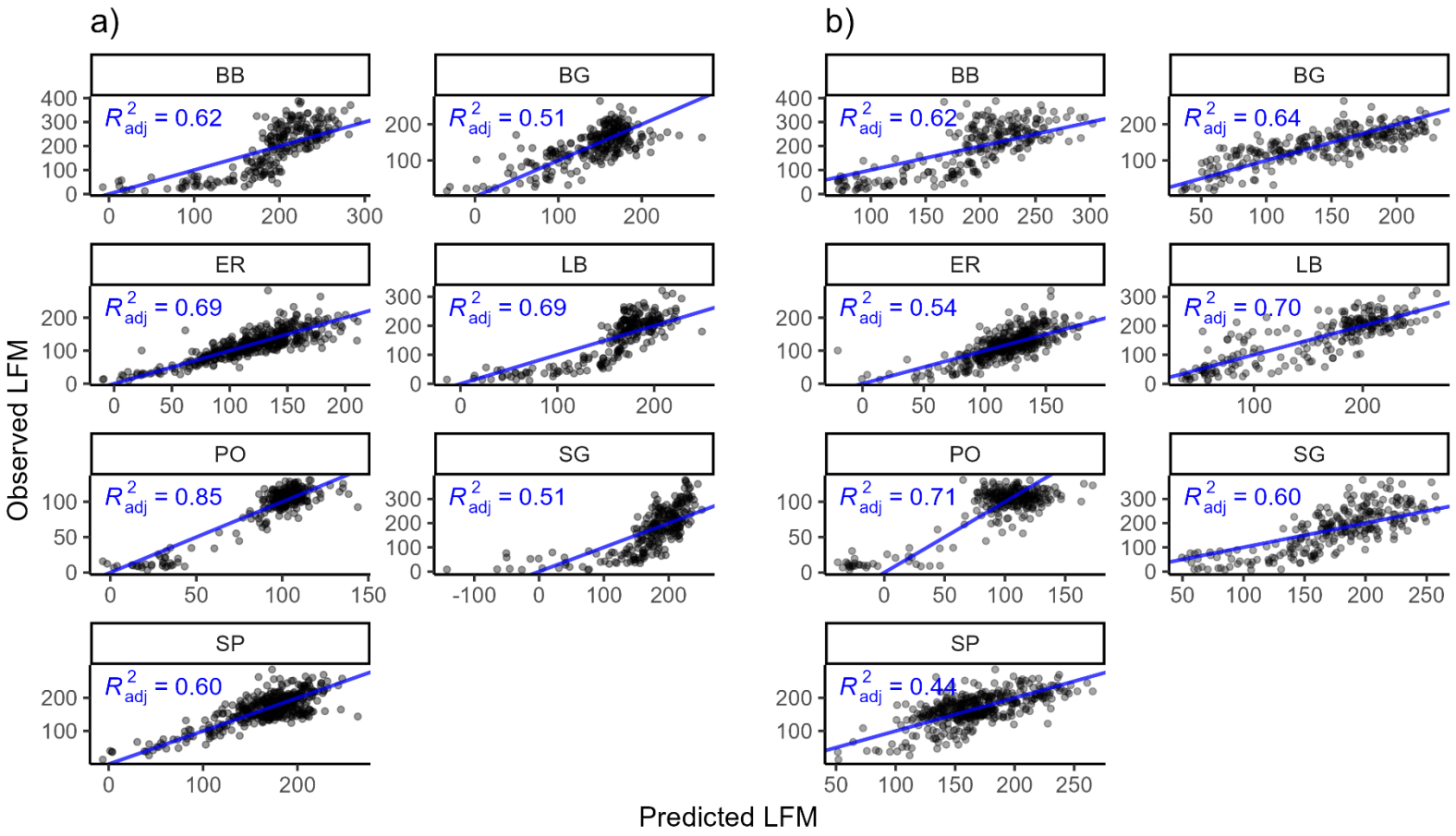

Figure S2.5 Model predictions vs observations by species from a) WI+WI² and b) VIgreen+VIgreen² models. See Table 2.1 for species codes.

APPENDIX B

Supplemental Tables and Figures for Chapter III

Table S3.1 Site/plant community collections by month. Many complete collections (all individuals and species) took more than one day.

	Oak-hickory-pine (cook)	Cross Timbers (cter)	Mixedgrass prairie (klem)	Shortgrass prairie (opti)	Tallgrass prairie (tgpp)	**Total**
Jan.	1	0	1	0	0	**2**
Feb.	0	0	0	0	0	**0**
Mar.	2	3	2	0	0	**7**
Apr.	0	3	2	0	0	**5**
May	1	2	2	1	1	**7**
Jun.	1	8	2	1	3	**15**
Jul.	4	4	2	3	1	**14**
Aug.	2	2	1	2	1	**8**
Sep.	1	3	1	0	1	**6**
Oct.	0	0	1	0	0	**1**
Nov.	0	1	0	0	0	**1**
Dec.	1	0	0	0	0	**1**
Total	**13**	**26**	**14**	**7**	**7**	**67**

Figure S3.1 Images of the vegetation at the collection site within Optima WMA (opti).

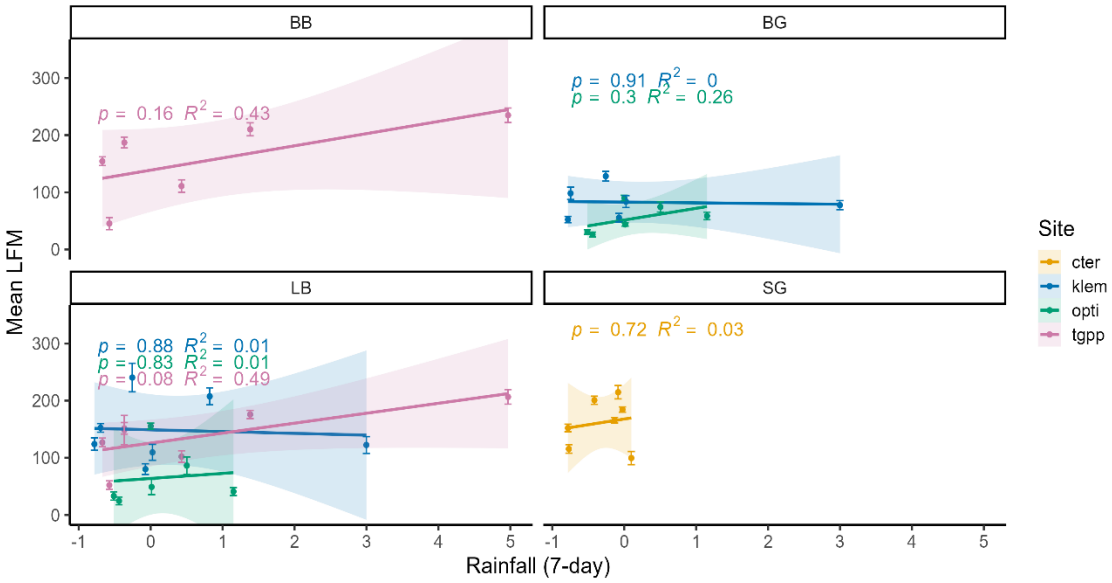

Figure S3.2 7-day average rainfall (centered and scaled) vs herbaceous mean LFM. Error bars represent the 95% CI for mean LFM and shading represents the 95% model CI. There is moderate, nonsignificant positive correlation at the tallgrass prairie preserve (pink). Site/species are listed in Table 3.1.

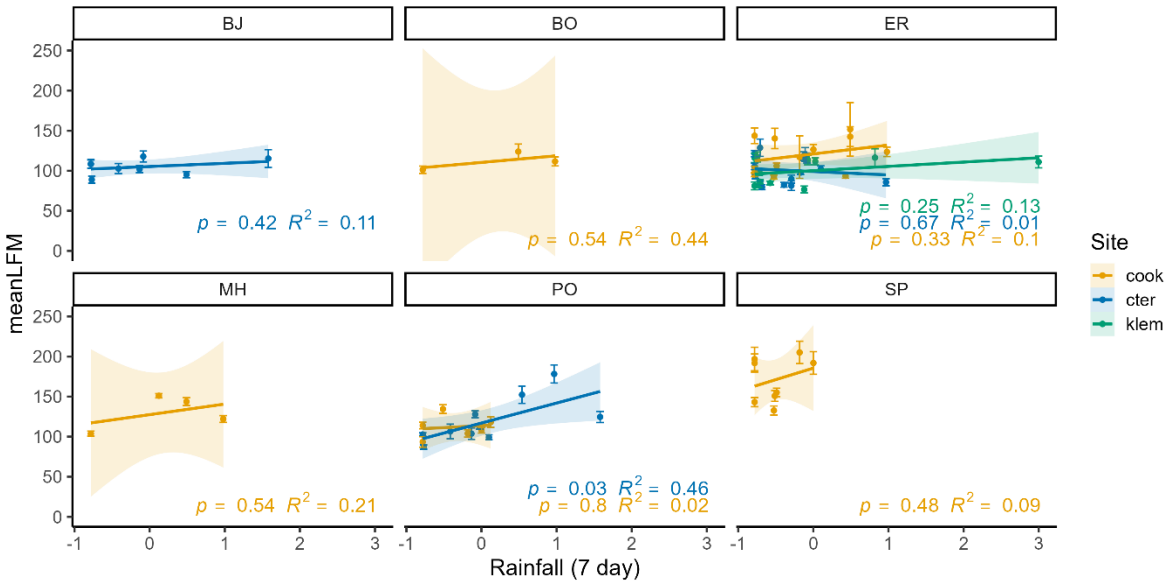

Figure S3.3 7-day average rainfall (centered and scaled) vs woody/tree mean LFM. Error bars are the 95% CI for mean LFM and shading is the 95% model CI. There is moderate positive correlation to PO* in the Cross Timbers (blue). Site/species are listed in Table 3.1. *p≤0.05

VITA

Antigone Jane Burke

Candidate for the Degree of

Master of Science

Thesis: ESTIMATING LIVE FUEL MOISTURE CONTENT IN OKLAHOMA PLANTS

Major Field: Natural Resource Ecology and Management

Biographical:

Education:

Completed the requirements for the Master of Science in Natural Resource Ecology and Management at Oklahoma State University, Stillwater, Oklahoma in May, 2023.

Completed the requirements for the Bachelor of Science in Botany at Kent State University, Kent, Ohio in 2019.

Experience:

Graduate Research Assistant, Oklahoma State University, 2021−2023
Vegetation Habitat Assessment Technician, The Great Basin Institute, Apr.−Oct. 2020
Natural Resource Management Intern, Jewel Cave National Monument, May−Aug. 2019
Undergraduate Researcher, Kent State University, Fall 2018−Spring 2019

Professional Memberships:

Xi Sigma Pi Honor Society
Phi Kappa Phi Honor Society
R-Ladies
Society of American Foresters
Botanical Society of America